Budgeting major elements in pelagic mesocosm studies

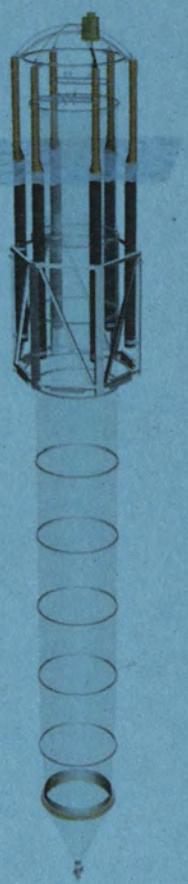

Dissertation
zur Erlangung des Doktorgrades
der Mathematisch-Naturwissenschaftlichen Fakultät
der Christian-Albrechts-Universität zu Kiel

vorgelegt von
Jan Czerny

Kiel 2013

Budgeting major elements in pelagic mesocosm studies

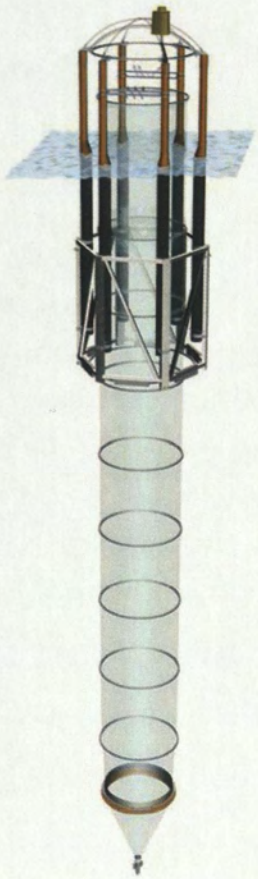

Dissertation

zur Erlangung des Doktorgrades

der Mathematisch-Naturwissenschaftlichen Fakultät

der Christian-Albrechts-Universität zu Kiel

vorgelegt von

Jan Czerny

Kiel 2013

(Zeichnung Deckblatt von Detlef Hoffmann)

Referent/in: Prof. Dr. Ulf Riebesell

Koreferent/in: Prof. Dr. Eric Achterberg

Tag der mündlichen Prüfung: 20.12.2013

Zum Druck genehmigt: 20.12.2013

gez. Prof. Dr. Wolfgang J. Duschl, Dekan

Table of contents

Zusammenfassung

Die vorliegende Dissertation behandelt die Optimierung eines pelagischen Mesokosmen-Systems zur quantitativen Messung von Stoffflüssen im marinen Planktonökosystem. Die KOSMOS (**K**iel **O**ff-**S**hore **M**esocosms for future **O**cean **S**imulation) Mesokosmen sind transparente zylindrische Kunststoffsäcke, in die repräsentative Unterproben des natürlichen Planktonnahrungsnetzes eingeschlossen werden können. Neun einzelne robuste Schwimmkonstruktionen tragen die, je nach Experiment, 20 bis 25 m langen wasserdichten Säcke. Hierbei soll der produktivste Abschnitt der Oberflächenschicht abgedeckt werden. Die in dieser Dissertation präsentierten Daten wurden im Rahmen eines Experimentes zu den Auswirkungen der Ozeanversauerung durch anthropogene CO_2 Emissionen erhoben. Zur Simulation der Ozeanversauerung wurde durch abgestufte CO_2 Zugaben ein Gradient von derzeitigen zu zukünftig prognostizierten Konzentrationen über die neun Mesokosmen erstellt. Ziel war es, Kohlenstoffflüsse von CO_2 in planktische Biomasse und über sinkende Partikel in tiefere Wasserschichten zu verfolgen. Durch erhöhte CO_2 Konzentrationen bedingte Änderungen im biologischen Kohlenstofftransport könnten weitreichende Folgen für den Ozean als wichtige Senke für anthropogenes CO_2 haben. Volle zeitlich aufgelöste Budgets der bioaktiven Hauptelemente Kohlenstoff, Stickstoff, Phosphor und Silizium wurden bisher noch nicht in marinen Planktongemeinschaften gemessen. Quantitative Daten zu Stoffflüssen dieser Elemente stellen wichtige Verbindungselemente zwischen Ökologie und Biogeochemie dar.

In einer kurzen Einleitung wird der Versuchsansatz Mesokosmos sowie Realisierungsmöglichkeiten mit besonderem Augenmerk auf pelagische Stoffflüsse anhand von Beispielen vorgestellt. Drei technisch methodische Publikationen, sowie eine darauf aufbauende Publikation der im Experiment gemessenen CO_2 bedingten Kohlenstoffflüsse bilden den Hauptteil der Arbeit. Die erste technische Publikation beschreibt den Versuchsaufbau (2.1); die zweite Publikation beschreibt ein Verfahren zur genauen Messung der eingeschlossenen Wassermenge (2.2) und der dritte Artikel ein Verfahren zur direkten Messung von Gasaustauschraten mit der Atmosphäre (2.3). Genaue Kenntnis der CO_2 Gasaustauschraten ist nicht nur unabdinglich zur Bilanzierung von Kohlenstoff, sondern gleichfalls relevant für Fragestellungen betreffs der marinen Produktion klimarelevanter Spurengase. Auf die drei technischen Publikationen folgt eine bisher unpublizierte kurze Beschreibung des von uns entwickelten Verfahrens zur quantitativen Messung von Sinkstoffflüssen. In dem ersten Experiment, in dem die beschriebenen Verfahren zum Einsatz gekommen sind, konnte bereits einige Erkenntnisse über Stoffflüsse durch das Nahrungsnetz und in tiefere Wasserschichten gewonnen werden. Ein deutlich zuträglicher Einfluss erhöhter CO_2 Konzentrationen auf das

Wachstum der zunächst bestandsbildenden Nano- und Picophytoplankter wurde nicht in Form messbar erhöhter Sinkstoffraten umgesetzt. Die später im Experiment stattfindende Blüte weitaus größerer Diatomeen führte sofort zu ansteigenden Sinkstoffflüssen. Das durch die vorausgehende Blüte bedingte Defizit an anorganischen Nährstoffen führte unter erhöhter CO_2 Konzentration jedoch zu verminderter Produktion von Diatomeen, welche womöglich selbst relativ unbeeinflusst von CO_2 wachsen.

Neben wichtigen Erkenntnissen zeigte sich allerdings auch noch Verbesserungspotential des Versuchsaufbaus. Daher folgt eine Beschreibung der wichtigsten technischen Neuerungen, die aus diesem Experiment hervorgegangen sind. In einem Perspektivenparagraph werden Verbesserungsvorschläge zur Datenerhebung sowie vielversprechende experimentelle Fragestellungen und Realisierungsmöglichkeiten in Bezug auf Tiefenwasserauftriebsereignisse in den Tropen vorgestellt.

Summary

This thesis deals with the optimisation of a marine pelagic mesocosm set-up for quantitative measurement of biogeochemical fluxes of matter within plankton ecosystems. The KOSMOS (**K**iel **O**ff-**S**hore **M**esocosms for future **O**cean **S**imulation) mesocosms are cylindrical transparent plastic bags designed to enclose representative samples of the naturally occurring plankton food web. Nine independent, rugged flotation frames support the 20 to 25 m deep watertight bags - depending on the specific experiment set-up - thereby covering the most productive part of the surface water layer. The data presented in this thesis were recorded in the context of an experiment designed to examine the effects of a projected future anthropogenic rise of aquatic CO_2 concentrations. This rise was simulated through graded addition of CO_2 across nine mesocosms. The objective was to trace natural carbon fluxes from the atmosphere into plankton biomass and via sinking of particles into deeper water layers. Changes in this biological carbon transport caused by increased CO_2 concentrations could have far-reaching consequences for the ocean in its function to naturally absorb large parts of the anthropogenic carbon emissions. Measuring the development of full budgets of carbon, nitrogen, phosphorus and silica over time in mesocosms of this size is unprecedented and could provide valuable quantitative data connecting ecology to biogeochemistry.

In a short introduction, an outline of the mesocosm approach as well as implementation options with particular regard to pelagic fluxes will be presented on the basis of examples. Three technical publications and a publication discussing measured carbon fluxes and budgets in the Svalbard 2010 ocean acidification study constitute the body of the thesis. The first technical note describes the mesocosm set-up; while the second manuscript deals with the measurement of the enclosed water volume in flexible wall mesocosms. A technique for tracer-based estimates of gas exchange with the atmosphere is described in a third technical publication. A precise knowledge of gas exchange rates is not only a prerequisite for carbon budgeting, but also relevant for issues concerning marine production of climate relevant trace gases. These publications on mesocosm methodology are followed by a so far unpublished description of a technology for quantitative measurement of sediment samples, developed for KOSMOS. In the first experiment using the described tools, some insights into the role of ecology for biogeochemical fluxes of matter through the plankton food web and into deeper water layers have already been gained. A significant beneficial influence of increased CO_2 concentrations on the growth of pico- and nanophytoplankton was not translated into measurably increased sedimentation rates. At a later point in the experiment, the flourishing of much larger diatoms immediately resulted in increased sedimentation rates at low CO_2 concentration levels. However, under conditions of increased

CO_2 concentrations, the deficit of inorganic nutrients, caused by the preceding pico- and nanophytoplankton, reduced the production of diatoms, whose growth is presumably relatively unaffected by CO_2 levels.

For all the important findings, there is still room for improvement of the experimental set-up. Therefore, a description of the most important technical improvements realised as a result of the 2010 experiment is enclosed. In the section entitled "Perspectives", some thoughts on the improvement of data collection and analyses as well as promising experimental concepts and implementation options with regard to tropical upwelling events are presented.

1. Introduction

1.1 Mesocosms

A mesocosm is an experimental enclosure containing more than two interacting species forming an ecosystem (Odum, 1984). The word "mesocosm" originates from the ancient Greek language and refers to the scale of a system. As a compromise between "cosmos"- the universe- and "microcosmos" - a small subunit of the universe - mesocosm describes a setup for controlled ecological experiments mimicking the field. From spatially defined field areas, through cages, to chemically isolated laboratory chemostats, the range of implementations of this concept seems endless (see book: "Enclosed Experimental Ecosystems" 2009). The common objective of mesocosm approaches is to provide experimental data on ecology within enclosed systems. Results of mesocosm experiments can form a basis for the extrapolation of physiological data on ecosystem components to natural communities observed in the field. As exchange of resources and biomass are restricted, transformations of matter become quantitatively traceable. Repeated sampling of precisely the same body of water is nearly impossible in aquatic field work, for oceanographers even more than for limnologists. Approaches to follow and re-sample ocean water masses using lagrangian drifters and chemical tracers (e.g. Landry et al., 2009; Bakker et al., 2005) are limited in time to a few days. Temporal succession within a series of field measurements can, due to mixing processes, never be as quantitatively precise as within a closed system. Important hints for understanding key processes like primary production in the sea (McAllister et al., 1961), bentho-pelagic coupling (Smetacek et al., 1976) or the formation of fast sinking marine aggregates (Alldredge et al., 1995) could thus already be achieved by following the succession of a plankton community over time in one single mesocosm. The effect of physical or chemical influences on community succession can be tested in perturbation experiments by using a set of replicated mesocosms. Recommendations for experimental design of pelagic mesocosm CO_2 perturbation studies are given in Riebesell et al. (2010).

Mesocosm experiments always represent a compromise between reality observed in the field and control and reproducibility achieved under laboratory conditions. Set-ups very close to the natural system might encounter a high level of variability and a large number of insufficiently determined variables, making obtained data in the end too complex to draw conclusions on many processes of interest. Highly controlled set-ups, on the other hand, premise a strong reduction of complexity and natural variability so that extrapolation of the described relationships to the natural system becomes questionable.

Observing natural communities in enclosures can be realised by simple means, however, the optimisation of a setup towards maximum realism at maximum control can become technically complex.

1.2 Elemental budgets in plankton mesocosm research – a historical review

Pelagic mesocosms have been an established tool in marine plankton research for more than 50 years (Strickland et al., 1969). Nevertheless, no standard protocols for mesocosm studies exist, nor even a common design of the enclosure. The diversity of shapes and sizes of in situ pelagic mesocosms similar to the enclosures being subject of this thesis is illustrated in Fig. 1.2. Beyond a well-reasoned choice of scale, all those designs are fitted to the specific type of question to be answered. Even more important in marine environments, however, is to construct a mesocosm that is durable enough to brave the elements for the duration of the planned experiment. For the following short review several designs of pelagic mesocosms were chosen, in size, research approach, or structure more or less directly comparable to the KOSMOS mesocosms.

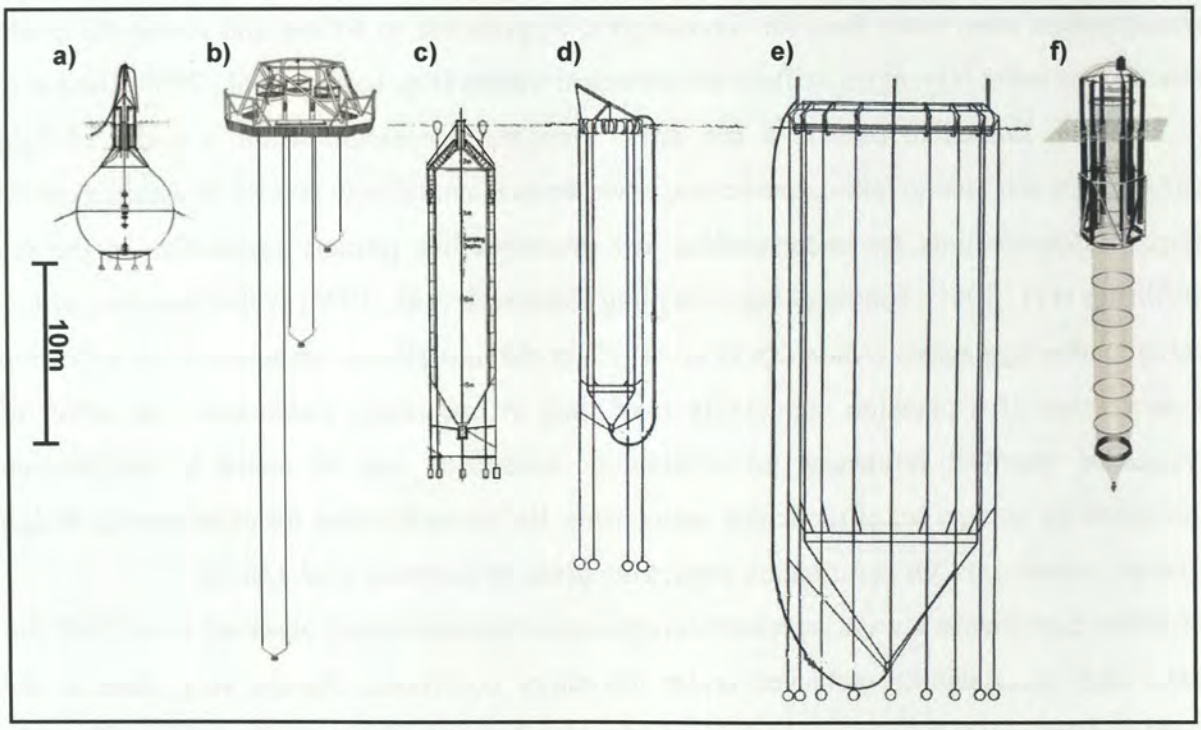

Figure 1.2. Examples for various enclosure designs used as marine plankton mesocosms. All chosen examples are designed for research from plankton ecology to biogeochemical fluxes. **a)** "Large plastic bag" (*113m³)* by Strickland and Terhune (1961). **b)** Seamless plastic tubes *(4-40m³)* described by Brockmann (1992), shown in the free drifting flotation frame with bags of different length. **c)** Loch ewe enclosure *(~100m³)* by Gamble et al. (1977). **d)** 0.25 CEE *(~68m³)* and **e)** full size CEE *(~1700m³)* as described by Menzel and Case (1977). **f)** KOSMOS *(~50-80m³)* as described by Riebesell et al. (2013).

First reported results from marine plastic bag enclosures by Strickland and Terhune (1961) (1. 2a) were published by McAllister et al. (1961) and Antia et al. (1963). One spherical bag equipped with a steering mechanism and pneumatic buoyancy compensation was filled with filtered seawater and inoculated with a natural phytoplankton community. Measurements of phytoplankton community composition and biogeochemical parameters were supplemented by a set of primary production estimates. In situ ^{14}C uptake, oxygen production, pH change as well as particulate organic carbon and cell production were in good agreement within this well stirred gas-tight bag (Fig. 1.3). The experiments gave a first impression of community primary production and dynamics of elemental composition of particles in the sea.

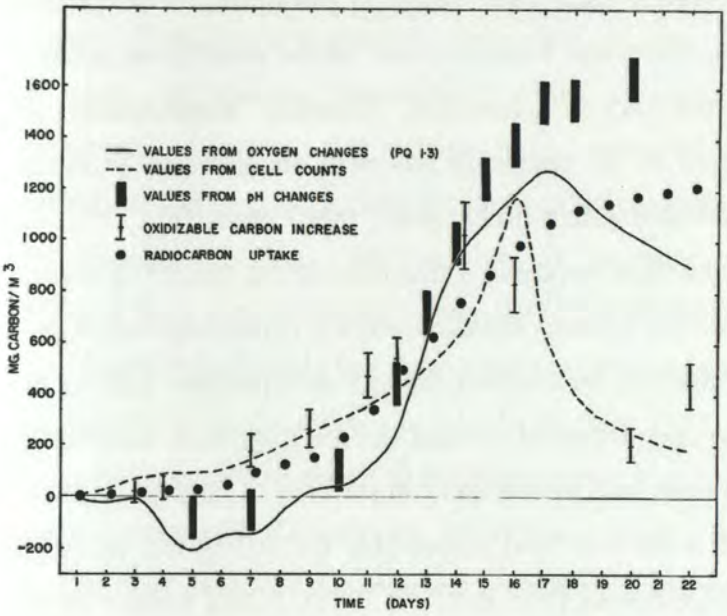

Figure 1.3. Net production of carbon during a phytoplankton bloom in the large volume plastic sphere measured by five different methods (McAllister et al., 1961).

Around ten years later, the mesocosm initiative CEPEX (**C**ontrolled **E**cosystem **P**ollution **Ex**periments) initiated parallel development of mesocosms around the world. Within the centre of investigation were questions concerning ecological effects and residence time of contaminants like heavy metals and crude oil within coastal waters. The Scotch Loch Ewe mesocosms (Fig. 1.2c; Gamble et al., 1977) were similar to the Strickland model tapered to the surface but, cylindrical in shape, they had the advantage of a linear representation of the light gradient within the euphotic zone. Instead of homogeneous mixing, a funnel-shaped bottom with a collecting cup for sediment sampling by scuba divers was attached. Full natural plankton communities were investigated including the simultaneous rearing of cod and herring larvae as well as lobster inside the mesocosms. Budget calculations were performed in one of the first experimental trials (Gamble et al., 1977). Due to obvious leakage of most of the bags, rough budgets were only calculated for nitrogen in the least corrupted bag. Around 4% more N than added was found after

55 days of daily fertilisation. This result was surprising, as strong wall growth, mentioned several times within the manuscript, should have absorbed large amounts of nutrients.

In Germany, several types of mesocosms were developed between 1970 and 1990. Among those, the seamless polyethylene bags of Brockmann (1992) represented the most productive concept. Simple bulk stock 1 m diameter plastic sleeve was used in combination with various flotation devices. Several years of research within Heligoland harbour focussed on the production and consumption of dissolved organic substances as well as ecological consequences of pollution. The three-bag conuration as shown in Fig. 1.2b was designed to perform drifting experiments within the North Sea. The POSER (**P**lankton **O**bservation with **S**imultaneous **E**nclosures in **R**osfjorden) project (Brockmann et al., 1983) used these seamless plastic tubes to compare results from bags of various dimensions. Elemental budgets could not be constructed because sinking material was neither extracted nor kept in suspension. Therefore, accumulation and remineralisation of material at the bottom of the enclosure represent an unknown exchange process. The Canadian CEE (**C**ontroled **E**cosystem **E**nclosures) mesocosms (Fig. 1.2d, e; Menzel and Case, 1977) were certainly the most impressive structures in the history of marine pelagic mesocosms. KOSMOS resembles CEE in many details; open top cylindrical bags with a bottom funnel forming a sediment trap that can be emptied through an extraction tube to the surface. CEEs were equipped with two to three layers of foil and Dacron to prevent failures due to bag damage, a permanent threat to flexible wall mesocosms. Absorption of large parts of the natural turbulence by these rather rigid walls was held responsible for falling out of larger phytoplankton in the beginning of the experiments (von Bröckel, 1982). A test version of the CEE, 25% of the original size, (Fig. 1.2d) was used for most studies due to the high costs and difficult handling of full size CEEs. One of the more elaborated nitrogen budgets within the 25% CEEs was published by Harrison et al. (1977). Calculations were based on nitrate additions, as well as measurements of particulate organic and dissolved inorganic nitrogen. Assuming a single pathway of nitrogen flow (inorganic N to particulate N to sediment), sedimentation was calculated by mass balance. Calculated sedimentation, that was sampled but could obviously not be measured, strongly resembled nitrate additions to the mesocosm. It was concluded that nitrogen export is a function of nitrogen input. Results merely document that nitrate added on a regular basis did not accumulate in the water column or in particles therein. Accumulation of dissolved organic nitrogen or wall growth featuring possible alternative nitrogen pools other than sediments were not discussed. Daily removed settled material was, also in later budget approaches (e.g. Hattori et al., 1980; Vadstein et al., 2012), at best qualitatively analysed. Examples where direct quantitative measurements of settled material were used for mesocosm

budget calculations could not be found. Reasons for the often problematic quantitative analyses of dense sediment samples are discussed in Section 2.4.

In a critical review article, Banse (1982) indicated the general shortage of studies evaluating elemental budgets. This critical point was picked up in a review by Brockmann (1990) who attributed it to a lack of interdisciplinary expertise needed to determine all the parameters within the same experiment. Still, substantial amounts of useful data, which could not be obtained by other means, were produced using mesocosms. Not only were the effects of pollutants on plankton ecology and production described, but important interactions within the planktonic food web in general could be quantified (Lalli, 1990). As one of the overall results, it was found that enclosed ecosystems reacted often far more sensitively to chemical perturbations than could be expected from single species lab experiments (Kuiper, 1982). Those responses are often initiated by shifts in species composition, which cannot be realistically represented within lab experiments on one or few species. Most mesocosm experiments since the 1980s focussed on ecological and biogeochemical interactions within parts of the enclosed ecosystem rather than on full elemental budgets. An overview of currently operating mesocosm facilities and their research focus is given on the homepage of MESOAQUA (mesocosm.eu). Some facilities have a long tradition in flexible bag mesocosm experiments; the Bergen-Espegrend mesocosm facility is performing experiments on a regular basis since 1978. Recently the impact of atmospheric dust deposition on carbon export in the oligotrophic Mediterranean was investigated using the "large clean mesocosms" (Guieu et al., 2013). The influence of dust ballast on aggregate formation and sinking was described by sediment carbon measurements as well as in situ optical instruments without applying a carbon budget approach. A clear correlation of dust input to export was shown, but the origin of the carbon exported from the mesocosms remains unclear (Bressac et al., 2013). A comprehensive experiment focussing on ecosystem carbon and nutrient flows using seven 40m^3 mesocosm bags was performed in Hopavågen lagoon close to Trondheim/Norway in 1997 (Vadstein et al., 2012; Olsen et al., 2007). Although many components of the carbon budget (e.g. inorganic carbon, sedimentation and gas exchange) were not directly measured, plausible elemental fluxes and budgets could be determined by mass balance and measured stoichiometry. Inverse modeling was combined with differential measurement of particulate matter and metabolic rates within four size fractions. A sophisticated sampling protocol harmonized with modeling allowed for presentation of plenty of metabolic rates that can, in parts, impossibly be measured directly in a natural system (see flow network Fig. 1.4).

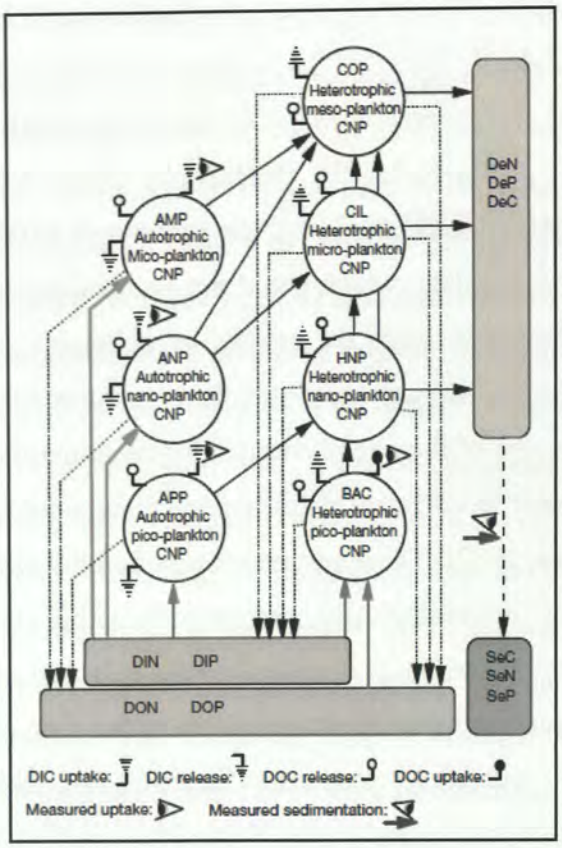

Figure 1.4. Flow network for inverse mesocosm ecosystem modeling from Vadstein et al. (2012) is fitted to a size fractionated data acquisition protocol. Abbreviations: DIC-dissolved inorganic carbon, DOC-dissolved organic carbon, DIN / DIP-dissolved inorganic nitrogen / phosphorus, DON / DOP-dissolved organic nitrogen / phosphorus, DeN / DeP / DeC-detritus nitrogen / phosphorus / carbon, SeN / SeP / SeC-sediment nitrogen / phosphorus / carbon, COP-copepods, CIL-ciliates, BAC-bacteria.

Whether more complete data coverage, also reducing the number of adjustable variables, would have increased capabilities of the model remains questionable. Measurement of carbon budgets, however, was not performed within large mesocosms until recently, when the transport of man-made atmospheric CO_2 by the biological carbon pump became a relevant research question. For the first time inorganic carbon concentrations were measured in large marine ecosystem experiments. Carbon mass balance calculations for experiments in shallow mesocosm bags in Bergen-Espegrend were used to draw conclusions on carbon export at future CO_2 levels (reviewed in Riebesell et al., 2008). Increased carbon loss from the budget at high CO_2 concentrations was thought to originate from polymerisation of exudates from CO_2 fertilised phytoplankton, leading to a measured increase in carbon content of the sedimenting material (Delille et al., 2005). This promising Bergen carbon budget approach would have profited from quantitative sediment sampling, as well as from data-based estimates for air-sea gas exchange. These first ocean acidification plankton mesocosm experiments acted as an impulse for the development of the methodology presented in this thesis.

1.3 The choice of scale

Scale is an integral feature in the definition of a mesocosm, representing a unit larger than a microcosm but smaller than a whole biotope. Depending on the size, behaviour, and generation

time of organisms studied, mesocosm experiments need appropriate spatial, structural and temporal dimensions in order to produce data applicable to the natural system (Petersen et al., 1999). Improving realism of experimental ecosystems can be achieved by increasing size and complexity. This is not only restricted by technical and financial limits, but also by the effort needed to gain sufficient data for description of the system.

Plankton communities in pelagic mesocosms are mainly composed of relatively small organisms with relatively short generation times (days to months). Additionally, the pelagial seems to be homogeneous and more or less unstructured compared to terrestrial or benthic habitats. Accordingly, it should be principally easy to enclose a relatively complete plankton ecosystem for a sufficient period to observe ecological and biogeochemical processes under realistic conditions. Yet, a closer second look shows that this is only partly true. The enclosure itself, necessarily a rigid structure, constitutes a major perturbation to the pelagic system. The walls of the mesocosm provide habitat for benthic species that compete with plankton (Chen et al., 1997). Inner walls of previous flexible wall mesocosms could generally not be cleaned. This procedure, which is standard for many rigid land-based mesocosms (see book: "Enclosed Experimental Ecosystems", 2009), is a basic prerequisite for budget calculations with an experimental duration of several weeks. Small-scale turbulence and large-scale convection, structuring the natural habitat of planktonic organisms, are significantly changed compared to open waters due to energy dissipation by the walls (von Bröckel, 1982). Especially in shallow set-ups, turbulence has to be deliberately generated to keep cells in suspension (reviewed by Sanford, 1997). The most efficient way of reducing wall artefacts is again by increasing the volume of the enclosure to decrease relative wall surface.

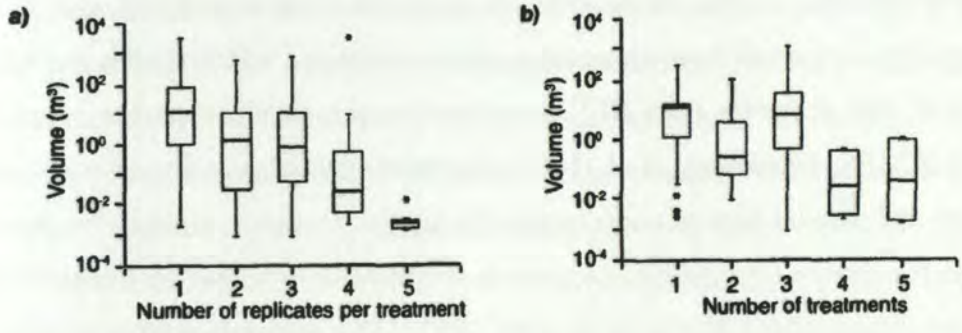

Figure 1.5. Box plots of mesocosm volume versus **a)** replicates per treatment **b)** and number of treatments. Data are sampled of 266 published papers on aquatic mesocosm research. Median values are represented by the bar within the box and the interquartile range by the top and bottom of the box. Whiskers represent data range within 1.5 times the interquartile, data outside this range are marked by asterisks. Plot modified from Petersen et al. (1999).

Due to increased costs and effort at increased size, the number of replicates is inversely related to mesocosm size, with negative effect on confidence in the findings (Petersen et al., 1999). MEERC (**M**ultiscale **E**xperimental **E**cosystem **R**esearch **C**entre) invested more than a decade to test scale-related theory, to improve experimental design and to develop rules and tools for extrapolation from experiments to nature. Results mainly achieved within land-based pelagic, benthic as well as salt marsh ecosystem enclosures are summarised in the Book "Enclosed Experimental Ecosystems and Scale: Tools for Understanding and Managing Coastal Ecosystems" (2009).

Besides turbulence, another structural feature relevant for deep pelagic mesocosm systems is horizontal stratification. Density gradients depict horizontal borders to the pelagic communities in the water column, mostly connected to chemical and physical gradients of the stratified water body. The upper mixed surface layer encounters the euphotic zone, where light is sufficiently available for photosynthetic primary production. Covering the entire euphotic zone with a pelagic mesocosm experiment enables estimating ocean primary production. While it is technically feasible to cover more than the eutrophic zone with less than 20 m long bags in turbid productive waters, the extension of the entire euphotic zone is usually beyond the reach of mesocosm instrumentation in oligotrophic waters. Theoretical considerations for the design of CEE in-situ pelagic mesocosms considered 1.3 times the depth of the euphotic zone as an optimal extension of an experimental unit (Menzel and Case, 1977). The design culminated in the construction of 29 m deep and 10 m wide mesocosms with a volume of 1700 m^3 (Fig. 1.2e). Additionally to vertical gradients also found in more narrow tubes, significant horizontal inhomogeneity was observed at 10 m diameter (Takahashi et al., 1975; Grice et al., 1977). A maximum of three mesocosms without replication was used within one experiment. Due to the large effort connected to a set-up of these dimensions, most published CEPEX studies (reviewed by Brockmann, 1990) report results from CEE mesocosms much smaller than these optimal dimensions. During POSER, Brockmann et al. (1983) compared phytoplankton and zooplankton succession in 1-2 m^3 and parallel bags of much larger dimensions. However, sinking flux lead to nutrient depletion in the surface layer within longer bags after a while, whereas growth in shorter bags was fuelled by remineralised nutrients (Kuiper, 1977). This principle applies mainly to simple bag constructions, where sinking material is not extracted during the experiment. A few m^3 was claimed to be sufficient to reproduce succession within size classes up to microplankton on short timescales. Introduction of carnivorous zooplankton like fish larvae poses additional requirements on the minimum volume of the experimental units (Kuiper, 1982). In this case the minimum size is given by the need to hold representative stock sizes of the larger animals as well

as their prey. Stock sizes have to be sufficiently large to enable representative sampling. In most experiments the number of trophic levels is reduced by removing large mesozooplankton or nekton.

Physical perturbations like temperature, light, turbulence or stratification, are for technical reasons mostly confined to land-based set-ups, whereas in situ pelagic mesocosms have been widely used to study chemical perturbations. The influence of anthropogenic impact on coastal communities due to increased nutrient runoff, atmospheric deposition, pollution by oil spills and especially heavy metals have been intensively studied in large mesocosm projects (Grice and Reeve, 1982). Most perturbation studies are targeted to detect thresholds of anthropogenic influence below which original biodiversity is widely preserved. Knowledge of these thresholds is necessary for policy makers to restrict emissions. Unfortunately, cost-intensive research such as mesocosm experiments become possible only once ecosystem services like fish yield and seaside recreational value or even the oceans' capacity as a dumping ground for toxic waste are endangered.

1.4 Thesis outline

This thesis documents the on-going technical development of a pelagic mesocosm system for quantitative measurement of biogeochemical fluxes. To date our investigations mainly focussed on testing the effect of projected future elevated aquatic CO_2 concentrations on carbon fluxes within plankton communities. The objective was to gain understanding of mechanisms and rates of conversion of dissolved inorganic carbon and nutrients into sinking particles or dissolved organics by a plankton community. The export of matter into deep waters is not only a function of photosynthetic production of particles, but depends much on the type of particles as well as their processing by the community. Especially within the context of man-made perturbation of global carbon cycles, the need of principle understanding of ocean carbon transport is urgently needed to ascertain projections of future global change. While hints from single ecosystem components tested are already abundant, integrated community experiments are rare. KOSMOS is a unique mobile platform for whole community experiments, applicable in most ocean regions. The KOSMOS mesocosms were often referred to as "giant test tubes". Within this thesis an approach to observe reactants and products of a biological reaction within mesocosms is presented. A quantitative budgeting approach in mesocosms is a simple and obvious idea, often thought but hardly ever published. Following articles describe methods and first data on mesocosm carbon budgets within KOSMOS mesocosms.

Technical Note: A mobile sea-going mesocosm system – new opportunities for ocean change research

To meet the specific requirements for investigation of this global scale biogeochemical issue a specific mesocosm was designed. Other than eutrophication or pollution being relevant predominantly on a regional scale in coastal waters, ocean acidification is equally occurring in offshore waters far from human activity. The previously mentioned mesocosms (Fig. 1.1) are not suitable for unsheltered regions where swell or waves might occur. They were mostly operated on fixed locations within bays close to the operating research facilities. The mobile KOSMOS system is designed for moored or free drifting deployment from mid-size research vessels to achieve data covering a variety of locally different ecosystems. Constructional features making the set-up withstand waves up to two meters were continuously improved within the last five years and open relevant marine areas for research previously inaccessible to mesocosms. Strategies to reduce bio fouling on the mesocosm surfaces enable long term studies. In bringing together scientists from a wide variety of research disciplines achieved datasets comprehensively describing chemical and biological processes.

With the focus on biological carbon sequestration, net community production and the export of organic particles are central variables. To account for the direct quantitative observation of inorganic matter input and organic matter output of the plankton system, several analytical methods were developed, adapted or improved.

Technical Note: The determination of enclosed water volume in large flexible-wall mesocosms "KOSMOS"

Manuscript 2.2 describes a precise method for determination of the enclosed water volume, showing that equally manufactured and filled KOSMOS bags vary in volume by up to 8%. The volume of the reaction vessel has to be precisely known to allow quantitative comparison of measured fluxes to aquatic standing stocks of carbon and relevant nutrients like nitrogen, phosphorus and silica. Volume estimates relied on pumping rates during filling within published mass balance calculations. For KOSMOS mesocosms, filled by enclosing a water column, geometric calculations based on the intended shape and dimensions were used. Even in case the intended shape of the submerged bag is approximately achieved, there might be considerable variability in the enclosed water volume within a flexible bag.

Technical Note: A simple method for air–sea gas exchange measurements in mesocosms and its application in carbon budgeting

Publication 2.3 describes a newly developed method to directly determine gas exchange velocities and compares the results to relevant literature values. Whereas in earlier mesocosm studies dissolved inorganic carbon (DIC) was generally not measured, in some more recent experiments mesocosm integrated net community carbon uptake was calculated on the basis of changes in DIC and CO_2 gas exchange. It could be shown that laboratory or field derived parameterisations can not readily be used to calculate mesocosm gas exchange. Robust estimates of net community carbon uptake can be however derived using direct tracer measurements to estimate CO_2 air sea exchange.

Sediment sample processing

A description of sediment sample processing elaborated for the KOSMOS mesocosms is described in Section 2.4. In the KOSMOS set-up, the whole enclosure is funnel shaped on the bottom end, so that all sinking material is collected. The material can be easily sampled from the surface at any interval using a tube connecting the funnel tip with the water surface. Frequent sinking flux measurements allow for the detection of sedimentation events, analyses of sediment composition unspoiled by degradation and the calculation of elemental budgets for each sampling day.

Implications of elevated CO_2 on pelagic carbon fluxes in an Arctic mesocosm study – an elemental mass balance approach

Publication 2.5 presents data on carbon and nutrient budgets from a high Arctic Ocean acidification experiment. Applying the presented methods, a comprehensive dataset could be produced describing the effects of elevated aquatic CO_2 on elemental cycling within the enclosed ecosystem. Fertilising CO_2 effects on picoplankton significantly affected carbon and nutrient fluxes within the water column. Increased production of these small algae however, did not result in increased export of sinking particles but in accumulation of dissolved organics. Increased nutrient consumption as a consequence of CO_2 fertilised production resulted in significantly reduced export of diatom aggregates later in the experiment. The presented dataset underlines the important role of plankton succession and trophic interaction in modifying the consequences of physiological responses on the ecosystem level.

In Section 3, the improvements of the KOSMOS system after the 2010 Svalbard experiment are discussed. Most importantly instrumentation that allows preventing relevant wall growth by regular cleaning of the inside walls is presented. Furthermore, the bottom construction was improved for more efficient sediment and water column sampling. Gas exchange estimates have been improved using more sophisticated sampling protocols and online measurement of physical boundary conditions. Furthermore, mesocosm methods were developed to observe and retrieve large animals like juvenile fish, being present in very low numbers.

In the Perspective Section 4, the determination of general biogeochemical patterns and universal mechanisms from mesocosm research is discussed. Hypotheses and questions for future experiments focussing on biogeochemistry in tropical upwelling events are presented, together with a concept for technical realisation of upwelling experiments.

Table 1. Record of all "KOSMOS" mesocosm deployments conducted so far.

Month	Project	Aim	exp. days	Location	Objective	Deployment mode
July 2008	SOPRAN I	Experiment	10	Bornholm Sea	Cyanobacterial blooms and ocean acidification	Free drifting
January-February 2011	IFM-GEOMAR	Test deployment	30	Kiel Bight	Mooring, bag construction and bottom closing mechanisms	Moored
May 2009	IFM-GEOMAR	Experiment	14	Kiel Bight	Spring bloom and ocean acidification	Moored
November 2009	IFM-GEOMAR	Test deployment	14	Rügen and Kiel Bight	Towing tests, mooring, diving equipment, sediment processing, volume and gas exchange measurement and filling nets	Moored
March 2010	IFM-GEOMAR	Test deployment	7	IFM-GEOMAR Pier	Large floating sediment traps, volume measurement	Attached to pier
June- July 2010	EPOCA	experiment	30	Kongsfjorden Svalbard	Plankton bloom/pteropods and ocean acidification	Moored
January 2011	IFM-GEOMAR	Test deployment	4	Flensburg fjord	New bottom flanges, 25m deep bags, volume measurement, silicate addition and surface layer sampling	Moored
May –June 2011	SOPRAN II	Experiment	30	Espegren Norway	Plankton bloom/coccolithophores/pteropods and ocean acidification	Moored
December 2011	BAG-1	Experiment	10	Pacific near Hawaii	Oceanic free drifting test, high temperature gas exchange, plankton bloom and artificial nutrient input	Free drifting
June-August 2012	SOPRAN II	Experiment	40	Tvärminne Finland	Cyanobacterial blooms and ocean acidification	Moored
January-July 2013	BIOACID 2	Experiment	120	Kristineberg Sweden	Spring bloom development until summer and phytoplankton adaptation to ocean acidification	Moored

1.5 References Introduction

Petersen, J. E., Kennedy, V. S., Dennison, W. C., and Kemp, W. M., editers: Enclosed Experimental Ecosystems and Scale, 1 ed., by: Springer New York, 221 pp., 2009.

Alldredge, A. L., Gotschalk, C., Passow, U., and Riebesell, U.: Mass aggregation of diatom blooms: Insights from a mesocosm study, Deep Sea Research Part II: Topical Studies in Oceanography, 42, 9-27, 1995.

Antia, N. J., McAllister, C. D., Parsons, T. R., Stephens, K., and Strickland, J. D. H.: Further measurements of primary production using a large-volume plastic sphere, Limnology and Oceanography, 8, 166-183, 1963.

Bakker, D. C. E., Bozec, Y., Nightingale, P. D., Goldson, L., Messias, M.-J., de Baar, H. J. W., Liddicoat, M., Skjelvan, I., Strass, V., and Watson, A. J.: Iron and mixing affect biological carbon uptake in SOIREE and EisenEx, two Southern Ocean iron fertilisation experiments, Deep Sea Research Part I: Oceanographic Research Papers, 52, 1001-1019, 2005.

Banse, K.: Experimental marine ecosystem enclosures in a historical perspective, in: Marine Mesocosms, edited by: Grice, G. D., and Reeve, M. R., Springer New York, 11-24, 1982.

Bressac, M., Guieu, C., Doxaran, D., Bourrin, F., Desboeufs, K., Leblond, N., and Ridame, C.: Quantification of the lithogenic carbon pump following a dust deposition event, Biogeosciences Discussions., 10, 13639-13677, 2013.

Brockmann, U.: Pelagic mesocosms: II. Process studies, in: Enclosed Experimental Marine Ecosystems: A Review and Recommendations, edited by: Lalli, C. M., Springer, New York, 81-108, 1990.

Brockmann, U. H., Dahl, E., Kuiper, J., and Kattner, G.: The concept of POSER (Plankton observation with simultaneous enclosures in Rosfjorden), Marine Ecology Progress Series, 14, 1-8, 1983.

Brockmann, U. H.: Enclosed plankton ecosystems in harbours, fjords, and the North Sea - release and uptake of dissolved organic substances, in: Marine Ecosystem Enclosed Experiments : proceedings of a symposium held in Beijing, People's Republic of China, edited by: Wong, C. S., and Harrison, P. J., IDRC, Ottawa, 66-86, 1992.

Chen, C.-C., Petersen, J. E., and Kemp, W. M.: Spatial and temporal scaling of periphyton growth on walls of estuarine mesocosms, Marine Ecology Progress Series, 155, 1-15, 1997.

Delille, B., Harlay, J., Zondervan, I., Jacquet, S., Chou, L., Wollast, R., Bellerby, R. G. J., Frankignoulle, M., Borges, A. V., Riebesell, U., and Gattuso, J.-P.: Response of primary production and calcification to changes of pCO_2 during experimental blooms of the coccolithophorid Emiliania huxleyi, Global Biogeochemical Cycles, 19.2, 2005.

Gamble, J. C., Davies, J. M., and Steele, J. H.: Loch Ewe bag experiment, 1974, Bulletin of Marine Science, 27, 146-175, 1977.

Guieu, C., Dulac, F., Ridame, C., and Pondaven, P.: Introduction to the project DUNE, a DUst experiment in a low Nutrient, low chlorophyll Ecosystem, Biogeosciences Discussions., 10, 12491-12527, doi:10.5194/bgd-10-12491-2013, 2013.

Grice, G. D., Reeve, M. R., Koeller, P., and Menzel, D. W.: The use of large volume, transparent, enclosed sea-surface water columns in the study of stress on plankton ecosystems, Helgoländer wissenschaftliche Meeresuntersuchungen, 30, 118-133, 1977.

Grice, G. D., and Reeve, M. R.: Marine mesocosms: biological and chemical research in experimental ecosystems, Springer-Verlag, 1982.

Harrison, W. G., Eppley, R. W., and Renger, E. H.: Phytoplankton nitrogen metabolism, nitrogen budgets, and observations on copper toxicity: controlled ecosystem pollution experiment, Bulletin of Marine Science, 27, 44-57, 1977.

Hattori, A., Koike, I., Ohtsu, M., Goering, J. J., and Boisseau, D.: Uptake and regeneration of nitrogen in controlled aquatic ecosystems and the effects of copper on these processes, Bulletin of Marine Science, 30, 431-443, 1980.

Kuiper, J.: Development of North Sea coastal plankton communities in separate plastic bags under identical conditions, Marine Biology, 44, 97-107, 1977.

Kuiper, J.: Ecotoxicological experiments with marine plankton communities in plastic bags, in: Marine Mesocosms, edited by: Grice, G. D., and Reeve, M. R., Springer, New York, 181-193, 1982.

Lalli, C. M.: Enclosed experimental marine ecosystems: A review and recommendations: A contribution of the scientific committee on oceanic research working group 85, Springer, New York, 218 pp., 1990.

Landry, M. R., Ohman, M. D., Goericke, R., Stukel, M. R., and Tsyrklevich, K.: Lagrangian studies of phytoplankton growth and grazing relationships in a coastal upwelling ecosystem of Southern California, Progress in Oceanography, 83, 208-216, 2009.

McAllister, C. D., Parsons, T. R., Stephens, K., and Strickland, J. D. H.: Measurements of primary production in coastal sea water using a large-volume plastic sphere, Limnology and Oceanography, 6, 237-258, 1961.

Menzel, D. W. a., and Case, J.: Concept and design: Controlled ecosystem pollution experiment, Bulletin of Marine Science, 27, 1-7, 1977.

Odum, E. P.: The mesocosm, BioScience, 34, 558-562, 1984.

Olsen, Y., Andersen, T., Gismervik, I., and Vadstein, O.: Protozoan and metazoan zooplankton-mediated carbon flows in nutrient-enriched coastal planktonic communities, Marine Ecology Progress Series, 331, 67-83, 2007.

Petersen, J. E., Cornwell, J. C., and Kemp, W. M.: Implicit scaling in the design of experimental aquatic ecosystems, Oikos, 85, 3-18, 1999.

Riebesell, U., Bellerby, R. G. J., Grossart, H. P., and Thingstad, F.: Mesocosm CO_2 perturbation studies: from organism to community level, Biogeosciences, 5, 1157-1164, 2008.

Riebesell, U., Lee, K., and Nejstgaard, J., C.: Pelagic mesocosms, in: Guide to best practices for ocean acidification research and data reporting, edited by: Riebesell, U., Fabry, V. J., Hansson, L., and Gattuso, J.-P., Publications Office of the European Union., Luxembourg, 95-112, 2010.

Riebesell, U., Czerny, J., Bröckel, K. v., Boxhammer, T., Büdenbender, J., Deckelnick, M., Fischer, M., Hoffmann, D., Krug, S. A., and Lentz, U.: Technical Note: A mobile sea-going mesocosm system - new opportunities for ocean change research, Biogeosciences, 10, 1835-1847, 2013.

Sanford, L. P.: Turbulent mixing in experimental ecosystem studies, Marine Ecology Progress Series, 161, 265-293, 1997.

Smetacek, V., von Bodungen, B., von Bröckel, K., and Zeitzschel, B.: The plankton tower. II. Release of nutrients from sediments due to changes in the density of bottom water, Marine Biology, 34, 373-378, 1976.

Strickland, J. D. H., and Terhune, L. D. B.: The study of in-situ marine photosynthesis using a large plastic bag, Limnology and Oceanography, 6, 93-96, 1961.

Strickland, J. D. H., Holm-Hansen, O., Eppley, R. W., and Linn, R. J.: The use of a deep tank in plankton ecology. I. Studies of the growth and composition of phytoplankton crops at low nutrient levels, Limnology and Oceanography, 14, 23-24, 1969.

Takahashi, M., Thomas, W. H., Seibert, D. L. R., Beers, J., and Koeller, P.: The replication of biological events in enclosed water columns, Archives of Hydrobiology, 76, 5-23, 1975.

Vadstein, O., Andersen, T., Reinertsen, H. R., and Olsen, Y.: Carbon, nitrogen and phosphorus resource supply and utilisation for coastal planktonic heterotrophic bacteria in a gradient of nutrient loading, Marine Ecology Progress Series, 447, 55-75, 10.3354/meps09473, 2012.

von Bröckel, K.: Sedimentation of phytoplankton cells within controlled experimental ecosystems following launching, and implications for further enclosure studies, in: Marine Mesocosms, Springer, 251-259, 1982.

Manuscript 2.1:

Technical Note: A mobile sea-going mesocosm system – new opportunities for ocean change research

Published in Biogeosciences

Biogeosciences, 10, 1835–1847, 2013
www.biogeosciences.net/10/1835/2013/
doi:10.5194/bg-10-1835-2013

Biogeosciences Open Access

Technical Note: A mobile sea-going mesocosm system – new opportunities for ocean change research

U. Riebesell, J. Czerny, K. von Bröckel, T. Boxhammer, J. Büdenbender, M. Deckelnick, M. Fischer, D. Hoffmann, S. A. Krug, U. Lentz, A. Ludwig, R. Muche, and K. G. Schulz

GEOMAR Helmholtz-Zentrum für Ozeanforschung Kiel, 24105 Kiel, Germany

Correspondence to: U. Riebesell (uriebesell@geomar.de)

Received: 23 August 2012 – Published in Biogeosciences Discuss.: 19 September 2012
Revised: 25 February 2013 – Accepted: 26 February 2013 – Published: 19 March 2013

Abstract. One of the great challenges in ocean change research is to understand and forecast the effects of environmental changes on pelagic communities and the associated impacts on biogeochemical cycling. Mesocosms, experimental enclosures designed to approximate natural conditions, and in which environmental factors can be manipulated and closely monitored, provide a powerful tool to close the gap between small-scale laboratory experiments and observational and correlative approaches applied in field surveys. Existing pelagic mesocosm systems are stationary and/or restricted to well-protected waters. To allow mesocosm experimentation in a range of hydrographic conditions and in areas considered most sensitive to ocean change, we developed a mobile sea-going mesocosm facility, the Kiel Off-Shore Mesocosms for Future Ocean Simulations (KOSMOS). The KOSMOS platform, which can be transported and deployed by mid-sized research vessels, is designed for operation in moored and free-floating mode under low to moderate wave conditions (up to 2.5 m wave heights). It encloses a water column 2 m in diameter and 15 to 25 m deep (~50–75 m^3 in volume) without disrupting the vertical structure or disturbing the enclosed plankton community. Several new developments in mesocosm design and operation were implemented to (i) minimize differences in starting conditions between mesocosms, (ii) allow for extended experimental duration, (iii) precisely determine the mesocosm volume, (iv) determine air–sea gas exchange, and (v) perform mass balance calculations. After multiple test runs in the Baltic Sea, which resulted in continuous improvement of the design and handling, the KOSMOS platform successfully completed its first full-scale experiment in the high Arctic off Svalbard (78°56.2′ N, 11°53.6′ E) in June/July 2010. The study, which was conducted in the framework of the European Project on Ocean Acidification (EPOCA), focused on the effects of ocean acidification on a natural plankton community and its impacts on biogeochemical cycling and air–sea exchange of climate-relevant gases. This manuscript describes the mesocosm hardware, its deployment and handling, CO_2 manipulation, sampling and cleaning, including some further modifications conducted based on the experiences gained during this study.

1 Introduction

Of the more than 260 scientific papers published until now on ocean acidification and its impacts on marine life less than 5 % have been conducted on communities or ecosystems, with the vast majority of studies performed on individual species (Gattuso and Hansson, 2011). Extrapolating from organism-based effects to community and ecosystem impacts is difficult, because the observed responses are typically obtained in the absence of competition, trophic interactions, and with low or no genetic diversity (Riebesell and Tortell, 2011). For the same reasons parameterizations of biological processes in ecosystem and biogeochemical models based on physiological responses of individual organisms are problematic. In benthic systems, natural high CO_2 environments, such as CO_2-venting sites, provide a powerful test bed to assess effects of ocean acidification at the community and ecosystem level. Studies at volcanic CO_2 vents have revealed drastic changes in benthic community composition and biodiversity when compared to adjacent areas not exposed to high CO_2 (Barry et al., 2011). Because of

lateral advection and mixing of water masses, CO_2-venting sites generally do not provide useful testing grounds to study ocean acidification impacts on pelagic communities (Riebesell, 2008). Oceanographic transects along natural CO_2 gradients, e.g. from temperate to high-latitude waters (Charalampopoulou et al., 2011) or from recently upwelled high-CO_2 waters downstream towards lower-CO_2 waters (Beaufort et al., 2011), offer the opportunity for community-level comparisons. Because of the many other environmental factors varying in concert with CO_2, the interpretation of observed biotic differences along those gradients is complex.

For pelagic systems mesocosms provide a powerful approach to maintain a natural community under close-to-natural self-sustaining conditions, taking into account relevant aspects from "the real world" such as indirect effects, biological compensation and recovery, and ecosystem resilience, which commonly are not accounted for in small-scale laboratory experiments (Riebesell et al., 2010). The mesocosm approach is therefore often considered the experimental ecosystem closest to the "real world", without losing the advantage of reliable reference conditions and replication (Petersen et al., 2003). The main advantages unique to mesocosm experimentation are as follows:

1. The ability to investigate community dynamics of three or more levels for an extended period of time.
2. The ability to measure the pools and fluxes of bio-active and particle reactive elements and compounds and to perform mass balance calculations in complex systems.
3. The ability to study interactions of ecosystem dynamics and biogeochemical processes under experimental conditions.
4. The ability to bring together scientists from a variety of disciplines, ranging from, e.g., molecular and evolutionary biology, ecophysiology, marine ecology and biogeochemistry to marine and atmospheric chemistry.

It needs to be acknowledged, however, that some constraints of enclosures are to be considered when extrapolating mesocosm results to natural systems (see Riebesell et al., 2010, for a review). Enclosures of all kinds are inherently limited in their ability to include higher trophic levels (e.g. fish, seabirds and mammals), and to approximate vertical mixing of water column and small-scale shear occurring in nature (Menzel and Steele, 1978; Carpenter, 1996). Enclosure effects may also influence food web dynamics to varying degrees, creating trophic interactions that can differ with mesocosm dimension and which may deviate from those of the natural system intended to be mimicked (Kuiper et al., 1983; French and Watts, 1989, Petersen et al., 2009). Despite these difficulties and the intense debate they have spurred over the past decades (e.g. Pilson and Nixon, 1980; Brockmann, 1990; Drenner and Mazumber, 1999), mesocosm enclosure studies still remain the most generally applicable means to experimentally manipulate and repeatedly sample multi-trophic planktonic communities.

Considering the wide range of topics in ocean change research where mesocosm experimentation could greatly advance our science, there are surprisingly few marine mesocosm facilities in operation. Moreover, existing facilities are either stationary or confined to well-protected waters, limiting their scope of application. Here we describe a newly developed sea-going mesocosm facility which can be used in moored and free-floating mode under low to moderate wave conditions (up to 2.5 m wave heights). The new design in combination with new developments in mesocosm handling and sampling are intended to optimize mesocosm performance, prolong the duration of mesocosm experiments, and perform mass balance calculations by accounting for all relevant pools and fluxes of elements and compounds of interest.

2 Material and methods

Most of the following description relates to the 2010 experiment off Svalbard. The corresponding sections are written in past tense. Some aspects of the mesocosm hardware and handling used in 2010 were modified in subsequent experiments. To avoid providing detailed descriptions of the KOSMOS approach for each new experiment, we have included descriptions of those modifications in this manuscript. To distinguish between aspects specific for the 2010 experiment and those applicable to KOSMOS hardware and handling in general, we will use past tense in the case of the former and present tense for the latter.

2.1 Mesocosm hardware

The Kiel Off-Shore Mesocosms for Future Ocean Simulations (KOSMOS) consist of 9 mesocosm units, which are operated independently. Each unit comprises a floatation frame, the mesocosm bag, a bottom shutter and sediment trap, a dome-shaped hood on top of the floatation frame, weights at the bottom of the floatation frame and the lower end of the bags to maintain an upright position when exposed to wind and wave activity, and various ropes needed for mesocosm operation. The total weight of each KOSMOS unit, including all components described below, is approximately 1.7 tons.

2.2 Floatation frame

The KOSMOS floatation frame consists of six 7.5 m-long, 30 cm-diameter closed glass fibre tubes which are fixed to a steel structure in the lower part and by a steel metal ring at the top end. Steel weights are attached to the horizontal junctions at the bottom of the steel structure. The diameter of the glass fibre tubes, which generate the buoyancy, is reduced at and above the waterline to lower the up- and downward movement of the floatation frame due to wave action.

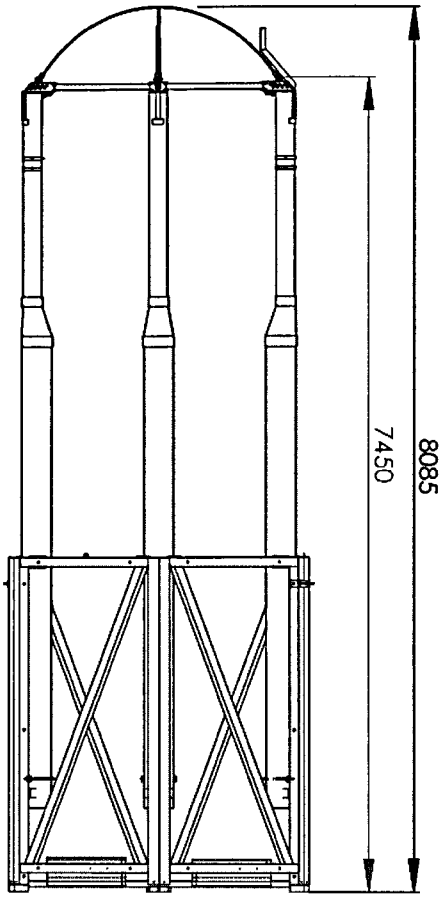

Fig. 1. Drawing of floatation frame with steel structure (lower part), glass fibre tubes for buoyancy, and steel ring at top, holding the dome-shaped PVC hoods. The tapering of the tubes in the above-surface section reduces buoyancy changes due to wave activity. Size indications in mm.

A dome-shaped roof made of polyvinyl chloride (PVC) covered with metal spikes is mounted on top of the floatation frame to reduce precipitation into the mesocosms and prevent seabirds from landing on the frame and defecating into the enclosures. The PCV foil has ca. 80 % light transparency in the spectral range > 400 nm wavelength. Below 400 nm the transparency strongly decreases, largely precluding the penetration of UV light. A flashlight with light sensor, solar panels and radar reflector is mounted on top of the frame, intended to alert passing ships. A set of clamps on either side of the frame above the waterline serves to fix various ropes needed to unfold, fix and operate the mesocosm enclosures (see mesocosm filling below). At the time of deployment the mesocosm bag is folded in a pack positioned above the water line (as displayed in Fig. 1).

2.3 Mesocosm bags

The enclosure bags are made of thermoplastic polyurethane (TPU) with a thickness of 1 mm in the upper 7 m and 0.5 mm below that. The bag diameter is 2 m. The length of the bag can be selected according to the scientific question and the conditions at the deployment location. For the 2010 experiment a total length of 17 m, 2 m above and 15 m below the water line, with a volume of approximately 50 m^3, was chosen. Follow-up experiments in the Raunefjord south of Bergen, Norway, in June/July 2011 used bag total lengths of 25 m, and off Hawaii in November/December 2011 and in the Finnish archipelago off Tvärminne in June to August 2012 19 m bag lengths. To maintain an approximately cylindrical shape of the mesocosm bags, rings of 2 m inner diameter made of 4 cm polyethylene pipes are positioned every 2 m in ring-shaped pockets made of TPU foil fixed onto the outside of the enclosure bag by high-frequency welding (Fig. 2).

Measurements of light intensities taken in parallel inside the mesocosms and outside in the fjord yielded similar surface layer light intensities and similar depth profiles in the PAR spectrum (see also Schulz et al., 2013). Light transparency measurements of the TPU foil revealed nearly 100 % absorbance of UV light. This together with the low light transparency below 400 nm of the PVC roof resulted in negligible UV light intensities inside the mesocosms.

2.4 Bottom shutter and sediment trap

At the bottom of the enclosure bag a steel ring holds two semi-circle plates made of 10 mm-thick Makrolon®. The plates are in upright position to allow water to enter the mesocosm bags during the lowering and unfolding of the bags (Fig. 3, left panel). A 2 m-long funnel-shaped sediment trap with a mouth of the same diameter as the mesocosm bag is connected to one of the bottom lids. It is tightly folded and attached between the bottom plates and unfolds and stretches automatically through an air-filled ring at the upper end of the funnel immediately after the bottom plates are closed (Fig. 3, right panel). A silicon tube connects to the lower end of the funnel from below the bottom lids and extends to the water surface on the outside of the mesocosms (Fig. 4). Material collected in the sediment trap is regularly sampled via this tube, using a manual vacuum pump system. Processing of the samples included sub-sampling for zooplankton counting, followed by concentrating the residual sediment material, freeze-drying, grinding and homogenizing for subsequent chemical analysis.

The sediment trap as described here created a "dead volume" underneath the funnel of approximately 8 % of the enclosure volume. Because this water gradually exchanged with the rest of the enclosed water over one to two days, there was a dilution effect after experimental manipulations such as CO_2 enrichment and nutrient addition. This complicated determining precisely the start value of the applied

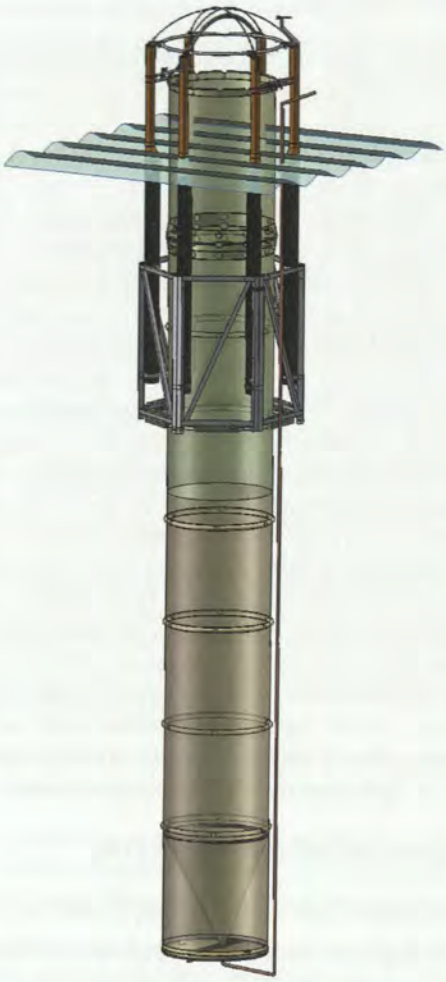

Fig. 2. Sketch of floatation frame with unfolded TPU enclosure bag; different colouring of the light-transparent bag indicates difference in TPU foil thickness: green, 1 mm; brown, 0.5 mm. The blue rippled plane represents the water line. At the bottom of the bag above the bottom plate the funnel-shaped sediment trap is indicated. The red line extending from the tip of the sediment trap to the water surface represents the tube used for sampling of sedimented matter.

manipulation. To avoid the dilution effect, a new sediment trap was designed after the 2010 campaign and applied in all later studies. This new trap is connected to the bottom of the mesocosm through a flange (Fig. 4). Mounted by divers after the filling of the bag, the trap closes off the mesocosm at the bottom end.

2.5 Mooring and deployment

The mesocosms can be operated in moored or free-floating mode. When moored, the mesocosms are deployed in groups of three at a distance of 30 to 50 m between mesocosm units (Fig. 5). Units of each group are connected to each other through ropes fixed to the floating frames at 2.5 m water depth. The groups are separated by approximately

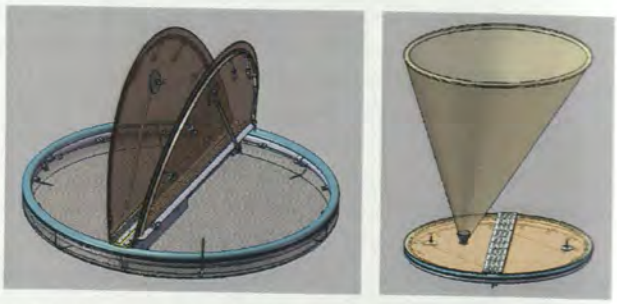

Fig. 3. Sketches of bottom plate. Left: lids in upright position, as applied during filling of the enclosure bags. A removable net (grey shaded area) with a mesh size of 3 mm is mounted below the bottom ring. Each bottom plate is equipped with 8 screws for tightening the lids after closing. Right: bottom plate in closed position with unfolded sediment trap.

Fig. 4. Left: sketch of sediment trap used in 2011 and 2012 campaigns. The funnel-shaped trap made of TPU foil is connected to the bottom of the enclosure bag via a flange (right panel). Note the tapering of the lowest section of the mesocosm bag. Sampling of sedimented matter is achieved via a silicon tube which connects to a 5 L sampling flask and a hand-operated vacuum pump. Right: flange ring made of laminated fibreglass to attach the external sediment trap to the lower end of the enclosure bag. The upper ring (connected to the bag) is equipped with steel weights to facilitate the sinking of the enclosure bag during mesocosm filling and to keep the bag in vertical position when exposed to currents. Bag and sediment trap are fixed to the upper and lower flanges by stainless steel clamps pressing the TPU foil in notches. Upper and lower flanges are connected with eight screws and sealed with a silicon rubber fitting.

50 m between each group and anchored on both ends with weights (1.2 tonnes) consisting of railway wheels. Buoys are mounted between mesocosms and the anchor weights to ensure that the downward pull generated by strong currents is absorbed by the buoys rather than acting directly on the mesocosms. When operated in moored mode, the water currents acting on the mesocosms should not exceed 0.5 knots to avoid strong vertical deflection of the mesocosm bags and wearing on the ropes. In free-floating mode, as applied in the 2011 campaign off Hawaii, a drogue was connected to one

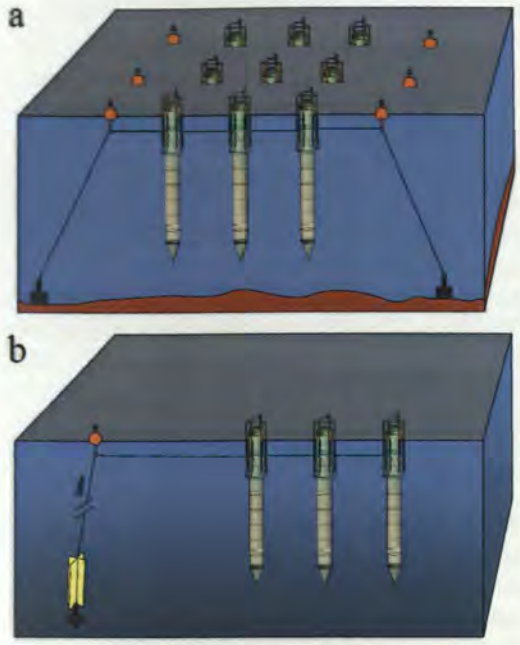

Fig. 5. Schematic drawing of the two modes of mesocosm operation: **(a)** mesocosms in moored mode in packs of three with anchor weight at each end as used in the Svalbard 2010 study; **(b)** mesocosms in free-floating mode connected to a weighted drogue hanging from a buoy at 150 m water depth. This approach was first tested in the 2011 campaign off Hawaii.

end of the three mesocosms. The weighted drogue was hanging from a large buoy at 150 water depth and thereby was exposed to water currents deviating from those at the surface. It served to generate a steady drag at one end of the mesocosm array in order to keep the mesocosms apart and in a straight line. In this mode there is no limit on the acceptable speed of water currents.

2.6 Filling and closing

The filling of the mesocosms started after all mesocosms were moored in position. For this the enclosure bags were untied at the bottom, allowing the weighted lower end of the bags to sink through the water column with open shutters until the bags were completely unfolded. With this approach the mesocosms were filled with minimal disturbance of the enclosed water body. To avoid capturing large organisms (e.g. fish, jelly fish) a removable net with a mesh size of 3 mm was mounted across the bottom opening. Several teams were involved in filling the mesocosms in parallel in close succession to reduce the effect of changing water masses due to lateral advection during the filling process. Nevertheless, because the mesocosms were not all filled simultaneously and because of possible small-scale patchiness in the plankton community (i.e. smaller than the distance between individual mesocosms), there was a risk of differences between enclosed water bodies in terms of seawater chemistry and plankton community abundance and composition. This could have caused large inter-mesocosm variability during the experiment. To minimize differences in starting conditions between enclosed water bodies, the mesocosms were left open for free exchange with the surrounding water for 48 h after filling. For this the bottom shutters were kept open and the upper part of the bags lowered to 1.5 m below the water surface with the top and bottom opening covered with a net of 3 mm mesh size. Test runs during previous years with dyes injected into the mesocosms indicated that, depending on bag length and current speed, a complete exchange of the enclosed water body occurs within 2–3 days. By gradually exchanging the enclosed and surrounding water masses, it is insured that spatial patchiness is averaged out over time. While the mesocosms were open for water exchange, frequent measurements were conducted for several chemical and biological parameters to test for differences between mesocosms. The absence of detectable differences in these parameters was a precondition for mesocosm closing.

The exchange between mesocosms and surrounding water was terminated by lifting the upper parts of the bags above the surface and having divers close the bottom plates. At this point the top and bottom nets are removed. With the closing of the bottom shutters the sediment trap, folded and fixed between the two bottom plates, unfolds and rises through an air-filled ring until fully extended (Figs. 2 and 3). The closing of the mesocosms marks the beginning of the experimental period.

As described above, bottom plate and internal sediment trap were replaced by a flange-connected external sediment trap after the 2010 campaign. In the following campaigns the sediment traps were put in place by divers after the full extension of the enclosure bags. In this new design the sediment trap also has the function of closing off the bottom of the bags. The sediment trap is put in place in two steps: initially it is connected by a hinge integrated in the flange (see Fig. 7, left side of the flange). At this stage the sediment trap is hanging parallel to the mesocosm bag, held by the hinge and tied to the first support ring. In a second step (e.g. on the following day), divers turn the lower flange ring in horizontal position to fully connect with the upper flange ring, thereby expending the TPU foil forming the funnel of the sediment trap. The two flange rings are tightly connected by 8 screws. As before, the mesocosms are closed by divers after 2–3 days of open exchange between mesocosm and surrounding water. After mounting of the sediment trap, three 5 kg weights are mounted at its lower end to keep the funnel stretched. A hose connected to the bottom of the funnel and reaching above the water surface is used for sampling of the sedimented material (Fig. 4).

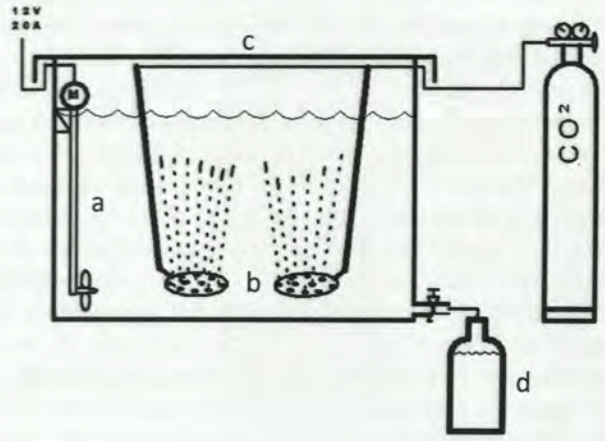

Fig. 6. Schematic drawing of the setup used for the preparation of CO_2-enriched water. An electric outboard motor **(a)** continuously mixed the water in the 1.4 m^3 polypropylene tank which was tightly closed by a lid **(c)**. Two large aerating disks **(b)** produced fine bubbles ensuring relatively low gas consumption. After aeration, the CO_2-enriched water was filled into 25 L polycarbonate carboys **(d)** for transport and quantitative addition into the mesocosms, using the "spider".

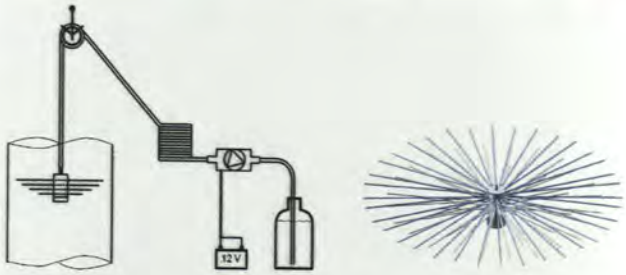

Fig. 7. Left: sketch of setup used for CO_2 manipulation. CO_2-enriched water is pumped from 25 L carboys via a garden hose into the "spider", which is gradually moved up and down over the entire length of the enclosure bag by manually heaving and hauling it via a pulley fixed above the centre of the enclosure bags underneath the hood. Right: the dispersion device ("spider") is composed of a polyoxymethylen body weighted with a 5 kg stainless steel stand. It has 84 jets (Ø 500 µm) of which 78 are equipped with elastic acryl branches of different lengths distributing the liquid evenly over a horizontal cross-section of the mesocosm. The diameter of the jets serves as a bottleneck, releasing ~ 80 mL min^{-1} of liquid dispensed through every jet irrespective of the length of the branch connected to it.

2.7 CO_2 and nutrient manipulation

CO_2 enrichment was carried out by adding CO_2-enriched fjord water into the mesocosms. The addition of CO_2-enriched seawater increases dissolved inorganic carbon (DIC) while leaving total alkalinity constant, perfectly mimicking on-going ocean acidification (cf. Schulz et al., 2009, Gattuso et al., 2010). With 9 mesocosms available for this study, the choice was made to apply a CO_2 gradient with 8 different CO_2 levels, duplicating only the ambient CO_2 conditions without CO_2 manipulation (considered as control). This approach involves the use of regression statistics for assessment of possible CO_2 effects. This choice was made for the following reasons:

(a) Because of the low number of experimental units available and considering the risk of losing one or several mesocosms (e.g. due to damage by ice floats), a CO_2-gradient approach carries a lower risk of failure compared to a replicated approach (e.g. 3 CO_2 treatments with triplicates each) relying on ANOVA statistics.

(b) If there is a threshold level for any of the CO_2/pH sensitive processes, a CO_2-gradient approach has a higher chance of detecting it.

(c) With a CO_2-gradient approach the opportunity arises to include one or two CO_2 levels outside the range recommended for ocean acidification perturbation experiments (Barry et al., 2010), which would be more difficult to justify if such extreme levels were replicated.

(d) Although CO_2 manipulation is relatively straightforward, it is challenging to precisely achieve the targeted CO_2 levels. While critical in a replicated approach, in a CO_2-gradient approach deviations from the targeted CO_2 levels can be tolerated.

It was decided to replicate the ambient CO_2 level (control treatment) in order to minimize the risk of completing the experiment with no control in case of losing one or several mesocosm units. The different CO_2 levels were randomly interspersed among the 9 mesocosms (cf. Riebesell et al., 2010).

The CO_2-enriched seawater was prepared in a 1.4 m^3 tank on land filled with filtered (pore size 20 µm) fjord water which was stirred by an electric propeller while aerated with pure CO_2 gas for approximately 24 h (Fig. 6). At this stage the CO_2 partial pressure in the water was close to saturation (pH ~ 4.4).

The DIC concentration in the CO_2-enriched water was calculated based on measurements of total alkalinity, pH (presented in total scale unless stated otherwise), salinity and temperature, using the computer program CO_2SYS (Lewis and Wallace, 1997). Based on this the amount of CO_2-enriched water needed to achieve the target pCO_2 levels in the different CO_2 treatments was calculated. The CO_2-enriched water was filled into 25 L carboys and transported to the mesocosms. Depending on target pCO_2, between 0 and 320 L (see Schulz et al., 2013) of the CO_2-enriched seawater was injected into the mesocosms by means of a membrane pump and a dispensing device (termed "spider"; Fig. 7, right panel). To achieve an even distribution of the CO_2-enriched water throughout the mesocosms, the "spider" was

slowly moved up and down during the injection over the entire length of the enclosure bags (Fig. 7, left panel). Vertical pH profiles were conducted after CO_2 additions to check whether an even distribution was achieved.

The injection of CO_2-enriched water was done in steps over 4 consecutive days starting in the afternoon of 6 June (t-1). Two mesocosms served as controls, while 7 mesocosms were manipulated to establish treatments of elevated pCO_2 with an initial range of 185–1420 µatm. Mean values of pCO_2 during the experimental period ranged from 175–1085 µatm (for details see Bellerby et al., 2012). In mesocosms with no or low addition of CO_2-enriched water, similar amounts of filtered fjord water were added in order to apply the same physical perturbation to all mesocosms. Some fine-tuning to reach target CO_2 levels was conducted on 11 June (t4), at which time the target pCO_2 levels where reached with an offset generally smaller than ±50 µatm. After this no further CO_2 manipulation was done in any of the mesocosms. Because of the slow exchange of water in the "dead volume" below the sediment trap with that in the rest of the enclosure bag, there was a dilution of the initial CO_2 enrichment due to mixing of the CO_2 manipulated (open bag) and non-manipulated ("dead volume") water during the first couple of days. Budget calculations based on carbonate chemistry measurements starting after CO_2 manipulations needed to account for this dilution effect (Czerny et al., 2012a, 2013; de Kluijver et al., 2013; Silyakowa et al., 2013).

In the early morning of 20 June (t13), inorganic nutrients were added using the same dispersion device as described above and shown in Fig. 7 at concentrations of 5 µmol L^{-1} NO_3, 0.32 µmol L^{-1} PO_4, and 2.5 µmol L^{-1} Si. The precise amounts of inorganic nutrients added to each mesocosm were calculated based on volume determinations conducted for all mesocosms through salt additions on 3 June (t4) and 11 June (t4). For a detailed description of the volume determination see Czerny et al. (2012b).

Approximately 200 live adult pteropods (*Limacina helicina)* sampled individually from the fjord were added to each mesocosm during 11–13 June (t4–t6) to study their response to ocean acidification. For unknown reasons the pteropods rapidly disappeared from the water column. Some pteropods were collected in the sediment traps; others were seen by divers accumulating in the dead volume underneath the sediment traps. Very few specimen survived the experiment.

2.8 Cleaning of the mesocosm walls

To estimate the contribution of wall growth to the overall production and accumulation of particular organic matter (POM) in the mesocosms, the inside of the enclosure bags was cleaned with a ring-shaped brush on 7 July (t30). Various biological parameters were determined on suspended particulate matter immediately before and after brushing of the walls to quantify the amount of biomass released into the water column. As reported in Czerny et al. (2012a) on average 16 % of the nitrate and 32 % of the phosphate added on t13 had accumulated on the mesocosm walls due to biofilm formation on t30. In follow-up campaigns, the formation of biofilms on the inside of the enclosure bags (wall growth) was prevented by regular cleaning (once per week) with a ring-shaped, double-bladed wiper using a similar configuration as depicted in Fig. 8.

Fig. 8. Ring-shaped brush used for cleaning the inside of the enclosure walls. The brush is pulled downwards by a weight attached by ropes below the ring and pulled upwards manually by a rope run over a pulley fixed above the centre of the enclosure bags underneath the hood. In follow-up experiments the brush was replaced by a double-bladed wiper.

2.9 Sampling

Vertical profiles of temperature, conductivity, pH, oxygen, fluorescence, turbidity and light intensity were taken daily in each mesocosm and the surrounding water between 14:00 and 16:00 LT with a CTD60M (Sun and Sea Technologies). Sampling of seawater from the mesocosms was conducted with a depth-integrating water sampler (Hydro-Bios). The sampler is equipped with a pressure-controlled motor and continuously collects water (5 L volume) while being lowered from the surface to 12 m depth. Samples were collected in the morning between 9:00 and 11:00 In addition discrete samples were taken at fixed depths using Niskin bottles and pumping systems with sampling tubes lowered into the mesocosms (for details see M&M in the corresponding manuscripts). For measurements of DIC, total alkalinity, N_2O, inorganic nutrients, dissolved organic matter, volatile organic compounds, oxygen incubations, and other samples sensitive for contamination and gas exchange, subsamples

Table 1. Starting conditions in the nine mesocosms (M1-M9) and the surrounding fjord water. Data for salinity, pH and oxygen concentration (determined in situ with a CTD equipped with pH and oxygen sensors) for day t-4, all others for day t0. pH is in total scale, concentrations for oxygen, nitrate, ammonium, phosphate and silicate are in $\mu mol\,L^{-1}$. See Schulz et al. (2013) for details on the methodologies.

	M1	M2	M3	M4	M5	M6	M7	M8	M9	Fjord
Salinity	33.90	33.90	33.90	33.91	33.91	33.90	33.90	33.93	33.93	33.58
pH	8.36	8.36	8.37	8.35	8.36	8.35	8.37	8.37	8.39	8.36
O_2	466	462	461	462	460	460	462	463	466	476
NO_3^-	0.03	0.03	0.02	0.03	0.01	0.01	0.02	0.02	0.03	0.01
NH_4^+	0.59	0.59	0.60	0.60	0.59	0.59	0.49	0.59	0.69	0.22
PO_4^{3-}	0.04	0.05	0.05	0.06	0.05	0.06	0.05	0.06	0.06	0.04
$Si(OH)_4$	0.15	0.16	0.15	0.17	0.12	0.12	0.12	0.10	0.12	0.23

were taken directly from the depth-integrating samplers in a fixed order. For bulk measurements of suspended particulate matter, photosynthetic pigments, biogenic silica, phyto- and microzooplankton abundance and composition, and various other components (see M&M in the corresponding manuscripts), the depth-integrated samples were transferred to 10 L polyethylene containers which were kept in a dark cold room at in situ temperature for later subsampling.

Net hauls were done about once a week (for details see Niehoff et al., 2013). To minimize the effect of zooplankton catches on the plankton abundance and composition, the cross-sectional area sampled by the sum of all net hauls conducted over the course of the experiment was kept to less than one-sixth of the total cross-sectional area of the enclosure bags.

All sampling gear and sensors were plunged into fjord water next to the sampling boats before being deployed in the mesocosms to avoid contamination by adhering materials. All instruments were cleaned with fresh water when returning to land.

3 Results

A mesocosm CO_2-enrichment experiment was conducted in Kongsfjorden on the north-west coast of Spitsbergen (Fig. 9) between 31 May and 8 July 2010. Nine sea-going mesocosms were loaded in Kiel and deployed on the southern shore of Kongsfjorden near Ny-Ålesund at 78°56.2′ N und 11°53.6′ E (Fig. 10) by M/V *Esperanza* of Greenpeace International on 31 May (t-7). Before mesocosm deployment mooring weights were laid out by R/V *Viking Explorer* of the University Centre in Svalbard (UNIS). Upon deployment the mesocosms were towed to the mooring site by small boats and tied in three groups of three mesocosms each as indicated in Fig. 10.

3.1 Conditions in the fjord

At the time of mesocosm deployment Kongsfjorden off Ny-Ålesund was ice-free, while parts of the inner fjord were covered by sea ice. During the course of the study, the sea ice broke off and the glaciers surrounding Kongsfjorden started to calve. Floats of sea ice and glacier ice drifted towards the mouth of the fjord starting in mid-June. Most of the ice transport occurred along the northern side of the fjord, i.e. on the opposite side of the mesocosm mooring, following the general current pattern in the fjord system. At times of persistent north to north-east winds some ice floats occasionally drifted towards the mesocosm array. A 24 h ice watch was on duty for the duration of the experiment. In a few cases ice floats needed to be pushed out of their path by small boats to avoid collision with the mesocosms.

The initial pCO_2 of the ambient water in the fjord was ~ 175 µatm, corresponding to a pH of ~ 8.3 (Bellerby et al., 2012). Concentrations of mineral nutrients in the water were close to detection limit at the beginning of the experiment (0.11 $\mu mol\,L^{-1}$ of nitrate, 0.7 $\mu mol\,L^{-1}$ of ammonia, 0.13 $\mu mol\,L^{-1}$ of phosphate). Additionally, there were 5.5 $\mu mol\,L^{-1}$ of dissolved organic nitrogen, 0.20 $\mu mol\,kg^{-1}$ of dissolved organic phosphorus (Schulz et al., 2013) and 75 $\mu mol\,L^{-1}$ of dissolved organic carbon (Engel et al., 2013). Reduced pCO_2 and inorganic nutrient concentrations as well as increased concentrations of organic carbon, nitrogen and phosphorus indicated a post-bloom situation in the fjord at the start of the experiment.

3.2 Conditions in the mesocosms

Comparing the initial conditions after closing of the mesocosms provided an indication of the similarity between bags at the start of the experiment. As indicated in Table 1, the chemical conditions were almost identical in all mesocosms. Small differences between mesocosms and the surrounding fjord water were due to changing water masses in the fjord after closing the bags. Close agreement also exists for phytoplankton biomass and taxonomic composition (Table 2). Differences in group-specific chlorophyll *a* equiva-

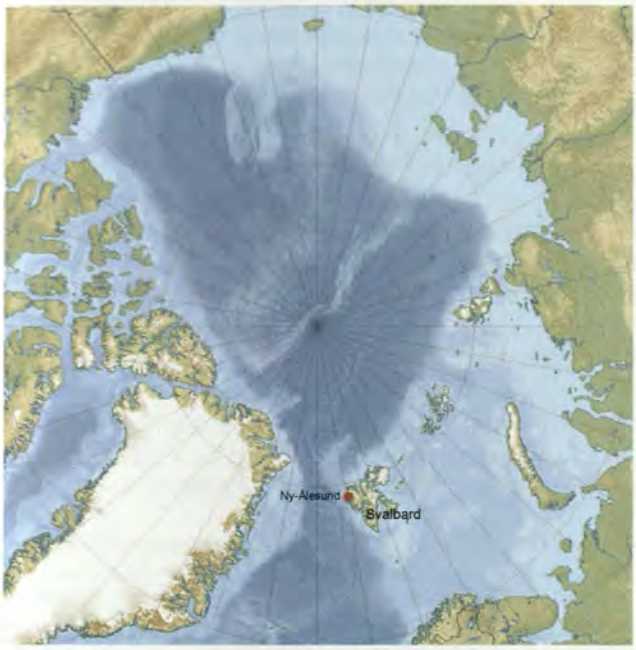

Fig. 9. Map of the Arctic. Red dot denotes the location of the study site (Kongsfjorden, Ny-Ålesund) on the north-west coast of Spitsbergen, the largest island of the Svalbard archipelago. Source: Wikipedia.

Fig. 10. Map of Kongsfjorden on the north-west coast of Svalbard. Insert shows the study area with the location and orientation of the mesocosm array. Source of map: Norsk Polarinstitutt.

lent concentrations between mesocosms for some of the taxonomic groups are more pronounced for those with predominantly large cell sizes combined with low abundances, such as diatoms and dinoflagellates. This difference is most likely due to a sampling bias rather than a true representation of biomass differences in the mesocosms. Almost identical concentrations in all mesocosms are obtained for bacteria and total virus counts (Table 2). Overall, the resemblance in initial values for a variety of chemical and biological parameters suggests proper conditions for the start of the experiment.

3.3 Temporal development

A short temporary increase in phytoplankton biomass during the first part of the experiment was probably fuelled by utilization of organic nutrients. Half way through the experiment inorganic nutrients were added to the mesocosms stimulating two additional phytoplankton blooms.

Based on the manipulations carried out over the course of the study, the deployment period is divided into 4 phases, one pre-experimental phase (phase 0) and three experimental phases (phases 1–3) as follows:

- phase 0: closing of the mesocosms until end of CO_2 manipulation (t-4 to t4),
- phase 1: end of CO_2 manipulation until nutrient addition (t5 to t12),
- phase 2: nutrient addition until 2nd chlorophyll minimum (t13 to t21),
- phase 3: 2nd chlorophyll minimum until end of experiment (t22 to t30).

The temporal changes in phytoplankton biomass and community composition observed in the mesocosms follow the same basic trends as those recorded in the waters surrounding the mesocosms (Brussaard et al., 2013; Schulz et al., 2013). Considering that lateral advection caused the water surrounding the mesocosms to exchange rapidly, the close agreement between enclosed and ambient plankton community development seems quite remarkable. This indicates that (1) major trends in plankton development persisted independent of small-scale patchiness in the study area and (2) the enclosed plankton community mimics the natural system reasonably well in terms of major developments in biomass and composition. The close agreement starts to weaken after nutrient addition in the mesocosms.

Aside from providing a comprehensive data set on plankton community responses to ocean acidification and their impacts on biogeochemical cycling, the study offered the opportunity for consistency checks between individual measurements. Particularly enlightening in this respect was the comparison of different approaches determining net community production, which was obtained from bottle incubations measuring O_2 production/consumption (Tanaka et al., 2013), estimates of changes in DIC concentration (Silyakowa et al., 2013), and incorporation of ^{13}C tracer added directly into the mesocosms (de Kluijver et al., 2013). These estimates were further compared with ^{14}C incorporation determined in bottle incubations (Engel et al., 2013). While at first sight the different approaches appeared to yield different rates and – more surprisingly – different relationships

Table 2. Concentrations of chlorophyll *a* equivalent (in ng L^{-1}) for eight taxonomic groups of phytoplankton determined from HPLC measurements using CHEMTAX and bacterial and viral numbers (10^6 mL^{-1}) measured by flow cytometry for day t0. See Schulz et al. (2013) for details on methodologies. Abbreviations for taxonomic groups refer to prasinophyceae, dinophyceae, crytophyceae, chlorophyceae, cyanophyceae, bacillariophyceae, chrysophyceae, and haptophyceae.

	M1	M2	M3	M4	M5	M6	M7	M8	M9	Fjord
Prasino	45.8	45.8	49.1	55.5	58.6	41.5	66.8	54.5	48.9	71.5
Dino	0	0.4	8.1	10.1	0	27.4	8.2	13.1	4.6	12.2
Crypto	25.2	15.5	19.7	34.6	45.6	23.1	29.5	20.7	18.3	73.3
Chloro	18.8	0	0	10.0	1.4	27.2	40.8	43.5	38.3	56.9
Cyano	29.9	31.3	41.4	41.4	44.2	36.5	28.3	22.2	38.7	37.2
Bacillario	28.4	18.5	27.7	31.4	31.8	19.6	37.2	15.3	35.7	97.8
Chryso	6.4	2.6	5.1	5.0	3.0	4.5	5.8	5.1	7.3	3.4
Hapto	28.0	65.4	28.7	35.1	51.3	25.3	16.1	25.4	19.7	18.5
Bacteria	2.0	2.1	2.0	2.1	2.0	2.1	2.2	2.0	2.0	1.7
Viruses	61.4	53.5	54.2	58.0	48.4	53.3	49.3	58.3	53.9	52.4

with CO_2 concentration, closer examination yielded some interesting insights into the underlying processes and eventually resulted in a coherent interpretation of plankton community responses to ocean acidification (see discussions in references cited above).

4 Discussions

4.1 The study area

The Arctic Ocean ecosystem is expected to undergo major climate-change-related transformations in the coming decades, ranging from surface layer warming and freshening to enhanced stratification and loss of sea ice. Due to the high CO_2 solubility and low carbonate saturation states of its cold surface waters, the Artic Ocean is also considered particularly vulnerable to ocean acidification. If CO_2 emissions continue to rise at current rates, half of the Artic Ocean will be undersaturated with respect to calcium carbonate and, therefore, corrosive for calcareous organisms within the next three to four decades (Steinacher et al., 2009). While several Arctic calcifying species have been shown to respond negatively to ocean acidification (e.g. Büdenbender et al., 2011; Comeau et al., 2009; Lischka et al. 2011; Walther et al., 2010; Wood et al., 2011), little is known about possible consequences of ocean acidification at the base of the Arctic food web. The experiment described here was intended as a first attempt at closing this gap by conducting a pelagic mesocosm CO_2-enrichment study in Kongsfjorden on the western coast of Spitsbergen – about 1000 nautical miles south of the North Pole.

Kongsfjorden, an open fjord system without sill, is about 26 km long and between 4 and 10 km wide, with a maximum depth of 400 m. The water in Kongsfjorden is influenced by (i) Arctic water masses transported by the coastal current flowing from the Barents Sea over the West Spitsbergen Shelf, (ii) Atlantic water masses coming in with the northbound West Spitsbergen Current, and (iii) freshwater input from calving and melting glaciers as well as precipitation (Hop et al., 2006). Discharge of freshwater and sediments from the adjacent glaciers strongly varies seasonally, peaking in the summer. During winter, the inner part of the fjord is covered by sea ice , with large interannual variability in ice thickness, time of formation and break-up (see Svendsen et al., 2002, for a detailed review of the physical environment of the Kongsfjorden area).

In the fjord the initiation of the phytoplankton spring bloom starts already under ice cover, culminating between April and early June after ice break-up (Eilertsen et al., 1989). The majority of studies conducted on the plankton community in Kongsfjorden focused on the spring period when high nutrient availability and increasing light levels support a substantial fraction of the annual primary production (Iversen and Seuthe, 2011; Seuthe et al., 2011). After the spring bloom, phytoplankton biomass remains moderately high during late spring and summer (Hop et al., 2002). At this time of the year, the plankton community is typically characterized by an efficient microbial loop (Iversen and Seuthe, 2011) that provides inorganic nutrients to phytoplankton and bacteria through rapid organic matter remineralization. These were the conditions encountered at the start of this mesocosm campaign. Accordingly, pico- and nanophytoplankton groups were the dominant autotrophs during the first part of this study (Brussaard et al., 2013). Due to the low seed population of dinoflagellates and diatoms, the dominance of pico- and nano-sized phytoplankton continued even after nutrient addition. The standing stock of microphytoplankton was building up slowly and dominated phytoplankton biomass only towards the end of the experiment (Schulz et al., 2013).

4.2 KOSMOS experimental facility

After a sequence of test runs in free-floating mode conducted in the Baltic Sea in 2006, 2007, and 2008, which led to considerable improvements in the mesocosm hardware and handling, and a four-week trial run in moored mode in 2009, which yielded some novel results on ocean acidification effects during a phytoplankton spring bloom (Schulz and Riebesell, 2012), the Svalbard 2010 campaign was the first full-scale experiment involving nine mesocosm units and covering a broad range of parameters over an extended period of time. Building on the experience gained during this campaign, this new sea-going experimental platform opens up new opportunities for mesocosm experimentation under a variety of hydrographic conditions and geographical locations. Important new features of this facility include

- the enclosure of large volumes (45–75 m^3) with minimal disturbance of the enclosed water body and plankton community,
- controlled carbonate chemistry manipulation with minimal agitation of the enclosed water,
- mass balance calculations through precise determination of mesocosm volume by full accounting of all relevant pools and fluxes for key elements (carbon, nitrogen, phosphorus, silica),
- extended experimental duration through routine cleaning of mesocosm walls (preventing extensive wall growth) and regular sediment sampling (preventing release of remineralization products from sedimented matter),
- operation in moored and free-floating mode under low to moderate wave conditions allowing mesocosm experimentation in areas previously not amendable to this kind of experimentation.

This mesocosm campaign, which involved 35 scientists from 12 institutes, provided the opportunity for a highly integrative, multidisciplinary study involving marine engineers, molecular and marine biologists, ecologists, biogeochemists, and marine and atmospheric chemists. By covering a wide range of parameters measured over 35 days (4 days prior to and 31 days after the start of CO_2 manipulation), it provided a comprehensive data set on pelagic community-level responses to ocean acidification and their impacts on nutrient cycling and air–sea exchange of climate-relevant gases.

Acknowledgements. The design, construction and field testing of the KOSMOS mesocosms was made possible through financial support of GEOMAR and the integrated project SOPRAN (Surface Ocean PRocesses in the ANthropocene) funded by the German Ministry for Education and Research (BMBF). GEOMAR and SOPRAN provided the KOSMOS facility for the Svalbard 2010 experiment and organized the logistics leading up to and during the experiment. GEOMAR was responsible for deploying the mesocosms, running the experiment and coordinating all scientific aspects before, during and after the experiment. The scientific work is a contribution to the European Project on Ocean Acidification (EPOCA), which received funding from the European Community's Seventh Framework Programme (FP7/2007–2013) under grant agreement no. 211384. Several participants of this study received funding from the European Community's Seventh Framework Programme under grant agreement no 228224, MESOAQUA. We gratefully acknowledge the logistical support of Greenpeace International for its assistance with the transport of the mesocosm facility from Kiel to Ny-Ålesund and back to Kiel. We also thank the captains and crews of M/V *Esperanza* of Greenpeace and R/V *Viking Explorer* of the University Centre in Svalbard (UNIS) for assistance during mesocosm transport and during deployment and recovery in Kongsfjorden. We thank the staff of the French-German Arctic Research Base (AWIPEV) at Ny-Ålesund, in particular Marcus Schumacher, for on-site logistical support.

The service charges for this open access publication have been covered by a Research Centre of the Helmholtz Association.

Edited by: J. Middelburg

References

Barry, J. P., Widdicombe, S., and Hall-Spencer, J. M.: Effects of ocean acidification on marine biodiversity and ecosystem function, in: Ocean acidification, edited by: Gattuso J.-P. and Hansson L., Oxford University Press, 192–209, 2010.

Barry, J. P., Tyrrell, T., Hansson, L., Plattner, G.-K., and Gattuso, J.-P.: Atmospheric CO_2 targets for ocean acidification perturbation experiments, in: Guide to best practices in ocean acidification research and data reporting, edited by: Riebesell, U., Fabry, V., Hansson, L., and Gattuso, J.-P., Office for Official Publications of the European Communities, Luxembourg, 53–66, 2011.

Beaufort, L., Probert, I., de Garidel-Thoron, T., Bendif, E. M., Ruiz-Pino, D., Metzl, N., Goyet, C., Buchet, N., Coupel, P., Grelaud, M., Rost, B., Rickaby, R. E. M., and de Vargas, C.: Sensitivity of coccolithophores to carbonate chemistry and ocean acidification, Nature 476, 80–83, 2011.

Bellerby, R. G. J., Silyakova, A., Nondal, G., Slagstad, D., Czerny, J., de Lange, T., and Ludwig, A.: Marine carbonate system evolution during the EPOCA Arctic pelagic ecosystem experiment in the context of simulated Arctic ocean acidification, Biogeosciences Discuss., 9, 15541–15565, doi:10.5194/bgd-9-15541-2012, 2012.

Brockmann, U.: Pelagic mesocosms: II. Process studies, in: Enclosed experimental marine ecosystems: A review and recommendations, edited by: C. M. Lalli, Springer-Verlag, New York, 81–108, 1990.

Brussaard, C. P. D., Noordeloos, A. A. M., Witte, H., Collenteur, M. C. J., Schulz, K., Ludwig, A., and Riebesell, U.: Arctic microbial community dynamics influenced by elevated CO_2 lev-

els, Biogeosciences, 10, 719–731, doi:10.5194/bg-10-719-2013, 2013.

Büdenbender, J., Riebesell, U., and Form, A.: Calcification of the Arctic coralline red algae *Lithothamnion glaciale* in response to elevated CO_2, Mar. Ecol. Progr. Ser., 441, 79–87, 2011.

Carpenter, S. R.: Microcosm experiments have limited relevance for community and ecosystem ecology, Ecology, 77, 677–680, 1996.

Charalampopoulou, A., Poulton, A. J., Tyrrell, T., and Lucas, M. I.: Irradiance and pH affect coccolithophore community composition on a transect between the North Sea and the Arctic Ocean, Mar. Ecol. Progr. Ser., 431, 25–43, 2011.

Comeau, S., Gorsky, G., Jeffree, R., Teyssié, J.-L., and Gattuso, J.-P.: Impact of ocean acidification on a key Arctic pelagic mollusc (Limacina helicina), Biogeosciences, 6, 1877–1882, doi:10.5194/bg-6-1877-2009, 2009.

Czerny, J., Schulz, K. G., Boxhammer, T., Bellerby, R. G. J., Büdenbender, J., Engel, A., Krug, S. A., Ludwig, A., Nachtigall, K., Nondal, G., Niehoff, B., Siljakova, A., and Riebesell, U.: Element budgets in an Arctic mesocosm CO_2 perturbation study, Biogeosciences Discuss., 9, 11885–11924, doi:10.5194/bgd-9-11885-2012, 2012a.

Czerny, J., Schulz, K. G., Krug, S. A., Ludwig, A., and Riebesell, U.: Technical Note: On the determination of enclosed water volume in large flexible-wall mesocosms, Biogeosciences Discuss., 9, 13019–13030, doi:10.5194/bgd-9-13019-2012, 2012b.

Czerny, J., Schulz, K. G., Ludwig, A., and Riebesell, U.: Technical Note: A simple method for air-sea gas exchange measurements in mesocosms and its application in carbon budgeting, Biogeosciences, 10, 1379–1390, doi:10.5194/bg-10-1379-2013, 2013.

de Kluijver, A., Soetaert, K., Czerny, J., Schulz, K. G., Boxhammer, T., Riebesell, U., and Middelburg, J. J.: A ^{13}C labelling study on carbon fluxes in Arctic plankton communities under elevated CO_2 levels, Biogeosciences, 10, 1425–1440, doi:10.5194/bg-10-1425-2013, 2013.

Drenner, R. W. and Mazumder, A.: Microcosm experiments have limited relevance for community and ecosystem ecology, Ecology, 80, 1081–1085, 1999.

Eilertsen, H. C., Taasen, J. P., and Weslawski J. M.: Phyto- plankton studies in the fjords of West Spitsbergen: physical environment and production in spring and summer, J. Plankton Res. 11, 1245–1260, 1989.

Engel, A., Borchard, C., Piontek, J., Schulz, K. G., Riebesell, U., and Bellerby, R.: CO_2 increases ^{14}C primary production in an Arctic plankton community, Biogeosciences, 10, 1291–1308, doi:10.5194/bg-10-1291-2013, 2013.

French, R. H. and Watts, R. J.: Performance of in situ microcosms compared to actual reservoir behavior, J. Environ. Eng., 115, 835–849, 1989.

Gattuso, J.-P. and Hansson, L.: Ocean acidification: background and history, in: Ocean acidification, Oxford, edited by: Gattuso, J.-P. and Hansson, L., Oxford University Press, Oxford, 1–20, 2011.

Gattuso, J.-P., Lee, K., Rost, B., and Schulz, K. G.: Approaches and tools to manipulate the carbonate chemistry, in: Guide to best practices in ocean acidification research and data reporting, edited by: Riebesell, U., Fabry, V., Hansson, L., and Gattuso, J.-P., Office for Official Publications of the European Communities, Luxembourg, 41–52, 2010.

Hop, H., Pearson, T., Hegseth, E. N., Kovacs, K. M., Wiencke, C., Kwasniewski, S., Eiane, K., Mehlum, F., Gulliksen, B., Wlodarska-Kowalczuk, M., Lydersen, C., Weslawski, J. M., Cochrane, S., Gabrielsen, G. W., Leaky, R. J. G., Lønne, O.J., Zajaczkowski, M., Falk-Petersen, S., Kendall, M., Wängberg, S.-Å., Bischof, K., Voronkov, A. Y., Kovaltchouk, N. A., Wiktor, J., Poltermann, M., di Prisco, G., Papucci, C., and Gerland, S.: The marine ecosystem of Kongsfjorden, Svalbard, Polar Res., 21, 167–208, 2002.

Hop, H., Falk-Petersen, S., Svendson, H., Kwasniewski, S., Pavlov, V., Pavlova, O., and Søreide, J. E.: Physical and biological characteristics of the pelagic system across Fram Strait to Kongsfjorden, Prog. Oceanogr., 71, 182–231, 2006.

Iversen, K. R. and Seuthe, L.: Seasonal microbial processes in a high-latitude fjord (Kongsfjorden, Svalbard): I. Heterotrophic bacteria, picoplankton and nanoflagellates, Polar. Biol., 34, 731–749, 2011.

Kuiper, J., Brockmann, U. H., van het Groenewoud, H., Hoornsman, G., and Hammer, K. D.: Influences of bag dimensions on the development of enclosed plankton communities during POSER, Mar. Ecol. Progr. Ser., 14, 9–17, 1983.

Lischka, S., Büdenbender, J., Boxhammer, T., and Riebesell, U.: Impact of ocean acidification and elevated temperatures on early juveniles of the polar shelled pteropod Limacina helicina: mortality, shell degradation, and shell growth, Biogeosciences, 8, 919–932, doi:10.5194/bg-8-919-2011, 2011.

Lewis, E. and Wallace, D. W. R.: Program developed for CO_2 system calculations. ORNL/CDIAC-105, Carbon Dioxide Information Center, Oak Ridge National Laboratory, US Department of Energy, Oak Ridge, Tennessee, 1998.

Menzel, D. W. and Steele, J. H.: The application of plastic enclosures to the study of pelagic marine biota, Rapp. P.-v. Réun. Cons. int. Explor. Mer., 173, 7–12, 1978.

Niehoff, B., Schmithüsen, T., Knüppel, N., Daase, M., Czerny, J., and Boxhammer, T.: Mesozooplankton community development at elevated CO_2 concentrations: results from a mesocosm experiment in an Arctic fjord, Biogeosciences, 10, 1391–1406, doi:10.5194/bg-10-1391-2013, 2013.

Petersen, J. E., Kemp, W. M., Bartleson, R., Boynton, W. R., Chen, C.-C., Cornwell, J. C., Gardner, R. H., Hinkle, D. C., Houde, E. D., Malone, T. C., Mowitt, W. P., Murray, L. Sanford, L. P., Stevenson, J. C., Sundberg, K. L., and Suttles, S. E.: Multiscale experiments in coastal ecology: Improving realism and advancing theory, BioScience, 53, 1181–1197, 2003.

Petersen, J. E., Kennedy, V. S., Dennison, W. C., and Kemp, W. M.: Enclosed experimental ecosystems and scale: tools for understanding and managing coastal ecosystems, Springer, New York, 221 pp., 2009

Pilson, M. E. Q. and Nixon, S. W.: Marine microcosms in ecological research, In Microcosms in ecological research, DOE Symposium series 52, Technical information center, US Department of Energy, Washington, DC, 724–741, 1980.

Riebesell, U.: Acid test for marine biodiversity, Nature 454, 46–47, 2008.

Riebesell, U. and Tortell, P.D.: Effects of Ocean Acidification on Pelagic Organisms and Ecosystems, in: Ocean Acidification, edited by: Gattuso, J.-P., Hansson, L., Oxford University Press, 99–121, 2011.

Riebesell, U., Lee, K., and Nejstgaard, J.C.: Pelagic mesocosms, in: Guide to best practices in ocean acidification research and data reporting, edited by: Riebesell, U., Fabry, V., Hansson, L., and

Gattuso, J.-P., Office for Official Publications of the European Communities, Luxembourg, 81–98, 2010.

Schulz, K. G. and Riebesell, U.: Diurnal changes in seawater carbonate chemistry speciation at increasing atmospheric carbon dioxide, Mar. Biol., doi:10.1007/s00227-012-1965-y, 2012.

Schulz, K. G., Barcelos e Ramos, J., Zeebe, R. E., and Riebesell, U.: CO_2 perturbation experiments: similarities and differences between dissolved inorganic carbon and total alkalinity manipulations, Biogeosciences, 6, 2145–2153, doi:10.5194/bg-6-2145-2009, 2009.

Schulz, K. G., Bellerby, R. G. J., Brussaard, C. P. D., Büdenbender, J., Czerny, J., Engel, A., Fischer, M., Koch-Klavsen, S., Krug, S. A., Lischka, S., Ludwig, A., Meyerhöfer, M., Nondal, G., Silyakova, A., Stuhr, A., and Riebesell, U.: Temporal biomass dynamics of an Arctic plankton bloom in response to increasing levels of atmospheric carbon dioxide, Biogeosciences, 10, 161–180, doi:10.5194/bg-10-161-2013, 2013.

Seuthe, L., Iversen, R. K., and Narcy, F.: Microbial processes in a high-latitude fjord (Kongsfjorden, Svalbard): II. Ciliates and dinoflagellates, Polar. Biol., 34, 751–766, 2011.

Silyakova, A., Bellerby, R. G. J., Czerny, J., Schulz, K. G., Nondal, G., Tanaka, T., Engel, A., De Lange, T., and Riebesell, U.: Net community production and stoichiometry of nutrient consumption in a pelagic ecosystem of a northern high latitude fjord: mesocosm CO_2 perturbation study, Biogeosciences Discuss., 9, 11705–11737, doi:10.5194/bgd-9-11705-2012, 2012.

Steinacher, M., Joos, F., Frölicher, T. L., Plattner, G.-K., and Doney, S. C.: Imminent ocean acidification in the Arctic projected with the NCAR global coupled carbon cycle-climate model, Biogeosciences, 6, 515–533, doi:10.5194/bg-6-515-2009, 2009.

Svendsen, H., Beszczynska-Møller, A., Hagen, J.O., Lefauconnier, B., Tverberg, V., Gerland, S., Ørbæk, J. B., Bischof, K., Papucci, C., Zajaczkowski, M., Azzolini, R., Bruland, O., Wiencke, C., Winther, J.-G., and Dallmann, W.: The physical environment of Kongsfjorden–Krossfjorden, an Arctic fjord system in Svalbard, Polar Res., 21, 133–166, 2002.

Tanaka, T., Alliouane, S., Bellerby, R. G. B., Czerny, J., de Kluijver, A., Riebesell, U., Schulz, K. G., Silyakova, A., and Gattuso, J.-P.: Effect of increased pCO_2 on the planktonic metabolic balance during a mesocosm experiment in an Arctic fjord, Biogeosciences, 10, 315–325, doi:10.5194/bg-10-315-2013, 2013.

Walther, K., Anger, K., and Pörtner, H. O.: Effects of ocean acidification and warming on the larval development of the spider crab *Hyas araneus* from different latitudes (54° vs. 79° N), Mar. Ecol. Progr. Ser., 417, 159–170, 2010.

Wood, H. L., Spicer, J. I., Kendall, M. A., Lowe, D. M., and Widdicombe, S.: Ocean warming and acidification; implications for the Artic brittlestar *Ophiocten sericeum*, Polar Biol., 34, 1033–1044, doi:10.1007/s00300-011-0963-8, 2011.

Manuscript 2.2:

Technical Note: The determination of enclosed water volume in large flexible-wall mesocosms "KOSMOS"

Published in Biogeosciences

Biogeosciences, 10, 1937–1941, 2013
www.biogeosciences.net/10/1937/2013/
doi:10.5194/bg-10-1937-2013

Biogeosciences Open Access

Technical Note: The determination of enclosed water volume in large flexible-wall mesocosms "KOSMOS"

J. Czerny, K. G. Schulz, S. A. Krug, A. Ludwig, and U. Riebesell

GEOMAR – Helmholtz Centre for Ocean Research Kiel, 24105 Kiel, Germany

Correspondence to: J. Czerny (jczerny@geomar.de)

Received: 29 August 2012 – Published in Biogeosciences Discuss.: 19 September 2012
Revised: 28 January 2013 – Accepted: 3 February 2013 – Published: 20 March 2013

Abstract. The volume of water enclosed inside flexible-wall mesocosm bags is hard to estimate using geometrical calculations and can be strongly variable among bags of the same dimensions. Here we present a method for precise water volume determination in mesocosms using salinity as a tracer. Knowledge of the precise volume of water enclosed allows establishment of exactly planned treatment concentrations and calculation of elemental budgets.

1 Introduction

Manipulation of a chemical parameter (e.g. nutrient or pollutant) in an experimental enclosure is usually accomplished by the following: (1) calculating the amount of the substance needed for a given volume of water, (2) adding the substance, (3) mixing the enclosed water to ensure homogeneity and (4) analysing the water to check if correct concentrations are achieved. In a large pelagic mesocosm like KOSMOS (**K**iel **O**ffshore **M**esocosms for future **O**cean **S**imulations) ($\sim$ 50–80 m^3 within each unit), some of these steps are technically difficult. The precise volume of water cannot be easily measured using standard volumetric or gravimetric methods and, as shown in this article, geometric calculations do not deliver satisfying results for a flexible-wall enclosure. Distributing a substance within an up to 25-m-deep water column can lead to vertical concentration gradients, and active mixing requires a large energy input. When a sample is analysed, it might be already too late to detect applied treatment concentrations inside the mesocosm as they might be rapidly altered by biological activity. Uncertainties and variability in treatment levels and budget calculations can be largely avoided if the exact water volumes of individual mesocosms are known. Many chemical parameters can be adjusted much more precisely as they can be determined later using seawater analytics. Here we present a method to precisely measure the volume within each experimental unit by addition of relatively small amounts of sodium chloride solution. Errors and uncertainties of the volume measurement are discussed.

2 Preparation of salt brine for volume measurements

Sodium chloride (NaCl) is used as a conductometric tracer for volume measurement because of its high solubility (359 $g\,L^{-1}$ at 20 °C). Complex sea salt mixtures cannot be prepared due to the relatively low solubility of some of the components. A NaCl concentration well below saturation (i.e. 250–300 $g\,kg^{-1}$) was chosen to ensure relatively quick dissolution and to prevent possible precipitation which could bias volume measurement. The source of the salt should be chosen with care, as impurities such as iron can cause enrichment of the enclosed water far beyond natural levels. To prevent this, one option is to use high purity grade salt. However, other salts are relatively pure and cost efficient depending on the production process. Attention should be paid to choosing a salt which does not contain commonly used anti-caking agents such as ferocyanide (e.g. Brezelsalz Bäckerstolz®, esco, Germany). The ion exchanger Lewatit™ MonoPlus TP 260® (Lanxess, Germany) removes metal anions efficiently from concentrated salt solutions. As soon as a subsample for calibration is taken after complete dissolution, the brine has to be stored in a tightly closed container to avoid evaporation. For a schematic drawing of our setup to prepare salt brine, see Fig. 1.

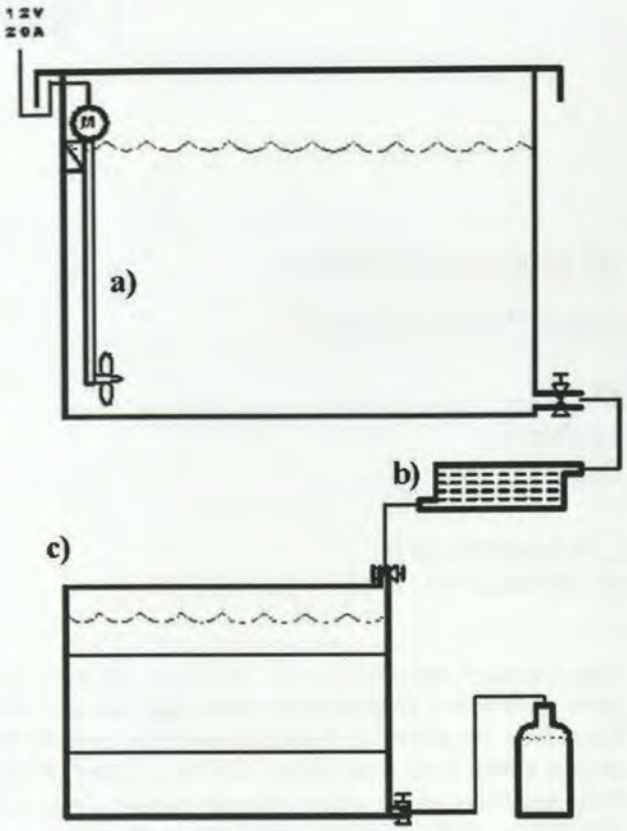

Fig. 1. Schematic drawing of the setup used for the preparation of salt brine in large amounts. An electric outboard motor **(a)** in the mixing tank speeds up the dissolution of salts, enabling preparation of nearly saturated solutions within a few hours. Produced solutions can be further processed (e.g. run over filters or purifying columns) **(b)** and stored in intermediate bulk containers **(c)** and dispensed into suitable carboys for quantitative addition into the mesocosms using the "spider".

3 Salt brine addition

Prior to brine addition the initial salinity in the mesocosms has to be determined precisely. Due to the slightly uneven shape of the enclosures, mean salinity of a CTD (conductivity, temperature and depth) profile made in a stratified mesocosm is not necessarily matching mean salinity of the same water without a salinity gradient (Fig. 2a). Therefore, the mesocosm water column has to be mixed prior to measurement until homogeneity is reached (if a salinity gradient is found). Mixing was performed by bubbling with compressed air for five minutes via a weighted ($\sim$ 13 mm inner diameter) hose lowered to the bottom of the mesocosm. After determination of initial salinity by three consecutive CTD profiles, a precisely weighted amount of salt brine was injected into each mesocosm. Amounts of brine added were calculated based on an approximated volume to achieve salinity increases of 0.2 to 0.4. The "spider" system (described by Riebesell et al., 2012) was designed to evenly distribute liquids of any density inside large mesocosms. The brine solution was pumped through the "spider" system which was continuously moved up and down the upper $\sim$ 90 % of the mesocosm depth, avoiding any resting of the device at the lowest point. Once the brine solution has been pumped into the mesocosms, the empty solution container was rinsed twice with mesocosm water and the remaining water was pressed out of the "spider" using compressed air. The established salt gradient with decreasing water density with depth is not stable. An overturning circulation mixes the water column during the following 12 h as light, low-salinity water is making its way up across the denser, high-salinity water sinking to the bottom (Fig. 2b). While temperature gradients establish within hours according to outside stratification, salinity distribution remains homogeneous throughout the procedure. A stable halocline can be later established by purposeful salt brine addition to deep water layers or by freshwater input to the surface.

4 Salinity measurement

Salinity profiles were collected using a data-logger-equipped, hand-held, multisensory CTD CTD60M (Sun and Sea Technologies), manually lowered at a speed of $\sim 0.2\,\mathrm{m\,s^{-1}}$. Reproducibility of mean salinity (standard deviation of mean salinity from three replicate profiles ($n = \sim$ 300 single measurements per profile) in four salinity measurements) was typically ≤ 0.0003 units. This is corresponding to a measurement-derived uncertainty for volume estimates of ~ 0.1 % for a salt addition increasing salinity (S) by 0.3.

5 Calibration

The calibration of the salt brine was performed at 20 °C in the laboratory, using surface water collected in the Flensburg Fjord ($S = 17.0$). Nine different mixing ratios were measured to construct a calibration curve (Fig. 3). For this, seawater has to be stirred in an appropriate calibration beaker to establish a constant flow across the salinity sensor of the CTD probe for a stable reading. Determination of initial salinity in the calibration beaker was followed by a first addition of brine, oriented at the largest expected mesocosm volume (highest dilution). Afterwards salinity was increased in small steps until the mixing ratio of the smallest expected mesocosm volume was reached. After plotting the first calibration curve, the batch of water was mixed again and a second calibration starting at $S = 17.1$ was performed.

Although conductivity was increased by NaCl addition and not using a complex sea salt mixture, measured increases in salinity were directly proportional to the added amount of salt brine. The algorithm used by our CTD (UNESCO PSS-78) assumes seawater ion composition to be conservative

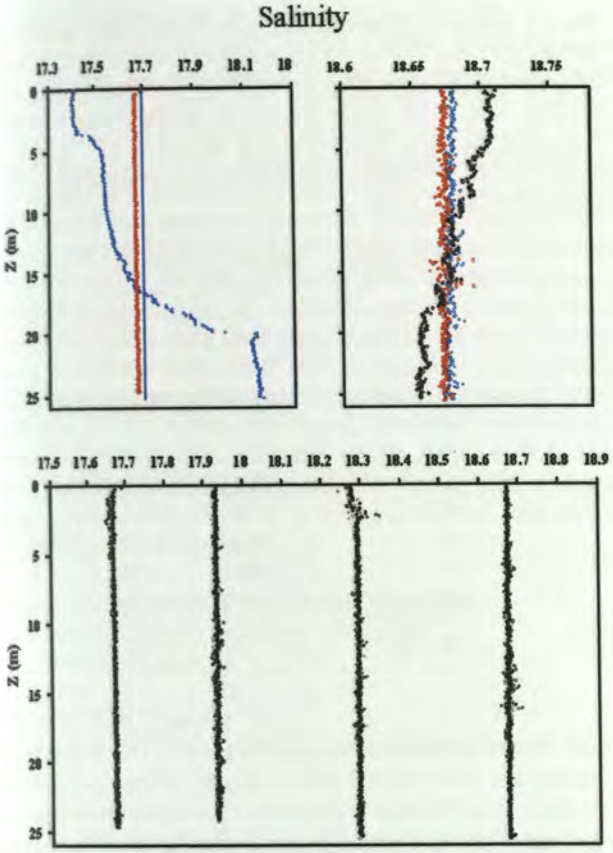

Fig. 2. **(a)** A natural vertical salinity profile in a 25-m-deep mesocosm (blue dots). The average salinity of the profile is indicated by a vertical blue line. Red dots are salinity measurements after mixing the water column using 5-min bubbling with compressed air. Differences are caused by the uneven shape of the bag (here especially the bottom funnel) **(b)** The black profile is collected right after injecting salt brine to the upper 22 m of the mesocosm, the blue profile is measured 6 h later and the red profile 18 h later. **(c)** Homogeneous S profile shown in **(a)** is increased in three steps, measured on three consecutive days using three replicated profiles shown as black, red and gray dots.

when calculating salinity from conductivity and temperature. However, changes in sea salt composition were found to have no significant influence on volume determination using this protocol.

When the gravimetric mixing ratio of seawater in the beaker per added brine (SW : Brine (kg)) is plotted versus measured salinity increase (ΔS), a power fit can be used to calculate volumes of mesocosms from ΔS (X) by multiplication of the mixing ratio (Y) with the added mass of brine (Fig. 3). To determine the precision of volume measurements, three consecutive salt additions were performed in a 25-m-deep mesocosm on a test cruise in the Flensburg Fjord in the western Baltic Sea in January 2011 (Fig. 2c).

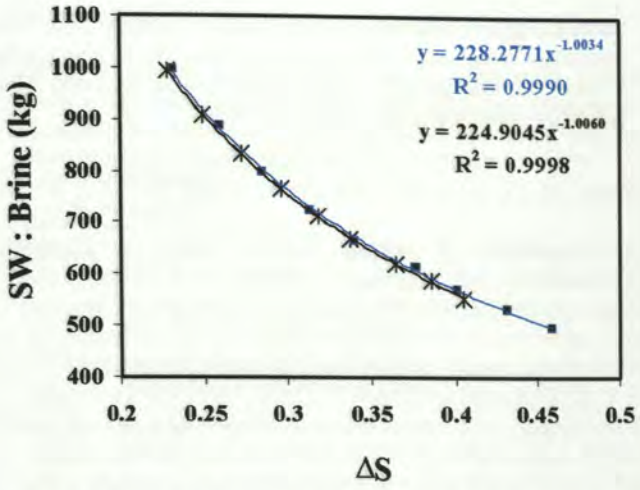

Fig. 3. Salt calibration curve. Exponential fits for two calibration datasets: calibration 1 (blue curve) is measured by increasing salinity from natural Baltic seawater $S = 17$; calibration 2 (black curve) is done after salinity was already increased from 17 to 17.1 by NaCl addition. Power formulas can be used to calculate mesocosm volume by multiplying y with the added amount of brine.

6 Potential side-effects of volume measurements using NaCl as a tracer

Every perturbation of the enclosed ecosystem in a mesocosm bares the risk of biasing results and reducing comparability to the natural system. Experiments on enclosed ecosystems cannot, however, be done without significant changes to natural physical and chemical side parameters such as turbulence, light or artificial nutrient additions. Perturbations equally performed in all parallel mesocosms are unproblematic when effects are compared among treatments. Homogenisation of the initial stratification and the addition of salt are equally performed in all units. Bubbles used to mix the mesocosms in the beginning of the experiment are presumably stressful for some of the enclosed organisms and might change initial dissolved gas concentration. Initial mixing of the water column in the beginning of the experiment has, beside the measurement of the salt inventory, a further advantage: it equalises differences in vertical nutrient distribution among parallel treatments arising from partial disruption of stratification after closing of the mesocosms. Harmful effects of temporary short bubbling on gases or organisms were not observed in prior experiments. In order to minimise stress on the enclosed ecosystem, the mesocosms should be mixed with large bubbles and not longer than absolutely necessary. Reports on physiological responses to a salinity increase of less than 1 could not be found for marine organisms. A minimum in species richness at intermediate salinities is observed along the natural salinity gradient (0 to 34) of the Baltic Sea estuary. However, changes in species distribution are generally attributed to salinity changes of

Table 1. Volumes calculated for three salinity additions to the same mesocosm using two calibrations, Cal 1 and Cal 2, were applied to each individual salinity increase. Results were corrected for increasing volume due to the addition of brine.

			Mesocosm Volume Estimates (t)	
Addition Nr.	Added brine (kg)	ΔS	Cal 1	Cal 2
1	83.05	0.264	72.44	71.1
2	113.16	0.359	72.40	71.1
3	122.27	0.381	73.53	72.2
Mean			72.79	71.5
St. Dev. %			0.88	0.89

several units with responses below 0.5 not being resolved (Remane, 1934; Paavola et al., 2005). Potential impacts of NaCl on freshwater ecosystems are summarised by Siegel (2007) within a risk assessment for salt use on roads. Responses to prolonged exposure are generally observed when several $g\,kg^{-1}$ NaCl were added. Single studies reported effects on Cladocera and some fish juveniles already at about $0.5\,g\,kg^{-1}$ of salt addition (see table and references within Siegel, 2007). Thus, NaCl could be generally also used as a tracer in freshwater mesocosm research if salt additions are below $0.2\,g\,kg^{-1}$. In any case, the risk of biasing results by additional manipulation of the enclosed system has to be evaluated against advantages of knowing the precise volume of the enclosure.

7 Discussion of measurement errors

Volumes calculated from three consecutive salt additions to the test mesocosm are summarised in Table 1. Deviations of about ±1 % are larger than expected from possible uncertainties in the amount of brine added and the precision of salinity measurements. Based on the reproducibility of measurements we would expect uncertainties of only up to ±0.1 %. With respect to the good reproducibility of salinity measurements inside the mesocosms, enrichments of 0.3 to 0.4 during the Baltic Sea test turned out to be unnecessarily high. Comparable results could have been achieved applying salinity increases of less than 0.1. Actual losses during addition of brine can be expected to be on the order of single grams. Observed deviations are therefore unlikely to be caused by addition or measurement errors inside the mesocosms, but from uncertainties arising from the calibration. Calculated volumes based on three salinity additions to the same mesocosm and two calibration curves were used to identify uncertainties. Using either calibration 1 or 2, results of the consecutive measurements vary by the same percentage (~ 0.9 %); however, using calibration 1, mean volume is 1.2 % higher than volume calculated using calibration 2. This offset is obviously due to a ~ 0.003 uncertainty in calibration initial S, to which all ΔS values in the calibration curve are referenced to. Parts of the calibration limitation might have been due to problems in measuring salinity with a CTD probe inside a beaker. Consequently, the method is more sensitive in determining differences between mesocosms than in determining the absolute amount of water enclosed. Most accurate results can be expected when calibration is done using seawater at in situ T and S, and the initial salinity is repeatedly measured.

Table 2. Measured volume of nine mesocosms in two experiments: Bergen 2011 and Svalbard 2010 including maximum and standard deviations from mean measured volumes. In Bergen 2011, bags reached overall 25 m below the surface, geometrically calculated volume for the bags, funnel shaped in the bottom 2 m, is 74.3 t. In Svalbard 2010, cylindrical 15-m-deep bags are geometrically calculated to hold 47 t.

Mesocosm. Nr.	Bergen 2011	Svalbard 2010
1	76.8	48.8
2	79.9	48.1
3	78.4	46.7
4	73.5	48.7
5	75.9	46.5
6	73.5	47.2
7	79.4	48.8
8	78.4	45.0
9	75.2	47.8
Max. Dev. %	8.4	7.9
St. Dev. %	3.2	2.7

8 Observed variability between mesocosms

Despite their nearly cylindrical appearance, measured volumes of nine KOSMOS mesocosms in two experiments deviated by up to 8 % between parallel units (standard deviation of ~ ±3 %; Table 2). The 25-m-deep setup in the Bergen 2011 experiment had slightly larger deviations than the 15-m-deep setup used in Svalbard 2010. The volumes of the 25-m-long bags were 4 % smaller than their geometrically calculated volumes during the test in the Baltic Sea. In Bergen 2011 the volumes of the same bags were averaged 3.3 % larger than geometrically calculated. These differences were probably caused by differences during filling – especially opening time – changing water densities, and slight lateral deformations caused by water currents acting on the moored mesocosms. During an earlier test cruise more than 20 % variation was measured between three mesocosms filled at a relatively strong current.

Acknowledgements. This work is a contribution to the "European Project on Ocean Acidification" (EPOCA) which received funding from the European Community's Seventh Framework Programme (FP7/2007-2013) under grant agreement no. 211384. Financial support was provided through Transnational Access funds by the European Union Seventh Framework Program (FP7/2007-2013) under grant agreement no. 22822 MESOAQUA and by the Federal Ministry of Education and Research (BMBF, FKZ 03F0608) through the BIOACID (Biological Impacts of Ocean ACIDification) project. We gratefully acknowledge the logistical support of Greenpeace International for assistance with the transport of the mesocosm facility from Kiel to Ny-Ålesund and back. We also thank the captains and crews of M/V *ESPERANZA* of Greenpeace, R/V *Viking Explorer* of the University Centre in Svalbard (UNIS) and R/V *Alkor* for assistance during mesocosm transport and during deployment and recovery in Kongsfjorden and the Flensburg fjord, respectively. We thank the staff of the French–German Arctic Research Base at Ny-Ålesund, in particular Marcus Schumacher, for on-site logistical support.

The service charges for this open access publication have been covered by a Research Centre of the Helmholtz Association.

Edited by: T. F. Thingstad

References

Paavola, M., Olenin, S., and Leppakoski, E.: Are invasive species most successful in habitats of low native species richness across European brackish water seas?, Estuar. Coast. Shelf Sci., 64, 738–750, doi:10.1016/j.ecss.2005.03.021, 2005.

Remane, A.: Die Brackwasserfauna, Verh. Deut. Z., 36, 34–74, 1934.

Riebesell, U., Czerny, J., von Bröckel, K., Boxhammer, T., Büdenbender, J., Deckelnick, M., Fischer, M., Hoffmann, D., Krug, S. A., Lentz, U., Ludwig, A., Muche, R., and Schulz, K. G.: Technical Note: A mobile sea-going mesocosm system – new opportunities for ocean change research, Biogeosciences Discuss., 9, 12985–13017, doi:10.5194/bgd-9-12985-2012, 2012.

Siegel, L.: Hazard identification for human and ecological effects of sodium chloride road salt Ph.D. theses, PE, State of New Hampshire, Department of environmental services, Water division, Watershed management, 2007.

Manuscript 2.3:

Technical Note: A simple method for air-sea gas exchange measurements in mesocosms and its application in carbon budgeting

Published in Biogeosciences

Biogeosciences, 10, 1379–1390, 2013
www.biogeosciences.net/10/1379/2013/
doi:10.5194/bg-10-1379-2013

Technical Note: A simple method for air–sea gas exchange measurements in mesocosms and its application in carbon budgeting

J. Czerny, K. G. Schulz, A. Ludwig, and U. Riebesell

GEOMAR – Helmholtz Centre for Ocean Research Kiel, 24105 Kiel, Germany

Correspondence to: J. Czerny (jczerny@geomar.de)

Received: 31 July 2012 – Published in Biogeosciences Discuss.: 3 September 2012
Revised: 27 January 2013 – Accepted: 11 February 2013 – Published: 1 March 2013

Abstract. Mesocosms as large experimental units provide the opportunity to perform elemental mass balance calculations, e.g. to derive net biological turnover rates. However, the system is in most cases not closed at the water surface and gases exchange with the atmosphere. Previous attempts to budget carbon pools in mesocosms relied on educated guesses concerning the exchange of CO_2 with the atmosphere. Here, we present a simple method for precise determination of air–sea gas exchange in mesocosms using N_2O as a deliberate tracer. Beside the application for carbon budgeting, transfer velocities can be used to calculate exchange rates of any gas of known concentration, e.g. to calculate aquatic production rates of climate relevant trace gases. Using an arctic KOSMOS (**K**iel **O**ff **S**hore **M**esocosms for future **O**cean **S**imulation) experiment as an exemplary dataset, it is shown that the presented method improves accuracy of carbon budget estimates substantially. Methodology of manipulation, measurement, data processing and conversion to CO_2 fluxes are explained. A theoretical discussion of prerequisites for precise gas exchange measurements provides a guideline for the applicability of the method under various experimental conditions.

1 Introduction

Pelagic mesocosms represent large volume (mostly between one and fifty m^3) experimental enclosures used to gather data on natural plankton communities (Petersen et al., 2003). Generally open towards the atmosphere, mesocosms, however allowing for air–sea gas exchange, make it difficult to calculate production or consumption of CO_2 and other volatile compounds inside an experimental unit. Climate relevant trace gases and other volatile carbon compounds produced in marine environments are increasingly investigated for their potential climate feedbacks and have been measured in previous mesocosm experiments (Sinha et al., 2007; Archer et al., 2012; Hopkins et al., 2012). Observed concentrations in a mesocosm are a product of water-column reactions and losses or gains from the atmosphere. Precise knowledge of air–sea gas exchange rates can be used to calculate net production rates of these compounds in the water column, which can be compared between various experiments. Aquatic production rates in concert with data on biological community composition and physiological state would help to understand observed open-ocean distributions.

Not only in the context of global change, biological CO_2 fixation and consequent carbon export by sinking particles is of special interest to biogeochemical experimentalists. Most mesocosm studies currently focus on investigating ecological interactions applying standard oceanographic methods on subsamples of the enclosed water. In principal, mesocosm experiments also provide the opportunity to compare biogeochemical element fluxes such as air–sea gas exchange and export to water-column production. With production rates, as usually measured in side experiments (e.g. O_2 production or ^{14}C incorporation), uncertainties arise from sample transfer into bottle incubations and from extrapolating back from incubation conditions to temperature and light gradients present in mesocosms. In situ primary production measurements using the whole enclosure as experimental vessel have to be elaborated, in order to produce estimates comparable to total mesocosm fluxes like sedimentation of organic matter. Calculating carbon fluxes from water-column pools of inorganic and organic carbon quantitatively related to air–sea fluxes and export rates could largely improve the

understanding of the system (Czerny et al., 2012a). To directly estimate cumulative net community production (NCP), changes in total dissolved inorganic carbon (CT) have to be corrected for CO_2 air–sea gas exchange and eventually for calcification and evaporation. In previous mesocosm experiments in a Norwegian fjord (Delille et al., 2005) and indoors (Wohlers et al., 2009; Taucher et al., 2012), net community production (NCP), calculated on the basis of measured changes in CT, were presented. To calculate air–sea gas exchange, Delille et al. (2005) used a parameterisation for wind dependent boundary layer thickness achieved from experimental data compiled by Smith (1985). Wind speed, the crucial input parameter, was set to zero, because the mesocosms were closed to the atmosphere and moored in a sheltered surrounding. Whereas most parameterisations result in zero gas exchange at zero wind speed (Wanninkhof, 1992), laboratory derived wind dependent parameterisations by Smith et al. (1985) resulted in positive exchange at zero wind speed. Under calm conditions, gas exchange is low, but not zero; it is governed by other energy inputs than wind, e.g. thermal convection due to evaporation and temperature changes (Liss, 1973; Wanninkhof et al., 2009). Although direct wind forcing might be negligible in most mesocosms, the general assumption that overall energy input is comparable to the conditions in the experimental tanks used by Smith et al. (1985), however, is not justifiable. Surface turbulence in many mesocosm experiments is unlikely to be very low. Active mixing systems, wave movement of the surrounding water, thermal mixing or the deployment of sampling gear might create turbulence within the enclosures, comparable to quite windy conditions. Taucher et al. (2012), for example, found wind speeds of more than $6\,m\,s^{-1}$ to be necessary for balancing the carbon budget in a Kiel indoor mesocosm experiment, applying the Smith et al. (1985) calculation. Parameterisations for wind speed dependent gas exchange over the ocean are obviously not suitable for calculating mesocosm air–sea gas exchange. Other than open-ocean gas exchange measurements, direct measurement of exchange velocities in an enclosed water volume can be relatively easily done.

Here, we present a simple method for direct measurements of air–sea gas exchange rates in mesocosm experiments using N_2O as a tracer. N_2O is a perfect choice as a gas tracer in this application, due to its well known atmospheric concentration, relatively simple detection and structural similarity to CO_2. Although N_2O is not an inert gas, conditions favouring its biological production are unlikely to occur in pelagic mesocosms. Possible bias by biological activity is assessd by parallel measurement of natural variations in N_2O and will be discussed later in the manuscript. The conversion of measured N_2O exchange rates to those of CO_2 and other gases is explained. We are providing a detailed description of the method and calculations including a discussion of prerequisites to achieve high quality data.

The measurement protocol and results are explained using a KOSMOS (Kiel Off Shore Mesocosm for Ocean Simulation, Fig. 1) experiment on ocean acidification in the Arctic as a model. Applicability of the method in the Kiel indoor mesocosm facility is further explained and discussed.

2 Methods

2.1 Setup of the Svalbard 2010 ocean acidification experiment

Nine 15 m deep KOSMOS mesocosms, each with a diameter of 2m were moored end of May 2010 in the Kongsfjorden, Svalbard. Seven different CO_2 treatment concentrations were achieved through addition of CO_2 saturated seawater. While the ambient ($\sim 180\,\mu atm\ pCO_2$) control treatment was replicated twice, the seven enriched mesocosms followed a gradient up to $\sim 1420\,\mu atm\ pCO_2$. Development of the enclosed natural plankton community was followed for 30 days after CO_2 manipulation, including addition of inorganic nutrients on day 13. For more details see Riebesell et al. (2012) and Schulz et al. (2013).

2.2 N_2O addition

One litre of saturated N_2O solution (N_2O medical, Air Liquide, purity > 98 %) was prepared via bubbling of seawater for two days in a narrow measurement cylinder covered with Parafilm®. Amounts of the solution to be added to the mesocosm were calculated using solubility constants by Weiss and Price (1980) with respect to in situ salinities (S) and temperatures (T). The targeted concentrations of N_2O should be adapted to the setup in order to achieve mesocosm to air fluxes, which can be measured at good precision over reasonable time scales. Here, seawater tracer concentrations were chosen in accordance to the highest certificated reference material for N_2O analyses available in our lab ($\sim 55\,nmol\,kg^{-1}$).

Assuming a background concentration of $13\,nmol\,kg^{-1}$, $40\,nmol\,kg^{-1}$ of medical grade N_2O was added. Based on experience, a surplus of approximately 20 % was added to the mesocosms to account for losses unavoidable during handling of the solution.

Addition of the solution to the mesocosms (about 1–$2\,mL\,m^{-3}$) can be calculated according to the formulation:

$$V_{ad} = \frac{V_w \cdot ad}{K_{TS} \cdot p}, \quad (1)$$

where V_{ad} is the volume of N_2O stock solution added (L), V_w the volume of the mesocosm (L), ad the desired addition ($mol\,L^{-1}$), and K_{TS} is the solubility constant by Weiss and Price (1980) for S and T of the N_2O stock solution ($mol\,L^{-1}\,atm^{-1}$) prepared at a pressure, p (atm), of one atmosphere.

A syringe with a large inlet diameter was used to transfer the stock solution carefully. Filling of the syringe was done

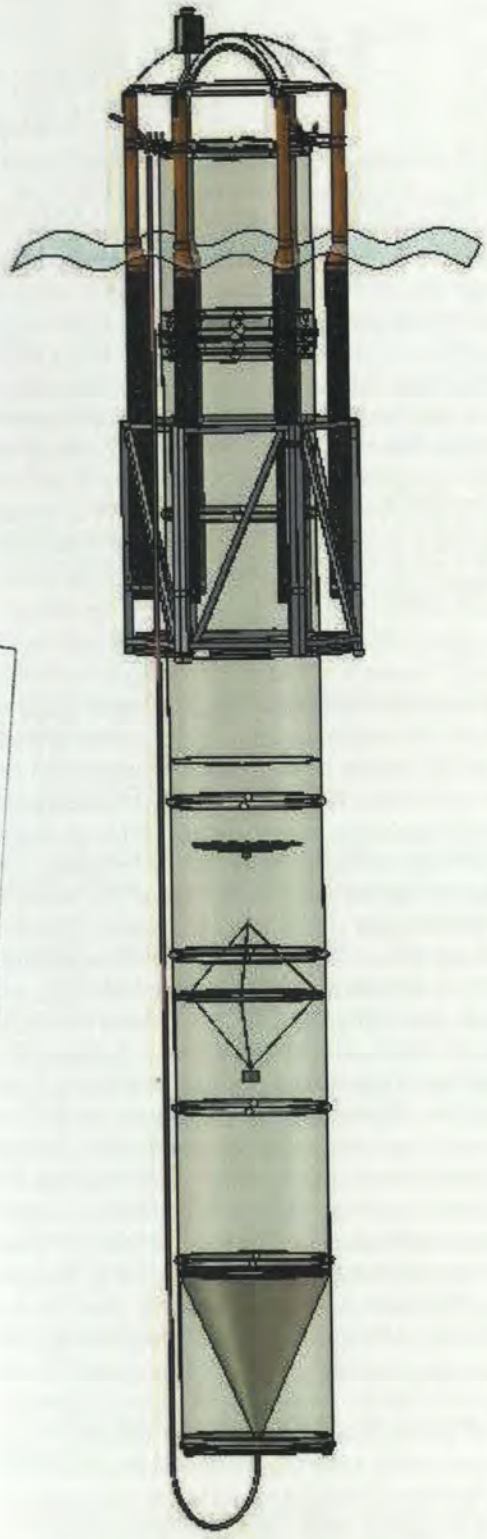

Fig. 1. Drawing of a KOSMOS mesocosm in the configuration used for the Svalbard experiment.

slowly as vacuum increases undesired outgassing of N_2O. The stock solution was first diluted with filtered seawater in 25 L carboys, which were filled almost to the rim. The content of the carboys was homogeneously distributed to the mesocosms by using the pumped injection device "Spider" (Riebesell et al., 2012).

2.3 Sampling

Three of the nine mesocosms were sampled every second day using integrating water samplers (IWS, Hydrobios). Equal amounts of sample were sucked into the sampling bottle at each depth between 0 and 12 m, electronically controlled via hydrostatic pressure sensors. These integrated water samples represent inventories of the 15 m deep water column. Triplicate samples were drawn directly from the sampler. The water was filled bubble free into 50 mL headspace vials via a hose reaching to the bottom of the vial. The vial volume was allowed to overflow about four times before closing. Vials were closed with butyl rubber plugs (N 20, Machery and Nagel), crimp sealed and stored at room temperature after addition of 50 µL of saturated mercury chloride solution.

2.4 Measurement procedures

Measurement of aquatic N_2O concentrations was performed via gas chromatography (GC) with electron capture detection (Hewlett Packard 5890 II), using a headspace static equilibration procedure as described by Walter et al. (2006, precision $\sim \pm 1.8$ %). The GC was equipped with a 6′/1/8″ stainless steel column packed with a 5 Å molecular sieve (W. R. Grace & CO) and operated at a constant oven temperature of 190 °C. A 95/5 argon-methane mixture (5.0, Air Liquide) was used as carrier gas. 10 mL of helium (5.0, Air Liquide) headspace was added to the sample vials and later injected into the sample loop of the GC after equilibration was achieved by manual shaking and storage of the vials for at least 10 h at a temperature of 21 °C. Certified gas mixtures of N_2O in artificial air (Deuste Steininger GmbH) with mixing ratios of 87.2 ± 0.2, 318 ± 0.2 and 1002 ± 0.2 ppb as well as 1 : 1 dilutions with helium were used to construct calibration curves with a minimum of three data points close to sample concentrations. Headspace to water phase ratios in the vials was determined gravimetrically.

Total dissolved inorganic carbon (CT) was determined via coulometric titration using a SOMMA system and total alkalinity (TAlk) via potentiometric titration (Dickson, 1981) (standard error of both methods $\sim \pm 1$ µmol kg^{-1}). CO_2 concentrations, partial pressures and pH (total scale) were calculated from CT and TAlk measurements with the program CO2SYS by Lewis and Wallace (1995). For more details on carbonate chemistry see Bellerby et al. (2012).

Determination of salinity and temperature in the mesocosms was performed with a data logger-equipped hand held multisensory CTD 60M (Sea and Sun Technology). Volume

of the mesocosms was determined with the same instrument using sodium chloride additions of $\sim 0.2\,g\,kg^{-1}$ as a tracer (Czerny et al., 2012b).

Wind velocity and direction measured at 10 m height onshore, about one mile from the mooring site, were provided by the staff of the AWI-PEV Station in Ny Alesund.

Atmospheric measurements of N_2O and CO_2 were measured on close by Zeppelin Mountain (~ 4.5 km from the experimental side) and provided to us by the NOAA Carbon Cycles Gases Group in Boulder, CO, USA and ITM in Stockholm University, Sweden, for N_2O and CO_2, respectively.

3 Results and discussion

Concentrations of N_2O added on day 4 decreased in the enriched mesocosms from initially measured $\sim 50\,nmol\,kg^{-1}$ on day 6 to $\sim 30\,nmol\,kg^{-1}$ on day 28 (Fig. 2). Concentrations measured in the fjord close to the mesocosms were slightly oversaturated compared to atmospheric equilibrium values, calculated for in situ seawater T, S and atmospheric mixing ratios measured close by on Zeppelin Mountain. Despite variable wind conditions, the concentration decrease inside the mesocosms could be fitted ($R^2 = 0.96$) using a standard diffusion relationship:

$$C_{N_2O} = 60.556 \cdot e^{-0.0241 \cdot d} \quad (2)$$

where the concentration of N_20 (C_{N_2O}) is described as an exponential function of the sampling day (d).

3.1 Calculation of CO_2 fluxes from changes in N_2O concentrations

Daily N_2O fluxes were calculated from the fitted N_2O concentration decrease over time and converted to volumetric units. Changes in the N_2O inventory, derived using the determined volume of the mesocosms (method described in Czerny et al., 2012b) were used to calculate fluxes in $\mu mol\,cm^{-2}\,h^{-1}$ (F_{N_2O}) across the water surface according to

$$F_{N_2O} = \frac{I_{w1} - I_{w2}}{A \cdot \Delta t} \quad (3)$$

where I_{w1} is the fitted bulk water N_2O inventory in µmol per mesocosm on t_1 and I_{w2} on t_2 with Δt as the time interval between t_1 and t_2 in h, while A is the nominal surface area of the mesocosm in cm^2. A N_2O transfer velocity (k_{N_2O}) in $cm\,h^{-1}$ is then calculated by dividing F_{N_2O} by the concentration gradient according to Eq. (4):

$$k_{N_2O} = \frac{F_{N_2O}}{(C_{N_2O\,w} - C_{N_2O\,aw})} \quad (4)$$

where $C_{N_2O\,w}$ is the fitted bulk water N_2O concentration ($\mu mol\,cm^{-3}$) at the point in time and $C_{N_2O\,aw}$ the calculated (Weiss and Price, 1980) equilibrium concentration of N_2O with the atmosphere at prevailing bulk water T and S. Using bulk water concentrations to derive a surface diffusion gradient perfect mixing of the mesocosm appears to be an absolute requirement. Referring from N_2O to inert gasses with air–sea gas exchange being the only exchange process, it is irrelevant whether exchange is limited by mixing processes close to the air–sea interface or within the water column. Yet, if a permanent stratification is formed inside the mesocosm, the decrease of N_2O bulk water concentration cannot be used to calculate mesocosm–atmosphere CO_2 exchange. Processes modulating the concentrations of biologically active compounds such as CO_2 are usually variable along the light gradient. Therefore, due to shallow primary production, considerable differences in the surface gradient of CO_2 might emerge compared to N_2O surface gradients that are governed by diapycnal mixing. For stratified mesocosms, gas exchange calculations require the integration of information about vertical distribution of tracer and gases of interest. Here, N_2O and CO_2 inventories have to be determined by integrated water samples independently from surface gradients determined from discrete surface water samples. Regardless of the specific sampling strategy applied, it is imperative to use the same protocol for the tracer as for the gases of interest.

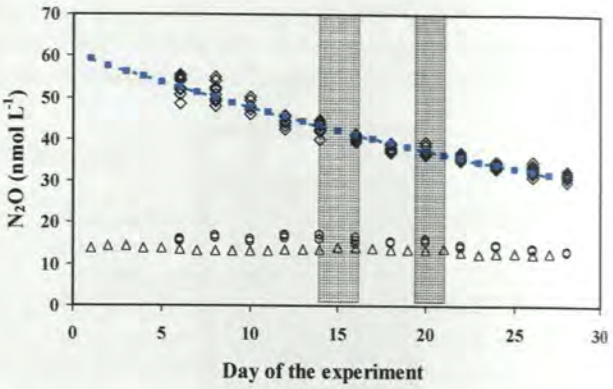

Fig. 2. N_2O concentrations during the experiment. Diamonds (◇) represent the measured concentration inside the three examined mesocosms; blue squares (□) are fitted daily concentrations according to equation 2, circles (○) are background N_2O concentrations measured in the surrounding fjord, triangles (△) are calculated equilibrium concentrations from atmospheric measurements at in situ T and S. Shaded areas indicate periods when waves (up to $H_{1/3} = 0.8$ m) occurred at the mooring site.

Due to convection caused by slight temperature changes in the surrounding water (Fig. 5) and an evaporation induced salinity increase (Schulz et al., 2013), the mesocosms in the Svalbard KOSMOS study could be considered to be homogeneous on time scales relevant for air–sea gas exchange. N_2O as well as CO_2 surface concentrations are therefore adequately represented by bulk water measurements.

k_{N_2O} can be translated into a transfer velocity for any other gas using its Schmidt numbers to correct for gas specific

properties as shown for the transfer coefficient of CO_2 (k_{CO_2}) in Eq. (5):

$$k_{CO_2} = \frac{k_{N_2O}}{\left(\frac{Sc_{CO_2}}{Sc_{N_2O}}\right)^{0.5}}. \quad (5)$$

The Schmidt number for N_2O (Sc_{N_2O}) published by Rhee (2000), and the Schmidt number for CO_2 (Sc_{CO_2}) derived from diffusion coefficients published by Jähne et al. (1987) were used. Using this pair of Schmidt numbers, k_{CO_2} is generally less than 1 % smaller than k_{N_2O}, similarly to when both Schmidt numbers are derived from coefficients published by Jähne et al. (1987). If both coefficients are taken from Wilke and Chang (1955) the difference is ~ 10 % and can become larger than 25 % if Sc_{CO_2} from Wilke and Chang (1955) is paired with (Sc_{N_2O}) derived from coefficients published by Broecker and Peng (1974). More recent wind and wave tank experiments have shown that a conversion of k_{N_2O} to k_{CO_2} is not necessary as gas exchange of the two gases is indistinguishable under conditions were chemical enhancement of CO_2 exchange is not relevant (Degreif, 2006). Fluxes for CO_2 (F_{CO_2}) can then be calculated by multiplication of k_{CO_2} with the diffusion gradient between bulk water CO_2 concentrations ($C_{CO_{2\,w}}$) and calculated equilibrium concentrations with the atmosphere ($C_{CO_{2\,aw}}$) as

$$F_{CO_2} = k_{CO_2} \cdot (C_{CO_{2\,w}} - C_{CO_{2\,aw}}). \quad (6)$$

Daily CO_2 fluxes were calculated for the nine mesocosms within the Svalbard ocean acidification experiment (Fig. 3). In the first days after CO_2 addition was completed (day 4), maximum efflux of ~ 2 µmol CO_2 per kg seawater and day could be observed in the highest CO_2 treatment (~ 1400 µatm) at a CO_2 gradient of ~ 980 µatm. In the following two weeks, the CO_2 gradient was diminished by outgassing CO_2 in concert with biological uptake, so that fluxes on day 27 were considerably lower (gradient ~ 450 µatm). Decrease of fluxes as a result of decreasing CO_2 gradients was less pronounced in the more moderately oversaturated mesocosms due to a higher buffer capacity of the carbonate system. About 0.5 µmol kg^{-1} d^{-1} CO_2 gassed into the water from the atmosphere in the non-manipulated control treatments (~ 175 µatm). Here, biological uptake was roughly balanced by influx so that the gradient remained rather constant over time.

3.2 Chemical enhancement of CO_2 air–sea gas exchange

Another correction has to be applied to derive accurate CO_2 fluxes in calm environments like the KOSMOS mesocosms. As CO_2 reacts with water, unlike N_2O, CO_2 gas exchange might be chemically enhanced due to buffering of diffusive concentration change by equilibration reactions within the boundary layer. Other than inert gases, CO_2 diffuses

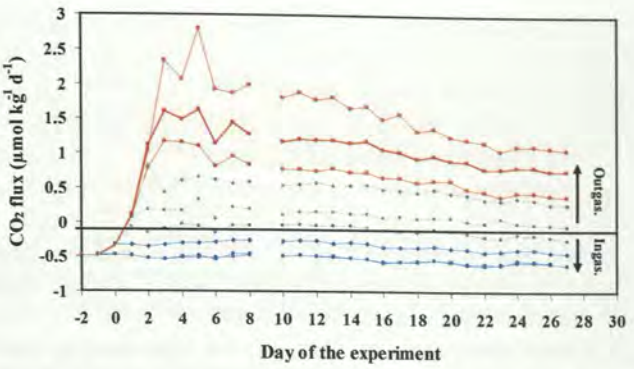

Fig. 3. Daily CO_2 fluxes for all CO_2 treatments over time. High CO_2 treatments are shown in red, medium in gray and low CO_2 are blue. Estimates include chemical enhancement according to Hover and Berkshire (1969).

are not necessarily exchanged through the boundary layer, but can also be formed from bicarbonate close to the interface. This applies only at low wind speeds and not when mixing is considerably faster because CO_2 hydration kinetics are slow. Thus, chemical enhancement is thought to be rather insignificant under turbulent conditions relevant for open-ocean CO_2 exchange (e.g. when $k > 5$ cm h^{-1}), but applies to the conditions found inside the mesocosms ($k \sim 1.8$–2.5 cm h^{-1}) (Wanninkhof and Knox, 1996). Moreover, the state of the carbonate system determines the extent of chemical enhancement, being negligible at pH < 6 and substantial at pH > 8. In the Svalbard ocean acidification experiment, the treatment pH_{tot} (total scale) ranged from 7.5 to 8.3 (Bellerby et al., 2012), therefore chemical enhancement created a pH effect on carbon flows that must be considered. To correct for this, theoretical parameterisations by Hoover and Berkshire (1969) were chosen, as currently no empirical parameterisations exist sufficiently describing the process in natural seawater (Wanninkhof and Knox, 1996). The enhancement factor α, the ratio between chemical enhanced flux and not enhanced flux can be calculated using Eq. (7):

$$\alpha = \frac{\tau}{[(\tau - 1) + \tanh(Qz)/(Qz)]}. \quad (7)$$

Here, dimensionless $\tau = 1 + [H^+]^2 \left(K_1^* K_2^* + K_1^* [H^+]\right)^{-1}$, with K_1^* and K_2^* being the first and second stoichiometric equilibrium constants for carbonic acid and $[H^+]$ the proton concentration. $Q = \left(r\tau D^{-1}\right)^{0.5}$ in cm^{-1}, where D is the diffusion coefficient for CO_2 by Jähne et al. (1987) and r describes the hydration of CO_2 either directly or via true carbonic acid. r in the unit s^{-1} can be calculated using Eq. (8):

$$r = KCO_2 + KOH^- K_w^* [H^+]^{-1} \quad (8)$$

with KCO_2 being the CO_2 hydration rate constant (s^{-1}), KOH^- is the CO_2 hydroxylation rate constant (L mol^{-1} s^{-1})

from Johnson (1982) and K_w^* is the equilibrium constant for water. The boundary layer thickness z (cm) can be calculated from determined transfer velocity ($z = Dk_{CO_2}{}^{-1}$). All constants used here can be found in Zeebe and Wolf-Gladrow (2001). Using the Hoover and Berkshire (1969) model, input conditions similar to our experimental conditions in Svalbard ($T = 5\,°C$, $S = 35$, $z = 0.002$ cm, $pH_{tot} = 8.2$) result in enhancement of about 8 % ($\alpha = 1.082$). For the same conditions, but at a temperature of 25 °C, CO_2 gas exchange would be enhanced by about 48 % ($\alpha = 1.479$).

Chemical enhancement factors using more complex models published by Quinn and Otto (1971), Emerson (1975), Smith (1985), and Keller (1994) give very similar results to the Hoover and Berkshire (1969) model (Wanninkhof and Knox, 1996). Experimental data from tank experiments reproduce calculated chemical enhancement relatively well (i.e. Hoover and Berkshire, 1969; Liss, 1973; Wanninkhof and Knox, 1996; Degreif, 2006). The simple pH dependent fit derived from enhancement experiments in natural Baltic seawater published by Kuss and Schneider (2004) is not recommended for use, as influences of T, S and z are not considered.

The relevance of chemical enhancement for open-ocean CO_2 exchange is controversial as the calculation of k from wind speed over the ocean itself still bears considerable uncertainty. As k in our experiments is measured directly, comparability to experimental results is quite straight forward.

Due to low temperatures during the Svalbard experiment, chemical enhancement of ~3 to 7 % is very low (Fig. 7). The influence of about three degree warming during the experiment in June 2010 is overall larger than the calculated difference arising from pH treatments (Fig. 4). Wrong pH-dependent chemical enhancement could produce artificial treatment effects in the carbon budget estimates especially in warm water ocean acidification studies. NCP estimates within this experiment by Silyakova et al. (2012) and Czerny et al. (2012a) at arctic temperatures are relatively unaffected by enhancement of this magnitude and possible uncertainties therein.

Evidence for a strong increase in chemical enhancement due to enzymatic catalysis by free carbonic anhydrases as suggested by Berger and Libby (1969) was not found in later experiments (Goldman and Dennett, 1983; Williams, 1983), but it might be interesting to reconsider this question in future mesocosm experiments.

The lack of empirical data coverage on chemical enhancement parameterisations in seawater poses the major quantitative uncertainty for NCP estimates based on CO_2 air–sea gas exchange using the presented method. Especially in setups were temperatures are high, the proportion of CO_2 exchange relying on theoretical considerations is high compared to the directly measured flux.

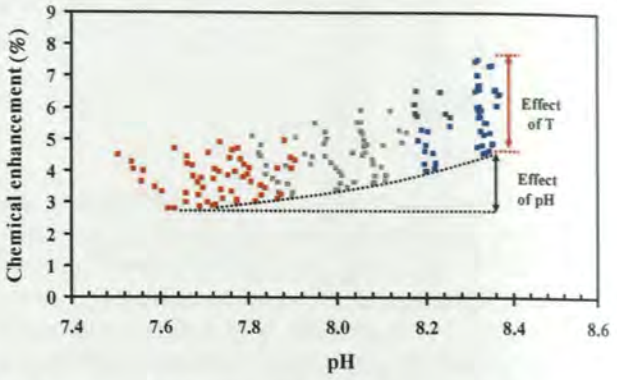

Fig. 4. Chemical enhancement of CO_2 compared to N_2O according to Hover and Berkshire (1969) calculated for measured k, S, T and pH_{tot} during the Svalbard experiment. High CO_2 treatments are red, medium are gray and low CO_2 are blue. The effect of pH_{tot} on chemical enhancement is indicated by the black arrow, while the effect of the ~3 °C temperature increase during the experiment is indicated by the red arrow.

3.3 The choice of N_2O as a gas exchange tracer and its biological stability

The N_2O molecule strongly resembles CO_2 in most physical properties; it has the same mass, nearly the same solubility and diffusivity. Other than CO_2, equilibrium reaction of N_2O with water lies strongly on the side of free N_2O so that air–sea gas exchange can be approximated as for inert gases. In laboratory experiments N_2O is a perfect tracer for CO_2 gas exchange. Because of the similarity of both gases a conversion of measured k_{N_2O} to k_{CO_2} is small and so are potential uncertainties. Wall effects relevant in laboratory experiments such as permeability or adhesion to plastic walls can be assumed to be comparable between similar molecules. In open waters, background concentrations of N_2O are slightly variable. Therefore, ^3He and SF_6 were used as gas exchange tracers in open-ocean applications as they are highly inert, their natural background concentration and detection limit is very low so that measurement is possible also after considerable dilution. Despite many practical advantages of N_2O in the application in mesocosms its prominent role as a biologically produced climate relevant trace gas is putting the inertness of N_2O into question.

The natural source of oceanic background N_2O concentrations is biological production. N_2O is produced predominantly as a side product of nitrification, when ammonia is incompletely oxidised in the course of deep remineralisation at low oxygen concentrations. Yet, most parts of the ocean are near equilibrium with the atmosphere (mean global saturation 103 %) (see Bange et al., 1996 and references herein), whereas significant N_2O oversaturation is predominantly found in tropical regions rather than in cold and temperate waters (Walter et al., 2006). Detectable nitrification in the euphotic zone was hypothesised to also be a source

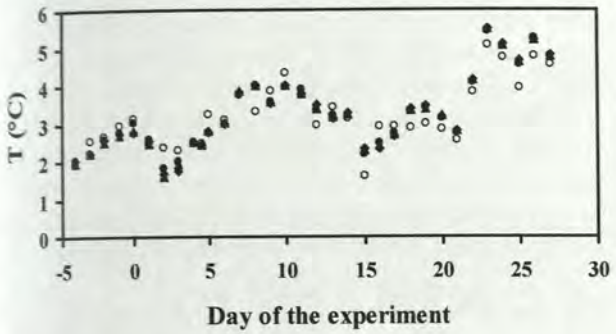

Fig. 5. Mean water temperatures between 0–12 m measured during the Svalbard experiment. The three examined mesocosms are shown as black symbols, while open circles represent measurements from the surrounding fjord.

of N_2O (Dore and Karl, 1996; Santoro et al., 2010), but this was not yet directly observed. Physiological results (Goreau et al., 1980; Loescher et al., 2012) suggest possible N_2O production by nitrification in fully oxygenated waters to be very low. However, even N_2O production at relatively high surface layer nitrification rates, as found in upwelling regions (Rees et al., 2011), are orders of magnitudes too low to significantly bias the large fluxes caused by deliberate N_2O addition. The only known pathway of biological N_2O uptake as a reactive nitrogen species is by denitrifiers at anoxic conditions ($<\sim 10\,\mu mol\,O_2\,kg^{-1}$) (Zumft, 1997; Zamora et al., 2012). Conditions favouring this process are unlikely to form in mesocosms and would result in a loss of the tracer (as N_2) but not into utilisation of N_2O as a nitrogen source. Side-effects of N_2O addition on biological activity in mesocosm experiments can therefore not be expected. Remineralisation of detritus at the bottom of the mesocosm could possibly be a source of N_2O. Conditions allowing for extensive remineralisation of accumulated organics inside pelagic mesocosms should thus be avoided. It is further strongly recommended to measure background natural N_2O concentrations preferably inside non-enriched experimental units, because N_2O is not considered as an inert gas.

3.4 Lateral gas exchange by diffusion through mesocosm wall material

Gas fluxes through the mesocosm walls can be calculated if temperature dependent permeability coefficients of the foil material and gases of interest are known.

Fluxes through the wall (F_{wall}) in $mol\,d^{-1}$ can be derived using the equation:

$$F_{wall} = \frac{D_t \cdot \Delta p \cdot A \cdot t}{z_m}. \quad (9)$$

Here D_t is the permeability coefficient at a given temperature in $mol \cdot \mu m\,atm^{-1}\,m^{-2}\,d^{-1}$, Δp is the partial pressure difference between inside and outside in atm, A is the submerged surface of the mesocosm walls in m^2, t is the duration in days and z_m is the thickness of the material in µm. Turbulence of the media in and outside the mesocosm is not relevant to this diffusion gradient as permeation of the materials is generally orders of magnitude slower than removal and advection of gases in the media.

Estimates of lateral gas exchange for the Svalbard experiment were calculated based on permeability coefficients published for Desmopan® 385, (Bayer). Desmopan® 385 is the raw material of our bag foil (Walopur®, Epurex Films). Direct measurements for Walopur® are not available for CO_2 and N_2O. Permeability for the specific temperatures was extrapolated.

For the experiments in the KOSMOS mesocosms, the fraction of the measured gas flux due to permeability of the bag material was maximal on the order of 1–2 %. Fluxes are low because of the relatively thick foil (0.5 to 1 mm) at comparatively low temperatures. In the perspective of CO_2 gas exchange estimates for carbon mass balance it is generally not interesting whether CO_2 exchanges through the walls or via the water surface. However, differences between N_2O and CO_2 in the material specific permeability of the bags have the potential to cause systematic errors if exchange is largely through the foil and not with the atmosphere. Such differences seemed at first unlikely because of the general similarity of N_2O and CO_2 in diffusivity and solubility, but permeability specifications for Desmopan® 385 suggest a considerably higher permeability for N_2O (27.1 and 51.7 $mol \cdot \mu m\,atm^{-1}\,m^{-2}\,d^{-1}$ for CO_2 and N_2O at 25 °C, respectively) (Bayer MaterialScience, TPU TechCentre). For the Svalbard experiment bias through lateral gas fluxes were not corrected, as the overall magnitude of these fluxes was negligible. The data basis in terms of permeability measurements would not have allowed for an exact correction of such bias. A set of permeability measurements at a relevant temperature range would improve gas exchange estimates especially at temperatures above 10 °C. If thin foil is used for mesocosms, a material with good gas barrier properties should be chosen and exact permeabilities should be known for the gases of interest.

When k_{N_2O} is translated into transfer velocities of poorly water soluble gases, dissolution and adhesion of those gases in and on the plastic material could cause a lateral sink of these substances in addition to the permeability issue.

3.5 Sensibilities of the results towards uncertainties in measured variables

Sensitivities of the overall resulting CO_2 fluxes to uncertainties in the determination of the most important measured variables for the presented method were estimated (Table 1). Water temperatures are used on numerous occasions for the calculation of gas exchange rates, e.g. for the calculation of CO_2 from CT and TAlk, for Schmidt numbers, for solubility

Table 1. Sensitivities of the overall resulting CO_2 fluxes to uncertainties in the determination of the most important measured variables of the presented method. The effect of systematic N_2O underestimation was tested using an alternative fit including only upper end values from the Svalbard dataset. The influence of errors in CO_2 gradient determination is denoted for an intermediate gradient of 400 µatm.

Parameter	Uncertainty in parameter	Uncertainty in CO_2 fluxes
Sea surface temperature	±1 °C	±3 %
Mesocosm volume	±1 %	±1 %
Mesocosm surface	±1 %	±1 %
Systematic error in N_2O measurement	Outliers due to losses during sampling	0.26 ± 0.29 %
Air–sea CO_2 gradient	±2 µmol in CT and TAlk	±5 %

and chemical enhancement. Errors in k_{CO_2}, in response to uncertainties in temperature, are mainly caused by the temperature dependence of N_2O solubility. Errors in resulting CO_2 fluxes are largely balanced by errors in CO_2 solubility calculated using identical temperatures. The remaining sensitivity of 3 % for 1 °C appears to be relatively low in respect of usually very precise temperature measurements using current technology. It has to be kept in mind that gas exchange is a continuous process; therefore, measurement frequency should be adequate for sufficient description of relevant temperature changes during the entire duration of the experimental duration. At water temperatures above 10 °C, chemical enhancement corrections become important so that precise temperature records gain additional relevance. Uncertainties in mesocosm volume or surface area translate directly into errors in calculated CO_2 fluxes (one to one %) when k_{CO_2} measured in one mesocosm is applied to calculate gas exchange in a parallel mesocosm with different volume or surface area. A random uncertainty in N_2O determination of 1.8 % as denoted by Walter et al. (2006) would be averaged out due to the large number of fitted measurements. However, a hypothetical systematic underestimation of N_2O by including outliers possibly caused by N_2O losses from oversaturated samples would influence k_{CO_2}. The effect of systematic N_2O underestimation was tested using an alternative fit including only upper end values. Resulting CO_2 fluxes differ by 0.7 % in the beginning of the experiment when N_2O concentrations were high and roughly equal fluxes calculated including all N_2O measurements at the end of the experiment. Maximum uncertainties in CO_2 fluxes of 5 % due to errors in the determination of air–sea CO_2 gradients are calculated on the basis of a maximum uncertainty of ±2 µmol kg^{-1} in CT as well as TAlk and an intermediate CO_2 gradient of ~ 400 µatm. As absolute errors in CO_2 determination have to be seen in relation to the air–sea gradient, percentile errors are small when gradients are large and vice versa. The effects of random errors in CO_2 determination on uncertainties in cumulative CO_2 mass flux over time are averaged out over time. A cumulative error of the applied constants cannot be given but it has to be highlighted that this is an additional source of uncertainty. Parameterisations of Schmidt numbers, solubility and rate constants, as well as diffusion coefficients cited in the text, were chosen to the best of our knowledge.

3.6 Processes driving gas exchange in mesocosms

The concentration of N_2O (C_{N_2O}) decreased quite steadily over the whole experimental period (Fig. 2). This indicates that N_2O fluxes were controlled by the diffusion gradient to the atmosphere. Variable external forcing by wind or waves as commonly observed in natural environments was of minor importance. Wind measurements at Bellevaja station at 10 m above sea level (U_{10}) reported velocities of up to 5 m s^{-1} during the experiment (Fig. 6). The water surface of the mesocosms, however, is sheltered from direct wind sheer by the two meter high plastic walls of the bag (Fig. 1; Riebesell et al., 2012).

Fetch, the distance wind could act on the water surface, was dependent on wind direction (maximum of ~ 10 nm in the Kongsfjorden). Waves that were able to propagate through the mesocosms (significant wave height ($H_{1/3}$) up to ~ 0.8 m) were only observed on the mooring site on three days when stronger winds were blowing along the fjord from southeast, the most exposed wind direction. Enhanced gas exchange during the days with waves could not be resolved by our measurements. However, CO_2 gas exchange inside the mesocosms was measured to be constantly about three times higher than calculated flux at zero wind as performed by Delille et al. (2005) (Fig. 7, stagnant film thickness calculated according to Smith, 1985, chemical enhancement according to Hoover and Berkshire, 1969).

Applying a quadratic wind dependent function (Wanninkhof, 1992) at constant wind speed of 3.15 m s^{-1}, resulting fluxes are very close to our empirical estimate over the whole period. Measured U_{10} wind speeds at the experimental site were generally lower than this (mean 2.1 m s^{-1}), and accordingly calculated mean air–sea gas exchange was also lower outside in the fjord than inside the mesocosms. Compared to relevant open-ocean gas transfer, estimated mesocosm CO_2 transfer velocities between ~ 1.9 to 2.5 cm h^{-1} in the Svalbard experiment are low. They are within a gray zone of baseline gas exchange where buoyancy fluxes and chemical enhancement contribute largely to gas exchange so that purely wind depended parameterisations are not applicable (Wanninkhof et al., 2009). Additional factors can be argued to be driving gas exchange in mesocosms compared to open waters. Rinsing of the plastic walls when waves are propagating through the setup presumably leads to enhanced air–sea surface renewal compared to open water. Slight temperature changes in the surrounding water mass were immediately

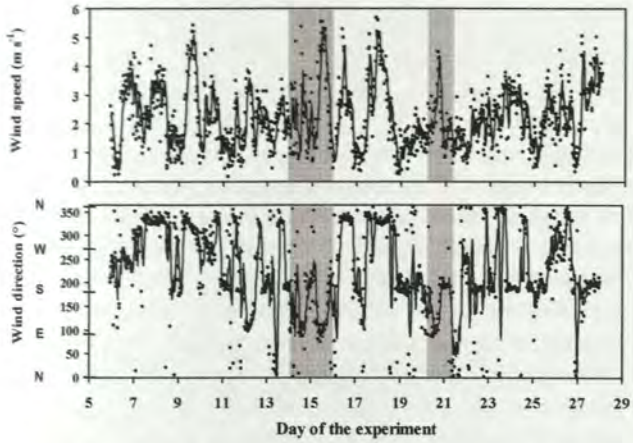

Fig. 6. Wind speed and direction during the course of the experiment, measured at 10 m height at Bayelva station, Ny Alesund. Waves (up to $H_{1/3} = 0.8$ m) were observed at the mooring site during time intervals indicated by shaded areas, when relatively strong wind was blowing along the fjord from southeast.

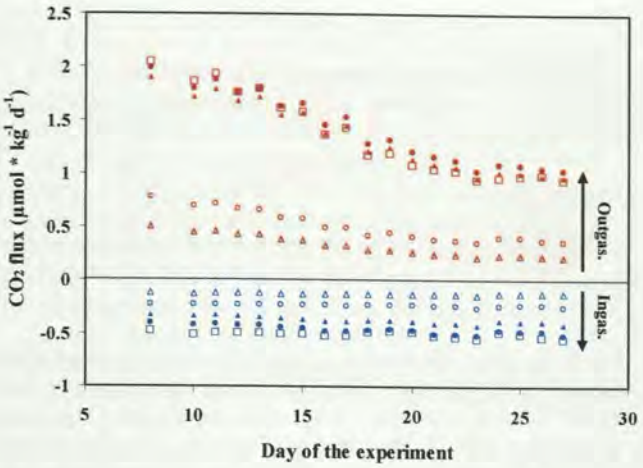

Fig. 7. Comparison of different approaches to estimate CO_2 air–sea gas exchange. Daily ingassing rates in the low CO_2 control treatment (average ~ 180 µatm) are shown in blue, while outgassing from the highest CO_2 treatment (average ~ 1085 µatm) is red. Filled symbols are estimates from the N_2O tracer approach, circles (•) for chemical enhanced flux and triangles (▲) for non chemical enhanced flux. Open squares (□) are an estimate using a quadratic wind dependent function according to Wanninkhof (1992) at a constant wind speed of 3.15 m s^{-1}, chosen to match the N_2O results. Open circles (○) are a chemically enhanced zero wind speed output, according to Smith (1985), while open triangles (△) are the same estimate without chemical enhancement.

heating or cooling the bags (Fig. 5), this probably caused considerably enhanced buoyancy fluxes that kept the experimental units relatively homogenous throughout the experiment. Last but not least, the extensive daily sampling with water samplers and probes contributed to gas exchange by active perturbation of the mesocosm surface.

3.7 Mesocosm proportions

Transfer velocities (k) in other mesocosm setups deployed in more sheltered surroundings, standing on land or inside climate controlled rooms might be lower or higher, depending on methodology used for sampling, temperature control, active mixing and gas specific permeability of the mesocosm material. Even more important than these influences on k, is the ratio between the mesocosm volume and its surface area (A/V), when exchange rates are normalised to units of water (kg^{-1} or L^{-1}). In an exemplary 15 m deep KOSMOS mesocosm (Fig. 1), holding ~ 45 m^3 of water, CO_2 gas exchange over 3.14 m^2 ($A/V = 0.07$) surface area is causing relatively moderate changes in aquatic concentrations despite large diffusion gradients (Fig. 3). Taking the example of the Kiel indoor mesocosm (Fig. 8a) of about 1.4 m^3 at 2 m^2 surface ($A/V = 1.4$), concentration change in response to the same gas exchange flux is 20 times faster. Additionally, air–sea gas exchange velocities are accelerated by continuous active mixing, necessary to keep plankton organisms in suspension (Fig. 8a). While after 20 days ~ 50 % of the N_2O added was still present during the Svalbard study (Fig. 1), the same tracer concentration was virtually gone after five days in the shallow indoor mesocosm (Fig. 8b) in the uncovered configuration. Here, inorganic carbon uptake by phytoplankton can be rapidly compensated by ingassing of CO_2 from the atmosphere. Ocean acidification experiments in setups with A/V similar to the Kiel indoor mesocosm would lose their treatment CO_2 within a few days. To maintain treatment levels in such shallow experiments, continuous measurement and control technology can be used (see e.g. Widdicombe and Needham, 2007) . Resulting controlled treatment levels are beneficial when physiological questions are investigated. However, CO_2 drawdown does not occur, and therefore DIC concentration change cannot be used to calculate NCP. Another option is to artificially decrease the surface area by covering the mesocosm with a low permeability transparent film. For comparison 50 nmol kg^{-1} N_2O was added to two Kiel indoor mesocosms, one in an uncovered configuration and one covered with a transparent floating foil to reduce surface in contact with the atmosphere (Fig. 8a). Both mesocosms were stirred at the same speed; samples were drawn using a tube. The thin polyurethane foil mounted on a light frame and floating on the surface, efficiently minimised air–sea gas exchange (Fig. 8b). If covers are used, reducing the surface area to a minimum, it has to be considered that the remaining open surface should be equally large. As the working principle of this approach is to minimise surface area, it can be assumed to be very sensible to the size of the remaining interface (leaks). Therefore, air–sea gas exchange should be measured in all experimental units to check for reproducibility of results.

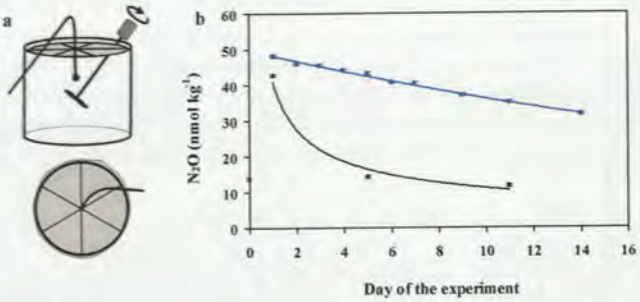

Fig. 8. (a) Schematic drawing of the Kiel indoor mesocosm. With stirrer, floating lid and sampling hose, below: vertical view on floating foil lid with enforcement frame. **(b)** Comparison of N_2O tracer outgassing in a Kiel indoor mesocosm, between a simple uncovered setup (black) and a setup using a floating foil lid reducing the water surface area available for air–sea gas exchange (blue).

4 Conclusion and outlook

Direct measurement of N_2O air–sea gas exchange can be used to estimate accurate CO_2 fluxes in various mesocosm setups, whereas common wind dependent parameterisations for air–sea gas exchange cannot be adapted to mesocosm conditions and their application is therefore prone to systematic errors. Within the mesocosm low energy physical surrounding, N_2O gas exchange measurements allow for direct estimation of CO_2 fluxes with uncertainties far below open-ocean dual tracer measurements due to a known, constant water volume. Measured transfer velocities are within the range of zero wind open-ocean baseline velocities assumed to be dominated by chemical enhancement and buoyancy fluxes (Wanninkhof et al., 2009). The influence of sea surface microlayers of surface active organic molecules is discussed to be responsible for large discrepancies in gas exchange between productive coastal waters and open-ocean conditions (Frew, 1997; Kock et al., 2012). The decrease in open-ocean k by 20–50 %, due to surfactants smoothening wind effects on the water surface (Tsai and Liu, 2003), can be expected to be of minor relevance to mesocosm gas exchange where wind stress is not the dominating energy input. The effect of these surfactants, possibly produced in high amounts during phytoplankton blooms in mesocosms, is difficult to include in theoretical calculations, but is inherently included in our direct measurements. Future mesocosm experiments combining the close observation of biological, chemical and physical processes might offer the opportunity to bring more light into origin and composition of organic surface microlayers.

The application of gas exchange measurements for calculation of NCP inside the mesocosm delivered satisfying results. Of the four community production estimates published for the Svalbard 2010 experiment, NCP calculated from changes in dissolved inorganic carbon corrected for air–sea gas exchange (Czerny et al., 2012a; Silyakova et al., 2012) seems to be quantitatively most plausible. Although overall quantity compares relatively well with results from oxygen and in situ ^{13}C- primary production estimates (Tanaka et al., 2013; de Kluijver et al., 2013), comparability to ^{14}C incubation data presented by Engel et al. (2012) is weak. Much higher ^{14}C fixation rates can be plausibly explained by the shallow (~ 1 m) incubation depth, while oxygen incubations obviously experienced more intermediate light and temperature conditions at ~ 4 m depth. ^{13}C tracer incorporation measurements inside the mesocosm deliver results representative for the entire mesocosm but only for a period before organic matter approached saturation with the tracer (de Kluijver et al., 2013). Rates measured in side experiments are more useful to compare community production between the treatments rather than giving quantitative cumulative estimates for in situ carbon uptake (see discussion in Engel et al., 2012). As incubations were performed only at one depth, it is impossible to integrate these data over time and depth in respect of variable light and temperature gradients. Summing up incubation results to achieve cumulative estimates could lead to further error propagation, whereas NCP calculated from in situ inorganic carbon measurements is per se cumulative and propagation of single measurement errors cannot occur.

Further development of the N_2O tracer concept is focussed on using it not only to determine air–sea gas exchange in stratified mesocosms, but also to estimate diapycnal mixing between surface layer and deep water inside mesocosms. For this purpose, N_2O gradients developing over time will be correlated to high resolution profiles of oxygen, pH and salinity, measured with CTD sensors. Especially in temperate turbid waters, mesocosm NCP is mostly not restricted by mesocosm length but by light penetration. The photoautotrophic surface layer communicates to some extent with a more nutrient rich deep layer where heterotrophic processes dominate. Budgeting these more naturally structured mesocosms is not only an interesting challenge, but will also introduce new ecological aspects connected to upward and downward elemental fluxes into the biogeochemical interpretation of the mesocosm system.

Acknowledgements. This work is a contribution to the "European Project on Ocean Acidification" (EPOCA) which received funding from the European Community's Seventh Framework Programme (FP7/2007-2013) under grant agreement no. 211384. Financial support was provided through Transnational Access funds by the European Union Seventh Framework Program (FP7/2007-2013) under grant agreement no. 22822 MESOAQUA and by the Federal Ministry of Education and Research (BMBF, FKZ 03F0608) through the BIOACID (Biological Impacts of Ocean ACIDification) project. We acknowledge Annette Kock and Hermann Bange for support in measuring N_2O as well as Allanah Paul and Scarlett Sett for providing measurements from the Kiel indoor mesocosms. We thank Thomas Conway from the NOAA Carbon Cycles Gases Group in Boulder, US, and Johan Ström from ITM,

Stockholm University, Sweden, for providing us with atmospheric N_2O and CO_2 measurements, respectively, from close by Zeppelin Mountain. We gratefully acknowledge the logistical support of Greenpeace International for its assistance with the transport of the mesocosm facility from Kiel to Ny-Ålesund and back to Kiel. We also thank the captains and crews of M/V *ESPERANZA* of Greenpeace and R/V *Viking Explorer* of the University Centre in Svalbard (UNIS) for assistance during mesocosm transport and during deployment and recovery in Kongsfjorden. We thank the staff of the French-German Arctic Research Base at Ny-Ålesund, in particular Marcus Schumacher, for on-site logistical support.

The service charges for this open access publication have been covered by a Research Centre of the Helmholtz Association.

Edited by: J. Middelburg

References

Archer, S. D., Kimmance, S. A., Stephens, J. A., Hopkins, F. E., Bellerby, R. G. J., Schulz, K. G., Piontek, J., and Engel, A.: Contrasting responses of DMS and DMSP to ocean acidification in Arctic waters, Biogeosciences Discuss., 9, 12803–12843, doi:10.5194/bgd-9-12803-2012, 2012.

Bange, H. W., Rapsomanikis, S., and Andreae, M. O.: Nitrous oxide in coastal waters, Global Biogeochem. Cy., 10, 197–207, doi:10.1029/95gb03834, 1996.

Bellerby, R. G. J., Silyakova, A., Nondal, G., Slagstad, D., Czerny, J., de Lange, T., and Ludwig, A.: Marine carbonate system evolution during the EPOCA Arctic pelagic ecosystem experiment in the context of simulated Arctic ocean acidification, Biogeosciences Discuss., 9, 15541–15565, doi:10.5194/bgd-9-15541-2012, 2012.

Berger, R. and Libby, W. F.: Equilibration of Atmospheric Carbon Dioxide with Sea Water: Possible Enzymatic Control of the Rate, Science, 164, 1395–1397, doi:10.1126/science.164.3886.1395, 1969.

Broecker, W. S. and Peng, T.-H.: Gas exchange rates between air and sea, Tellus, 26, 21–35, 1974.

Czerny, J., Schulz, K. G., Boxhammer, T., Bellerby, R. G. J., Büdenbender, J., Engel, A., Krug, S. A., Ludwig, A., Nachtigall, K., Nondal, G., Niehoff, B., Siljakova, A., and Riebesell, U.: Element budgets in an Arctic mesocosm CO_2 perturbation study, Biogeosciences Discuss., 9, 11885–11924, doi:10.5194/bgd-9-11885-2012, 2012a.

Czerny, J., Schulz, K. G., Krug, S. A., Ludwig, A., and Riebesell, U.: Technical Note: On the determination of enclosed water volume in large flexible-wall mesocosms, Biogeosciences Discuss., 9, 13019-13030, doi:10.5194/bgd-9-13019-2012, 2012b.

de Kluijver, A., Soetaert, K., Czerny, J., Schulz, K. G., Boxhammer, T., Riebesell, U., and Middelburg, J. J.: A ^{13}C labelling study on carbon fluxes in Arctic plankton communities under elevated CO_2 levels, Biogeosciences, in press, 2013.

Degreif, K. A.: Untersuchungen zum Gasaustausch: Entwicklung und Applikation eines zeitlich aufgelösten Massenbilanzverfahrens, Ph.D., Naturwissenschaftlich-Mathematische Gesamtfakultät, Ruprecht-Karls-Universität, Heidelberg, 183 pp., 2006.

Delille, B., Harlay, J., Zondervan, I., Jacquet, S., Chou, L., Wollast, R., Bellerby, R. G. J., Frankignoulle, M., Borges, A. V., Riebesell, U., and Gattuso, J.-P.: Response of primary production and calcification to changes of pCO_2 during experimental blooms of the coccolithophorid Emiliania huxleyi, Global Biogeochem. Cy., 19, GB2023, doi:10.1029/2004gb002318, 2005.

Dickson, A. G.: An exact definition of total alkalinity and a procedure for the estimation of alkalinity and total inorganic carbon from titration data., Deep-Sea Res., 28, 609–623, 1981.

Dore, J. E. and Karl, D. M.: Nitrification in the euphotic zone as a source for nitrite, nitrate, and nitrous oxide at Station ALOHA, Limnol. Oceanogr., 41, 1619–1628, 1996.

Emerson, S.: Chemically enhanced CO_2 gas exchange in a eutrophic lake: a general model, Limnol. Oceanogr., 20, 743–753, 1975.

Engel, A., Borchard, C., Piontek, J., Schulz, K., Riebesell, U., and Bellerby, R.: CO_2 increases ^{14}C-primary production in an Arctic plankton community, Biogeosciences Discuss., 9, 10285–10330, doi:10.5194/bgd-9-10285-2012, 2012.

Frew, N. M.: The role of organic films in air-sea gas exchange, in: The Sea Surface And Global Change, edited by: Liss, P. S. and Duce, R. A., Cambridge University Press, Cambridge, 121–171, 1997.

Goldman, J. C. and Dennett, M. R.: Carbon Dioxide Exchange Between Air and Seawater: No Evidence for Rate Catalysis, Science, 220, 199–201, doi:10.1126/science.220.4593.199, 1983.

Goreau, T. J., Kaplan, W. A., Wofsy, S. C., McElroy, M. B., Valois, F. W., and Watson, S. W.: Production of NO_2- and N_2O by Nitrifying Bacteria at Reduced Concentrations of Oxygen, Appl. Environ. Microb., 40, 526–532, 1980.

Hoover, T. E. and Berkshire, D. C.: Effects of Hydration on Carbon Dioxide Exchange across an Air-Water Interface, J. Geophys. Res., 74, 456–464, doi:10.1029/JB074i002p00456, 1969.

Hopkins, F. E., Kimmance, S. A., Stephens, J. A., Bellerby, R. G. J., Brussaard, C. P. D., Czerny, J., Schulz, K. G., and Archer, S. D.: Response of halocarbons to ocean acidification in the Arctic, Biogeosciences Discuss., 9, 8199–8239, doi:10.5194/bgd-9-8199-2012, 2012.

Jähne, B., Heinz, G., and Dietrich, W.: Measurement of the Diffusion Coefficients of Sparingly Soluble Gases in Water, J. Geophys. Res., 92, 10767–10776, 10.1029/JC092iC10p10767, 1987.

Johnson, K. S.: Carbon dioxide hydration and dehydration kinetics in seawater, Limonol. Oceanogr., 27, 849–855, 1982.

Keller, K.: Chemical enhancement of CO_2 transfer across the Air sea interface, M.S., Mass. Inst. Technol., Boston, 120 pp., 1994.

Kock, A., Schafstall, J., Dengler, M., Brandt, P., and Bange, H. W.: Sea-to-air and diapycnal nitrous oxide fluxes in the eastern tropical North Atlantic Ocean, Biogeosciences, 9, 957–964, doi:10.5194/bg-9-957-2012, 2012.

Kuss, J., and Schneider, B.: Chemical enhancement of the CO_2 gas exchange at a smooth seawater surface, Mar. Chem., 91, 165–174, 2004.

Lewis, E. L. and Wallace, D. W. R.: Basic programs for the CO_2 system in seawater, Brookhaven National Laboratory Informal Report, BNL# 61827, 1995.

Liss, P. S.: Processes of gas exchange across an air-water interface, Deep Sea Res., 20, 221–238, 1973.

Löscher, C. R., Kock, A., Könneke, M., LaRoche, J., Bange, H. W., and Schmitz, R. A.: Production of oceanic nitrous oxide

by ammonia-oxidizing archaea, Biogeosciences, 9, 2419–2429, doi:10.5194/bg-9-2419-2012, 2012.

Petersen, J. E., Kemp, W. M., Bartleson, R., Boynton, W. R., Chen, C.-C., Cornwell, J. C., Gardner, R. H., Hinkle, D. C., Houde, E. D., Malone, T. C., Mowitt, W. P., Murray, L., Sanford, L. P., Stevenson, J. C., Sundberg, K. L., and Suttles, S. E.: Multiscale experiments in coastal ecology: Improving realism and advancing theory, BioScience, 53, 1181–1197, 2003.

Quinn, J. A. and Otto, N. C.: Carbon Dioxide Exchange at the Air-Sea Interface: Flux Augmentation by Chemical Reaction, J. Geophys. Res., 76, 1539–1549, doi:10.1029/JC076i006p01539, 1971.

Rees, A. P., Brown, I. J., Clark, D. R., and Torres, R.: The Lagrangian progression of nitrous oxide within filaments formed in the Mauritanian upwelling, Geophys. Res. Lett., 38, L21606, doi:10.1029/2011gl049322, 2011.

Rhee, T. S.: The process of air water gas exchange and its application, Ph.D. thesis, College Station, A&M University, Texas, 2000.

Riebesell, U., Czerny, J., von Bröckel, K., Boxhammer, T., Büdenbender, J., Deckelnick, M., Fischer, M., Hoffmann, D., Krug, S. A., Lentz, U., Ludwig, A., Muche, R., and Schulz, K. G.: Technical Note: A mobile sea-going mesocosm system – new opportunities for ocean change research, Biogeosciences Discuss., 9, 12985–13017, doi:10.5194/bgd-9-12985-2012, 2012.

Santoro, A. E., Casciotti, K. L., and Francis, C. A.: Activity, abundance and diversity of nitrifying archaea and bacteria in the central California Current, Environ. Microbiol., 12, 1989–2006, doi:10.1111/j.1462-2920.2010.02205.x, 2010.

Schulz, K. G., Bellerby, R. G. J., Brussaard, C. P. D., Büdenbender, J., Czerny, J., Engel, A., Fischer, M., Koch-Klavsen, S., Krug, S. A., Lischka, S., Ludwig, A., Meyerhöfer, M., Nondal, G., Silyakova, A., Stuhr, A., and Riebesell, U.: Temporal biomass dynamics of an Arctic plankton bloom in response to increasing levels of atmospheric carbon dioxide, Biogeosciences, 10, 161–180, doi:10.5194/bg-10-161-2013, 2013.

Silyakova, A., Bellerby, R. G. J., Czerny, J., Schulz, K. G., Nondal, G., Tanaka, T., Engel, A., De Lange, T., and Riebesell, U.: Net community production and stoichiometry of nutrient consumption in a pelagic ecosystem of a northern high latitude fjord: mesocosm CO_2 perturbation study, Biogeosciences Discuss., 9, 11705–11737, doi:10.5194/bgd-9-11705-2012, 2012.

Sinha, V., Williams, J., Meyerhöfer, M., Riebesell, U., Paulino, A. I., and Larsen, A.: Air-sea fluxes of methanol, acetone, acetaldehyde, isoprene and DMS from a Norwegian fjord following a phytoplankton bloom in a mesocosm experiment, Atmos. Chem. Phys., 7, 739–755, doi:10.5194/acp-7-739-2007, 2007.

Smith, S. V.: Physical, chemical and biological characteristics of CO_2 gas flux across the air-water interface, Plant Cell Environ., 8, 387–398, doi:10.1111/j.1365-3040.1985.tb01674.x, 1985.

Tanaka, T., Alliouane, S., Bellerby, R. G. B., Czerny, J., de Kluijver, A., Riebesell, U., Schulz, K. G., Silyakova, A., and Gattuso, J.-P.: Effect of increased pCO_2 on the planktonic metabolic balance during a mesocosm experiment in an Arctic fjord, Biogeosciences, 10, 315–325, doi:10.5194/bg-10-315-2013, 2013.

Taucher, J., Schulz, K. G., Dittmar, T., Sommer, U., Oschlies, A., and Riebesell, U.: Enhanced carbon overconsumption in response to increasing temperatures during a mesocosm experiment, Biogeosciences, 9, 3531–3545, doi:10.5194/bg-9-3531-2012, 2012.

Tsai, W.-T. and Liu, K.-K.: An assessment of the effect of sea surface surfactant on global atmosphere-ocean CO_2 flux, J. Geophys. Res., 108, 24.21–24.16, 2003.

Walter, S., Bange, H. W., Breitenbach, U., and Wallace, D. W. R.: Nitrous oxide in the North Atlantic Ocean, Biogeosciences, 3, 607–619, doi:10.5194/bg-3-607-2006, 2006.

Wanninkhof, R.: Relationship between wind speed and gas exchange over the ocean, J. Geophys. Res., 97, 7373–7382, doi:10.1029/92jc00188, 1992.

Wanninkhof, R. and Knox, M.: Chemical enhancement of CO_2 exchange in natural waters, Limonol. Oceanogr., 41, 689–697, 1996.

Wanninkhof, R., Asher, W. E., Ho, D. T., Sweeney, C., and McGillis, W. R.: Advances in quantifying air-sea gas exchange and environmental forcing, Annu. Rev. Mar. Sci., 1, 213–244, 2009

Weiss, R. F. and Price, B. A.: Nitrous oxide solubility in water and seawater, Mar. Chem., 8, 347–359, 1980.

Widdicombe, S. and Needham, H. R.: Impact of CO_2-induced seawater acidification on the burrowing activity of Nereis virens and sediment nutrient flux, Mar. Ecol.-Prog. Ser., 341, 111–122, 2007.

Wilke, C. R. and Chang, P.: Correlation of diffusion coefficients in dilute solutions, AICHE J., 1, 264–270, doi:10.1002/aic.690010222, 1955.

Williams, G. R.: The Rate of Hydration of Carbon Dioxide in Natural Waters, Environ. Biogeochem., 35, 281–289, 1983.

Wohlers, J., Engel, A., Zöllner, E., Breithaupt, P., Jürgens, K., Hoppe, H.-G., Sommer, U., and Riebesell, U.: Changes in biogenic carbon flow in response to sea surface warming, P. Natl. Acad. Sci., 106, 7067–7072, doi:10.1073/pnas.0812743106, 2009.

Zamora, L. M., Oschlies, A., Bange, H. W., Huebert, K. B., Craig, J. D., Kock, A., and Löscher, C. R.: Nitrous oxide dynamics in low oxygen regions of the Pacific: insights from the MEMENTO database, Biogeosciences, 9, 5007–5022, doi:10.5194/bg-9-5007-2012, 2012.

Zeebe, R. E. and Wolf-Gladrow, D.: CO_2 in seawater: equilibrium, kinetics, isotopes, Elsevier Oceanography Series, edited by: Halpen, D., Elsevier, Amsterdam, 2001.

Zumft, W. G.: Cell biology and molecular basis of denitrification, Microbiol. Mol. Biol. Rev., 61, 533–616, 1997.

Manuscript 2.4:

Sediment sample processing

by Jan Czerny, Tim Boxhammer, Klaus von Bröckel, Andrea Ludwig, and Ulf Riebesell

Sediment sample processing

Similar to many previous mesocosm setups, KOSMOS prior to 2010 used sediment traps placed within the mesocosm to quantify sinking material. Sediment data were found to be of a more qualitative than quantitative nature. Within published experiments, sinking fluxes were calculated on the basis of those data often only when combining measured elemental composition with mass balance calculations based on water column data (Riebesell et al., 2008; Vadstein et al., 2012). After analysing the first sediment dataset from the 2009 Baltic Sea experiment, problems in gathering qualitative data on sinking fluxes within the mesocosms became evident. Daily measured sediment quantities as well as elemental composition of the material were strongly variable, impeding publication of the dataset. A correlation to parallel water column data could hardly be detected. Variability was presumably caused by resuspension of already settled material and uneven distribution of sinking matter within the mesocosm. Sinking flux measurements were improved on several stages of the protocol for the 2010 Svalbard experiment. Firstly, the collection of the sinking material was expanded from sampling a sub-unit of the bottom surface to a sediment trap covering the entire bottom surface. Secondly, the sampling method was improved in terms of technical reliability, sampling speed and most importantly in preserving the integrity of the sediment particles. Therefore the diameter of the extraction hoses was enlarged (from 5 to 10 mm) and the battery driven peristaltic pump was replaced by a hand operated vacuum system. This procedure keeps aggregates fairly intact instead of dispersing the sediment material within the attendant water. Blurry sediment samples with large parts of the aggregates dispersed can only be sampled by filtration techniques, impracticable at prevailing particle densities. Consequently, as a third innovation, the sample preservation and sub-sampling method was changed from a filtration technique as applied to water samples to a centrifugation technique taking advantage of particles sinking.

The aim of the sediment processing technique, developed for the Svalbard 2010 experiment, was to quantitatively extract and homogenize all settling particles sampled from the mesocosm for representative sub-sampling. Even the largest sinking items e.g. dead juvenile fish are represented in all homogenized sub-samples analysed for this sampling day, instead of producing an outlier in one of the measurements.

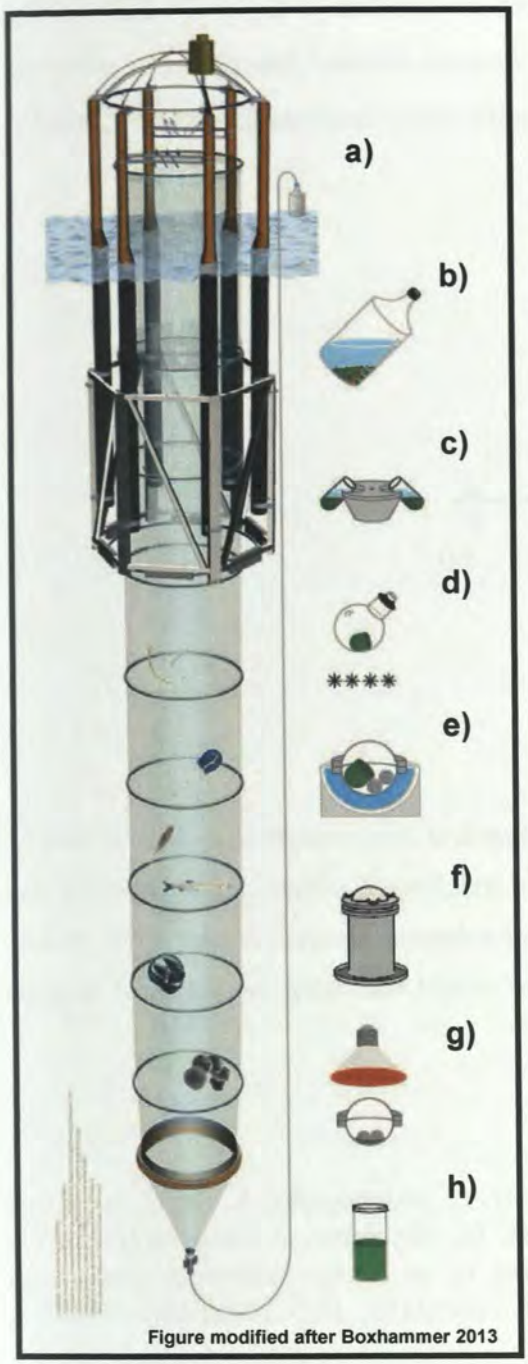

Figure 2.1. Processing of the sediment samples. a) Extraction of settled material in regular intervals, b) settling and decantation, c) centrifugation d) lyophilisation, e) embrittlement, f) grinding, g) warming, h) storage.

Sedimented material collecting in the funnel tip at the bottom of KOSMOS mesocosms is extracted by applying a hand pumped vacuum on a 5 L glass bottle connected to a silicon rubber hose reaching from the sea surface down to the funnel tip (Fig. 2.1a). The bottles with sediment material and attendant water are kept in a cool room for about two hours to settle, allowing extraction of the clear supernatant. In later experiments, a solution of $FeCl_3$ together with NaOH was used to speed up aggregation by precipitating the small fraction of fine particles within the water phase (Fig. 2.1b). The dense material left is centrifuged to a compact pellet (Fig. 2.1c) and stored at -20 °C. Pellets are later dried by lyophilisation, avoiding evaporation or decay of sensitive organic compounds (Fig. 2.1d). Prior to grinding, lipids and tough components within the dried material are embrittled by cooling with liquid nitrogen (Fig. 2.1e). A custom-built stainless steel ball mill is used for the grinding process (Fig. 2.1f). After warming to room temperature, the fine powder is transferred into storage vessels that are kept cold and dark (Fig. 2.1g, h). Elemental analyses for carbon, nitrogen, phosphorus and biogenic silica on sub-samples of the ground material show high reproducibility similar to homogenous reference material (Fig. 2.2).

There is usually sufficient material available for test measurements and replication, and even repetition of entire analytic runs. After test analyses, sample size is adjusted to the required range for any specific analytical method. For the Svalbard 2010 experiment, ground material was analysed for inorganic and organic carbon, as well as total nitrogen, phosphorous and biogenic silica (Czerny et al., 2013). Furthermore, $\delta^{13}C$ elemental composition of specific fatty acids in the sediment was analysed to track the contribution of different food web components to sinking

flux after deliberate ^{13}C enrichment in the water column (de Kluijver et al., 2013). HPLC (**H**igh **P**ressure **L**iquid **C**hromatography) analyses of phytopigments showed that pigments were well preserved allowing analyses of the contribution of specific phytoplankton taxa to sediment flux (unpublished results).

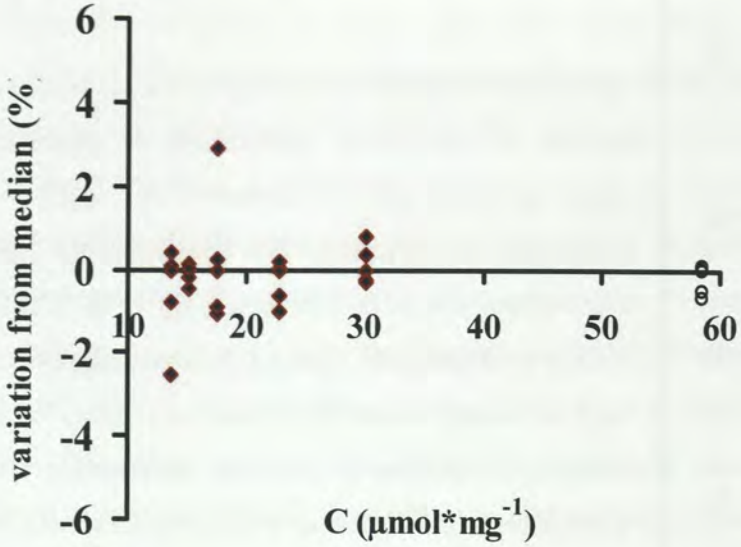

Figure 2.2. Variation in carbon of replicate carbon measurements of five homogenised sediment samples (black dots) featuring carbon contents between 13 and 30 µmol*mg^{-1}C. Open circles represent five replicate measurements of acetanilide used as homogeneous reference material. Measurement of each ~4mg sample and 0.4mg acetanilide in tin capsules was carried out using an elemental analyser (EuroVektor EA) according to Sharp (1974).

References sediment sample processing

Czerny, J., Schulz, K. G., Boxhammer, T., Bellerby, R. G. J., Büdenbender, J., Engel, A., Krug, S. A., Ludwig, A., Nachtigall, K., Nondal, G., Niehoff, B., Silyakova, A., and Riebesell, U.: Implications of elevated CO_2 on pelagic carbon fluxes in an Arctic mesocosm study - an elemental mass balance approach, Biogeosciences, 10, 3109-3125, 10.5194/bg-10-3109-2013, 2013.

de Kluijver, A., Soetaert, K., Czerny, J., Schulz, K. G., Boxhammer, T., Riebesell, U., and Middelburg, J. J.: A ^{13}C labelling study on carbon fluxes in Arctic plankton communities under elevated CO levels, Biogeosciences, 10, 1425-1440, 10.5194/bg-10-1425-2013, 2013.

Riebesell, U., Bellerby, R. G. J., Grossart, H. P., and Thingstad, F.: Mesocosm CO_2 perturbation studies: from organism to community level, Biogeosciences 5, 1157-1164, 2008.

Sharp, J. H.: Improved analysis for "particulate" organic carbon and nitrogen from seawater., Limnology and Oceanography, 19, 984-989, 1974.

Vadstein, O., Andersen, T., Reinertsen, H. R., and Olsen, Y.: Carbon, nitrogen and phosphorus resource supply and utilisation for coastal planktonic heterotrophic bacteria in a gradient of nutrient loading, Marine Ecology Progress Series, 447, 55-75, 10.3354/meps09473, 2012.

Manuscript 2.5:

Implications of elevated CO_2 on pelagic carbon fluxes in an Arctic mesocosm study – an elemental mass balance approach

Published in Biogeosciences

Biogeosciences, 10, 3109–3125, 2013
www.biogeosciences.net/10/3109/2013/
doi:10.5194/bg-10-3109-2013

Biogeosciences Open Access

Implications of elevated CO_2 on pelagic carbon fluxes in an Arctic mesocosm study – an elemental mass balance approach

J. Czerny[1], K. G. Schulz[1,6], T. Boxhammer[1], R. G. J. Bellerby[2,3,4], J. Büdenbender[1], A. Engel[1], S. A. Krug[1], A. Ludwig[1], K. Nachtigall[1], G. Nondal[4], B. Niehoff[5], A. Silyakova[2], and U. Riebesell[1]

[1]GEOMAR Helmholtz Centre for Ocean Research Kiel, 24105 Kiel, Germany
[2]Bjerknes Centre for Climate Research, 5007 Bergen, Norway
[3]Geophysical Institute, University of Bergen, 5007 Bergen, Norway
[4]Norwegian Institute for Water Research (NIVA), 5006 Bergen, Norway
[5]Alfred Wegener Institute for Polar and Marine Research, 27515 Bremerhaven, Germany
[6]Centre for Coastal Biogeochemistry, Southern Cross University, Lismore, NSW 2480, Australia

Correspondence to: J. Czerny (jczerny@geomar.de)

Received: 31 July 2012 – Published in Biogeosciences Discuss.: 31 August 2012
Revised: 28 March 2013 – Accepted: 7 April 2013 – Published: 8 May 2013

Abstract. Recent studies on the impacts of ocean acidification on pelagic communities have identified changes in carbon to nutrient dynamics with related shifts in elemental stoichiometry. In principle, mesocosm experiments provide the opportunity of determining temporal dynamics of all relevant carbon and nutrient pools and, thus, calculating elemental budgets. In practice, attempts to budget mesocosm enclosures are often hampered by uncertainties in some of the measured pools and fluxes, in particular due to uncertainties in constraining air–sea gas exchange, particle sinking, and wall growth. In an Arctic mesocosm study on ocean acidification applying KOSMOS (Kiel Off-Shore Mesocosms for future Ocean Simulation), all relevant element pools and fluxes of carbon, nitrogen and phosphorus were measured, using an improved experimental design intended to narrow down the mentioned uncertainties. Water-column concentrations of particulate and dissolved organic and inorganic matter were determined daily. New approaches for quantitative estimates of material sinking to the bottom of the mesocosms and gas exchange in 48 h temporal resolution as well as estimates of wall growth were developed to close the gaps in element budgets. However, losses elements from the budgets into a sum of insufficiently determined pools were detected, and are principally unavoidable in mesocosm investigation. The comparison of variability patterns of all single measured datasets revealed analytic precision to be the main issue in determination of budgets. Uncertainties in dissolved organic carbon (DOC), nitrogen (DON) and particulate organic phosphorus (POP) were much higher than the summed error in determination of the same elements in all other pools. With estimates provided for all other major elemental pools, mass balance calculations could be used to infer the temporal development of DOC, DON and POP pools.

Future elevated pCO_2 was found to enhance net autotrophic community carbon uptake in two of the three experimental phases but did not significantly affect particle elemental composition. Enhanced carbon consumption appears to result in accumulation of dissolved organic carbon under nutrient-recycling summer conditions. This carbon overconsumption effect becomes evident from mass balance calculations, but was too small to be resolved by direct measurements of dissolved organic matter. Faster nutrient uptake by comparatively small algae at high CO_2 after nutrient addition resulted in reduced production rates under future ocean CO_2 conditions at the end of the experiment. This CO_2 mediated shift towards smaller phytoplankton and enhanced cycling of dissolved matter restricted the development of larger phytoplankton, thus pushing the system towards a retention type food chain with overall negative effects on export potential.

Published by Copernicus Publications on behalf of the European Geosciences Union.

1 Introduction

Increasing atmospheric CO_2 concentration is the major man-made geochemical perturbation characterising the anthropocene (Doney, 2010; Revelle and Suess, 1957). Atmospheric CO_2 partial pressure already increased by 40% since the beginning of industrialisation, while rates of CO_2 emissions are continuing to increase beyond most modelled worst-case scenarios, e.g. SRES (Special Report on Emissions Scenarios) A1FI (Meehl et al., 2007; Friedlingstein et al., 2010). Correlations of increasing CO_2 concentrations to global warming are predictable and documented by current measurements as well as in the geological record (Hansen et al., 2006; Petit et al., 1999). About one third of the currently emitted CO_2 is dissolving in the world oceans, serving as a buffer for global climate change (Sabine et al., 2004). However, most of the absorbed CO_2 is accumulating in the surface ocean, separated from deep water masses by thermal stratification, which will further strengthen under global warming. In surface waters, ocean carbonation (increasing CO_2 concentrations) and consequential ocean acidification (decreasing pH) are affecting marine organisms, thereby modulating ecosystem functioning (Riebesell et al., 2009). A predominant geochemical function of the marine planktonic ecosystem is the formation of organic matter from dissolved CO_2. Sinking of this organic matter, transporting carbon across barriers of physical mixing into the ocean interior is referred to as the biological carbon pump (Sarmiento and Le Quéré, 1996; Volk and Hoffert, 1985). Increasing temperatures affect the ocean's function as a physical CO_2 sink, but acidification and carbonation are likely to impact also future biological carbon sequestration (Riebesell and Tortell, 2011; Gruber, 2011).

The Arctic Ocean plays a key role in sequestration of anthropogenic carbon for several reasons. From the physical perspective, high solubility of CO_2 in cold water leads to a high physical sequestration potential of anthropogenic CO_2 in areas of deep water formation. From the biological perspective, nutrient supply to the surface layer during winter deep mixing can promote pulses of high productivity with a large potential for carbon export via the biological pump (Lutz et al., 2007). Whether there is a net release or sequestration of atmospheric carbon depends on the carbon to nutrient ratio and sinking rate of the material exported after a mixing event. These properties are known to be highly variable, depending on food web structure. Deep sedimentation events in the Arctic Ocean may occur when fast sinking particles are formed, i.e. through coagulation of diatom blooms (Klaas and Archer, 2002) or by pteropods and their sticky nets (Bathmann et al., 1991). But efficient recycling of material by a surface layer retention food web may keep export at a low level (von Bodungen et al., 1995). Ocean warming and acidification are expected to impact ecosystems particularly in Arctic regions. Sea-surface warming will likely result in elevated primary production due to a reduction of sea ice cover and the shoaling of mixed layer depth in the light limited Arctic. Estimates for these effects of sea-surface warming are implemented in various global carbon flux models (Bopp et al., 2001; Sarmiento et al., 2004; Schmittner et al., 2008), whereas effects of changing seawater carbonate chemistry and pH on Arctic community export production are more difficult to quantify.

Ocean acidification and carbonation have the potential to directly affect ecosystem functioning in numerous ways. Of those, the adverse effect of future decreasing pH and carbonate ion concentrations on marine calcification is the most investigated mechanism (Riebesell, 2004; Fabry et al., 2008). Pteropods and foraminifera, the only calcifying organisms of significant relevance to the high Arctic pelagic ecosystem examined, were found to be very sensitive to ocean acidification (Comeau et al., 2009; Lombard et al., 2010; Lischka et al., 2011). Carbonation is also found to directly affect photoautotrophic carbon fixation of cultured marine phytoplankton and natural plankton assemblages (Riebesell and Tortell, 2011). In most studies, elevated CO_2 is reported to enhance carbon fixation, however, CO_2 affinity differs between different algal taxonomic groups (Reinfelder, 2011). In addition to effects of ocean carbonation on primary production, bacterial enzymatic rates were found to be directly affected by decreasing seawater pH (Piontek et al., 2010). Moreover, chemical speciation of potentially limiting micronutrients seems to be pH dependent in the range of projected ocean acidification (Millero et al., 2009).

Increased inorganic carbon consumption in response to elevated pCO_2 was already found in incubated natural plankton communities of the North Atlantic (Hein and Sand-Jensen, 1997) and in mesocosm studies in a Norwegian Fjord compiled by Riebesell et al. (2008). CO_2 induced overconsumption of carbon that was presumably exuded by phytoplankton cells in form of organic matter, which was measured as transparent exopolymer particles (TEP). The sticky carbon-rich TEP aggregated with other particles in the water column, thereby potentially increasing carbon export (Engel, 2002; Engel et al., 2004a). Enrichment of carbon relative to nitrogen in the exported matter would cause a substantial increase in the total amount of carbon sequestered in the future ocean (Oschlies, 2009).

This study investigates the response of a natural Arctic plankton community, including all trophic levels from bacteria to millimetre-sized zooplankton, to changes in seawater carbonate chemistry. Treatment levels ranged from ~ 180 µatm CO_2, as prevailing during the early summer situation in the beginning of the experiment, over present day and year 2100 atmospheric projections to extreme values of up to 1420 µatm CO_2. Using tracer gas exchange measurements and quantitative high resolution sediment sampling, we are able to present daily budget calculations for carbon, nitrogen, and phosphorus in all mesocosms. Mass balance calculations were used to crosscheck measured trends and to provide a quantitative evaluation of biogeochemical

fluxes. A "Pool X" representing the carbon not reproducibly measured on a daily basis will be discussed to evaluate the performance of the applied methods and to identify problematic measurement parameters. Those parameters (DOC, DON and POP) will be then estimated based on mass balance calculations. CO_2-induced changes in carbon fluxes within the water column, towards export and in exchange with the atmosphere are detected using correlation statistics. The presented dataset focuses on carbon fixation and export, but is however too unspecific to provide detailed insights into ecosystem functioning. Based on the presented mass balance, elemental cycling and export is discussed with reference to publications on the same experiment, putting biogeochemistry in the context of the observed plankton community composition.

2 Material and methods

2.1 Experimental set-up

Nine KOSMOS (Kiel Off-Shore Mesocosms for future Ocean Simulation) mesocosms were moored in the Kongsfjord, Svalbard (78°56.2′ N, 11°53.6′ E). The enclosures were cylindrical polyurethane bags 2 m in diameter, 17 m long and reaching ~ 15 m deep into the water. The bags were supported by a stainless steel and glass fibre flotation frame and weighted at the bottom with steel rings closable with polycarbonate watertight shutters. The bags reaching 2 m above the water surface were open to the atmosphere. A spiked roof was mounted at the top to prevent birds from resting on the structures and introducing nutrients into the system (Fig. 1). The fjord water, enclosed by lowering of the bags on the 31 May 2010 (t-7), had a salinity of about 34. The mesocosms contained a natural plankton community, though larger plankton and nekton were excluded using a net (3mm mesh size) covering the upper and lower opening of the mesocosms during filling. After simultaneous watertight closure of the systems on t-5, flotation rings (Fig. 1) were released from the bottom shutters to buoy upwards, unfolding funnel-type sediment traps of 2 m height. This upper ring of the funnel was of the same diameter as the bag (2 m), therefore touching it on all sides. The rather tight fit of the funnel was chosen to minimise sediment losses at the sides but resulted in ~ 4.5 m^3 of water below the funnel, which had only limited exchange with the bulk of enclosed water above the funnel. Depending on water/bag movement, water exchange between mesocosms and this "dead volume" happened on a timescale of days. Sediment lost into this dead volume was observed by divers to be very low (for calculated estimates see Table 1); nonetheless additions of dissolved substances (e.g. manipulations) to the water column had to mix with this dead volume before reliable budgets could be calculated. Pteropods of the species *Limacina helicina,* individually collected in the fjord, were added to each mesocosm (100, 20 and 70 individuals on day t4, t5 and t6, respectively). Most of them died within a few days in the tight gap between sediment funnel and mesocosm wall. Dead pteropods were picked from sediment samples or ended up in the dead volume. For more detail on the set-up see Riebesell et al. (2013) and find detailed information on abiotic conditions and standing stock succession of phytoplankton, dissolved and particulate matter in Schulz et al. (2013).

2.2 Manipulation

The water volume enclosed in flexible wall mesocosms can vary by some percent and was therefore determined using small additions of a calibrated NaCl solution as a tracer (~ 1mL L^{-1} = 0.2 g L^{-1}). Salinity measurements allowed calculation of the enclosed water volume of each individual mesocosm with uncertainties of less than 1 % (Czerny et al., 2013a). Measurements were performed twice, on t-4 and t4, because of considerable uncertainties in salinity measured before the first tracer addition on t-4. Measured volumes were consulted to plan further manipulation steps and to calculate elemental budgets. From t-1 to t4, CO_2 enriched filtered seawater solution was added to achieve eight CO_2 treatments between 185 and 1420 µatm CO_2, spanning a pH gradient from 8.31 to 7.51 (measured after mixing with the dead volume on t8). The two ~ 180 µatm CO_2 "control" mesocosms were undersaturated with respect to atmospheric CO_2 at the time the mesocosms were deployed and were blank manipulated using 55 µm filtered fjord water. All mesocosms were enriched with N_2O as a gas exchange tracer to a final concentration of ~ 50 nmol kg^{-1} on t4, when the second salt addition was performed. Before sampling on t13, a seawater-based mixed nutrient solution, calculated for the volumes of each single mesocosm, was added to establish equal concentrations of NO_3^- (5 µmol kg^{-1}), PO_4^{3-} (0.31 µmol kg^{-1}) and SiO_3^{2-} (2.5 µmol kg^{-1}) in all mesocosms. All additions were performed using the "Spider" injection system (Fig. 1a). For a more detailed description of the mesocosm manipulation technique see Riebesell et al. (2013). And for a description of inorganic nutrient dynamics see Schulz et al. (2013).

2.3 Sampling

The entire experiment from filling (t-7) to the last sampling of the mesocosms (t31) lasted 39 days. Sampling started at t-3, two days prior to the beginning of the CO_2 manipulation and lasted until t30 for most variables presented here. Daily water sampling for dissolved and particulate matter (representing total inorganic carbon (CT), dissolved inorganic nitrogen (DIN) and phosphorus (DIP), dissolved organic carbon (DOC), nitrogen (DON) and phosphorus (DOP), as well as particulate carbon (PC), organic nitrogen (PON) and phosphorus (POP)) was between 09:00 and 11:00 LT (local time) from boats. Samples were taken using 5 L depth-integrating

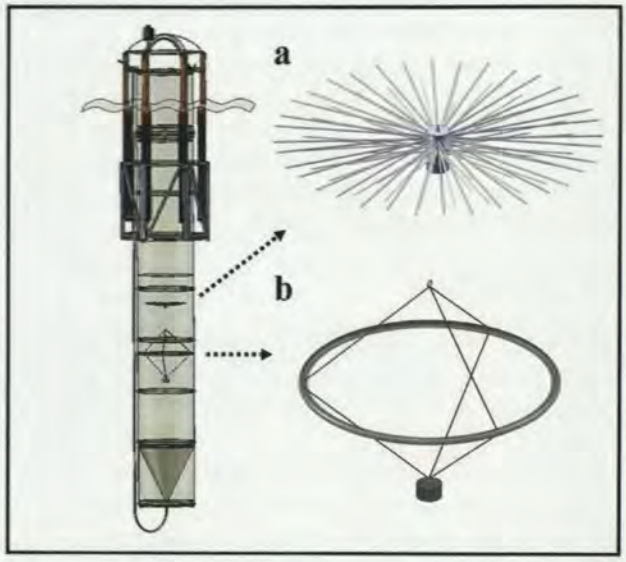

Fig. 1. Sketch of one of the nine experimental units. Total view of the mesocosm with **(a)** manipulation device "Spider" and **(b)** wall brush.

water samplers (IWS, Hydrobios, Kiel, Germany) that delivered one mixed sample from the upper 12 m, representing total water-column inventories. Sampling depth was restricted to 12 m to prevent dispersion of sediment from the 2 m-high collecting funnel at the bottom of the mesocosms. Immediately after water collection, gas samples for N_2O and carbonate chemistry (CT and total alkalinity (TAlk)) were collected directly from the sampler into gas-tight bottles. The rest of the water was transferred into 20 L polyethylene carboys using a silicon tube. Carboys were transported into the lab, screening them from sunlight using black plastic foil. Samples for dissolved and particulate matter were subsampled from carboys. Vertical (0–12 m depth) Apstein net hauls (opening Ø 17 cm, mesh size 55 µm) were performed to determine zooplankton abundance and biomass. To minimise effects on zooplankton density, samples were taken only once per week (days t-2, t2, t11, t18, t24 and t30). For more details see Niehoff et al. (2013).

Sediment was sampled every other day using silicone tubes (10 mm inner diameter) connecting the tips of the sediment funnels to the water surface (Fig. 1). Sediment dispersed in approximately 3 L of water was drawn from the silicone tube into a glass bottle under low vacuum pressure. After gravimetric determination of the sediment-water volume sampled, 20 to 30 mL sub-samples for microscopic inspection were taken with a pipette from the stirred bottles. For bulk chemical analyses (PC, PON, POP and biogenic silica (BSi)), particles were concentrated by settling and centrifugation, and the resulting compact sediment pellets were frozen at −80 °C.

2.4 Measurement procedures

Aliquots of water samples for analyses of chlorophyll *a* (Chl *a*; 250–500 mL) , PC, PON and POP (400–500 mL) were filtered under low vacuum (200mbar) on glass fibre filters (Whatman GF/F 25 mm Ø, pre-combusted at 450 °C for 5h) and stored frozen at −20 °C. Chl *a* was determined fluorometrically according to Welschmeyer (1994) using a Turner fluorometer 10-AU (Turner BioSystems). Quantification of PC and PON was carried out using an elemental analyser (EuroVektor EA) according to Sharp (1974). POP and BSi was determined following the method by Hansen and Koroleff in Grasshoff et al. (1983). For POP this method was modified to the measurement of samples on glass fibre filters. Here, particulate matter was completely oxidised by heating the filters in 50 mL glass bottles with 40 mL of purified water and the reagent Oxisolv (Merck) in a pressure cooker. Solutions were measured colorimetrically on a Hitachi U 2000 spectrophotometer. DOC, DON and DOP were determined from filtered (Whatman GF/F 25 mm Ø, pre-combusted at 450 °C for 5 h) water samples. DOC was analysed on a Shimadzu TOC_{VCN} using the HTCO (high-temperature catalytic oxidation) method (Qian and Mopper, 1996); for details see Engel et al. (2013). DON and DOP were oxidised as described for POP and subsequently measured as inorganic nutrients, for nitrate (NO_3^-), nitrite (NO_2^-) and phosphate (PO_4^{3-}) according to Hansen and Koroleff (1999), and for ammonia (NH_4^+) according to Holmes et al. (1999). The sum of NO_3^-, NO_2^- and NH_4^+ is presented as dissolved inorganic nitrogen (DIN). For a more detailed description of particulate matter (POM) and dissolved organic matter (DOM) and inorganic matter (DIM) analyses see Schulz et al. (2013). CT was determined via coulometric titration using a SOMMA (Single Operator Multiparameter Metabolic Analyser) system, and TAlk via potentiometric titration (Dickson, 1981). CO_2 concentrations, partial pressures and pH (total scale) were calculated from CT and TAlk measurements with the program CO2SYS by Lewis and Wallace (1998). For more details on carbonate chemistry see Bellerby et al. (2012).

Frozen sediment pellets were freeze dried at a pressure of ~ 50 mbar for 1–2 days without additional heat input until room temperature was reached. Subsequently, the dried sediment was ground in a stainless steel ball mill at low temperatures using liquid nitrogen to cool the sample before grinding. Sub-samples adjusted to the analytic measurement range (5–10 mg) were weighed on a precision scale. Analyses of particulate matter were performed as described above for PC, PON, POP and BSi on filters. 20 to 30 mL sub-samples of the sediment suspension, as well as samples from vertical net hauls were analysed for zooplankton composition, abundance and biomass under a dissecting microscope. At the same time, sediment samples were also inspected for general composition (detritus and phytoplankton). Zooplankton was sorted into tin cups for bulk carbon and nitrogen analyses as

described above for water-column PC and PON. For more details on zooplankton analyses see Niehoff et al. (2013).

2.5 CO_2 gas exchange estimate

Daily air–sea gas exchange velocities (k) were estimated using N_2O as a gas tracer. Calculations were based on fitted concentration decrease inside the mesocosm in relation to calculated equilibrium concentrations estimated using water T/S and atmospheric N_2O concentrations monitored on Zeppelin Mountain ($\sim$4 km distance from the experimental site). Daily CO_2 fluxes were calculated using k (adapted to CO_2 using published Schmidt numbers) together with CO_2 air–sea diffusion gradients. CO_2 gradients were derived from bulk aquatic CO_2 concentrations calculated from CT and AT as well as estimated using bulk water T/S and atmospheric CO_2 concentrations recorded on Zeppelin Mountain. Corrections for chemical enhancement by Hoover and Berkshire (1969) were applied. For a detailed discussion on gas exchange measurements in mesocosms including complete references on used constants see Czerny et al. (2013b). Zeppelin Mountain atmospheric data were provided by Thomas Conway from the NOAA Carbon Cycles Gases Group in Boulder, US, and Johan Ström from ITM (Department of Applied Environmental Science), Stockholm University, Sweden; atmospheric N_2O and CO_2 measurements, respectively.

2.6 Wall growth estimate

After sampling on the last day of the experiment (t30), a special brush (Fig. 1b) was used to mechanically remove and suspend biomass growing on the inner surface of the mesocosm bag as described in Riebesell et al. (2013). The detached biomass was then quantified by POM measurements of the water column before and right after brushing as described above.

2.7 Data presentation

Budget calculations for carbon (C), nitrogen (N) and phosphorus (P) are based on changes in pool sizes over time (Δpool) relative to a reference point in time. The addition of CO_2 enriched seawater caused major changes in the CT budget that could only be precisely quantified by direct measurements of CT inside the mesocosms. The earliest reference points for CT budgets were measured after complete mixing of the water column above and below the sediment traps. In the high CO_2 mesocosms this took until t8, while CT values were found to be stable in the non-manipulated control and in some low CO_2 mesocosms earlier. N and P budgets were calculated starting on t13, after inorganic nutrients were added. As a reference value for ΔDIN and ΔDIP from t13 onwards, concentrations measured on t12 plus the known amounts of added inorganic nutrients were used. This particular reference point was chosen because, in this way, budget calculation could be started on the day of nutrient addition, e.g. before the added nutrients were fully mixed into the dead volume below the sediment traps (see Sect. 2.1). For dissolved and particulate organic matter, starting values (t0, t8, t13, t20) for the analysed phases were obtained by averaging measured concentrations of the respective days with those of the days before and after. As measurement precision for inorganic matter is much higher than for organic material, averaging over three consecutive days was not needed and the concentrations of dissolved inorganic pools measured on the reference days were used as starting values.

Measured changes in inorganic matter that cannot be accounted for by the combined changes in pools of dissolved and particulate organic matter, cumulative gas exchange and sedimentation were assigned as "Pool X", representing a combination of measurement errors and the following pools unaccounted for in daily sampling: (1) a small amount of sedimented material accumulated in the space surrounding the sediment trap (dead volume) that could not be sampled. (2) A biofilm growing on the mesocosm walls became visible towards the end of the experiment. The size of this pool was estimated from water-column measurements taken immediately before and after brushing the mesocosm walls. (3) Fast-swimming zooplankton such as copepods were not quantitatively sampled with the depth-integrating sampler and are therefore not adequately represented in PC/PON/POP measurements. Biomass of zooplankton larger than 55 µm was estimated by weekly Apstein net hauls. Estimates for these three contributors to Pool X within the three phases of the experiment are based on theoretical considerations combined with available data on wall growth, zooplankton, and sediments (Table 1). Due to a rather constant elemental composition of particulate matter close to Redfield ratios of 106/16/1, those uncertainties in nitrogen and phosphorus are proportionally smaller than presented uncertainties in carbon (data not shown).

Corrections for the effect of water evaporation on dissolved and particulate matter concentrations as well as corrections for the effect of sampling-derived volume decrease on the calculation of air–sea and sediment fluxes were not included to keep calculations traceable. With a range of $\sim$0.2 % and $\sim$ 1 %, respectively, over the whole experiment, corrections are below the detection limit of most of the applied methods. Moreover, the effects of small changes in water volume would be identical in all mesocosms.

Changes in Pool X ($\Delta X_{C/N/P}$) were calculated for the three phases of the experiment as the summed amount of changes in all major pools as:

$$\Delta X_C = \Delta CT + \Delta GX + \Delta PC + \Delta DOC + \Delta Sed_C, \quad (1)$$

$$\Delta X_N = \Delta DIN + \Delta PON + \Delta DON + \Delta Sed_N, \quad (2)$$

$$\Delta X_P = \Delta DIP + \Delta POP + \Delta DOP + \Delta Sed_P. \quad (3)$$

Table 1. Estimates for the contribution of undetermined carbon pools (or not daily determined pools) to Pool X or ΔDOC_{calc}. Sediment losses were estimated on the basis of the ratio of areas of funnel opening relative to the gap around the funnel and the average cumulative sediment trapped during each phase. The area from which particles would collect in the gap was estimated as radius × length of the sediment trap flotation ring. Copepod biomass changes were estimated from average counts and carbon content determined from weekly net hauls. The depicted value was calculated assuming copepods were not at all represented in the particulate carbon measurements from water samples. Wall growth for phases II and III (after nutrient addition) was estimated, assuming exponential growth of the wall-grown carbon measured on t30 (8.31 ± 3.1 µmol kg^{-1}) at rates of 1 to 0.3 per day (Hagseth et al., 1992). "Maximum contribution of undetermined pools" depicts the sum of estimated mean changes within the three listed pools plus one standard deviation, or in the case of wall growth, the largest estimate.

Phase	I [µmol kg^{-1}]	II [µmol kg^{-1}]	III [µmol kg^{-1}]
Sediment lost into dead volume	0.046 ± 0.007	0.10 ± 0.015	0.17 ± 0.063
Copepod biomass changes	$0.0 + 0.11$	0.26 ± 0.43	1.11 ± 0.78
Wall growth	none	0.081 to 0.82	1.0 to 3.4
Maximum contribution of undetermined pools	0.12	1.63	5.52
Observed range of ΔDOC_{calc} on the last day of the phase	−0.93 to 11.09	−7.02 to 8.81	19.32 to 30.5

With ΔCT = change in total inorganic carbon concentrations, ΔGX = cumulative exchange of carbon with the atmosphere (flux in = negative/out = positive), ΔPC = change in total particulate carbon concentrations, ΔDOC = change in dissolved organic carbon concentrations, ΔSed = cumulative amounts of the respective element found in the sediment trap, ΔDIN = change in dissolved inorganic nitrogen concentrations, ΔPON = change in particulate organic nitrogen concentrations, ΔDON = change in dissolved organic nitrogen concentrations, ΔDIP = change in dissolved inorganic phosphorus concentrations, ΔPOP = change in particulate organic phosphorus concentrations, ΔDOP = change in dissolved organic phosphorus concentrations.

Pool X should be ideally zero as changes in one of its components should always be balanced by changes in one or several others. To trace back the source of changes in Pool X, regression analyses were performed, thus testing the degree of variance in all daily Pool X within each phase to be explained by changes in each of the single components on corresponding days (Fig. 2, Table 2). In this way, unexplained variability in measured concentrations of DOC, DON and POP were found to explain most of the variability in Pool X for carbon, nitrogen and phosphorus, respectively. Therefore mass balance calculations were used to estimate possible changes in DOC, DON and POP on the basis of all other budget components. Those estimates are presented as DOC_{calc}, DON_{calc} and POP_{calc}. Bias in these estimates, composed of summed measurement uncertainties and errors in the combined variables as well as undetermined pools (Table 1), is considerably lower than measurement errors in DOC, DON and POP.

Thus, estimates of DOC_{calc}, DON_{calc} and POP_{calc} were calculated using mass balances according to the following equations:

$$\Delta DOC_{calc} = \Delta CT + \Delta GX + \Delta PC + \Delta Sed_C, \quad (4)$$

$$\Delta DON_{calc} = \Delta DIN + \Delta PON + \Delta Sed_N, \quad (5)$$

$$\Delta POP_{calc} = \Delta DIP + \Delta DOP + \Delta Sed_P. \quad (6)$$

As sediment traps were sampled every other day, measured values were linearly interpolated for days in between. Also missing data points of other parameters were linearly interpolated between preceding and subsequent measurements. This applies for DON and DOP of all mesocosms on t16 and t19 and for 8 single data points of DOC.

2.8 Statistics

The set-up with 8 different CO_2 treatment levels and no replication of treated mesocosms was designed for regression analyses. Delta values of all tested phases are calculated using the first day of the respective phase as a reference point. Means of changes in measurement parameters (Δvalues) of single mesocosms during the three phases of the experiment were plotted against mean pCO_2 in the mesocosms during that specific phase. The null hypothesis that the overall slope is zero and that there is no linear relationship between treatment pCO_2 and mean Δ values was statistically tested with an F test. Data satisfied assumptions for normal distribution, as confirmed by a Shapiro–Wilk test. Analyses were performed using the program Statistica 6.0 (StatSoft Inc., Tulsa, USA). The same statistical procedure was applied to regression of Pool X to single budget components.

Table 2. Linear regression of daily Pool X of all mesocosms during each phase versus corresponding budget components (see Fig. 2). Coefficients of determination depict the share of variances in daily Pool X explained by variances in the datasets it is based on.

Regression of Pool X versus		ΔPC	ΔDOC	ΔCT	ΔGX	Sed
Phase I	r^2	0.01	0.85	0.01	0.00	0.03
	p	0.49	0.00	0.51	0.69	0.27
Phase II	r^2	0.00	0.90	0.11	0.09	0.10
	p	0.89	0.00	0.01	0.02	0.01
Phase III	r^2	0.08	0.51	0.24	0.08	0.22
	p	0.03	0.00	0.00	0.03	0.00

3 Results

3.1 Chlorophyll *a* and the analysed phases of the experiment

The experiment can be divided into three phases of autotrophic bloom development. An increase in Chl *a* (Fig. 3) started in all mesocosms already during CO_2 manipulation and peaked on t7. A CO_2 effect on Chl *a* concentrations during phase I was not observed. After nutrient addition (t13), there was a lag phase of 2 to 3 days until Chl *a* started to increase. Phase I carbon budget-calculation starts on t8, just after the phase I peak, and is thus describing processes during the bloom decay until t15. During phase II, from t13 onwards, large parts of added inorganic nutrients were consumed and budgets for C, N and P were calculated for build-up and decay of the second bloom peak until t20. Here, the Chl *a* peak of the high CO_2 treatments was higher than the one at intermediate and low CO_2 levels. During phase III, starting on t20, Chl *a* at low and intermediate CO_2 started to increase exponentially, reaching maximum concentrations on t27 and declining thereafter. In contrast, at high pCO_2 Chl *a* increased more slowly, not reaching peak values until the end of the experiment.

Maximal Chl *a* concentrations of $\sim 3\,\mu g\,L^{-1}$ during the course of the experiment are rather low considering the $5\,\mu mol\,kg^{-1}$ NO_3^- and $0.32\,\mu mol\,kg^{-1}$ PO_4^{3-} added. Chl *a* concentrations were transformed into estimates of organic carbon for the autotrophic community using Chl *a* to carbon ratios by Li et al. (2010), with $0.02\,g\,Chl\,a\,g\,C^{-1}$ for a phytoplankton community with low contribution of diatoms. Transformation reveals that the contribution of photoautotrophic biomass (up to $15\,\mu mol\,kg^{-1}$ C) to the standing stock of particulate carbon, PC, (up to $40\,\mu mol\,kg^{-1}$) was rather low.

3.2 Carbon budget of the replicated control treatment

In Fig. 4 carbon pools of the untreated control mesocosms are plotted over the entire period of the experiment. The bloom development as displayed in Chl *a* (Fig. 3) is mirrored by build-up of ΔPC, while cumulative sedimentation of this

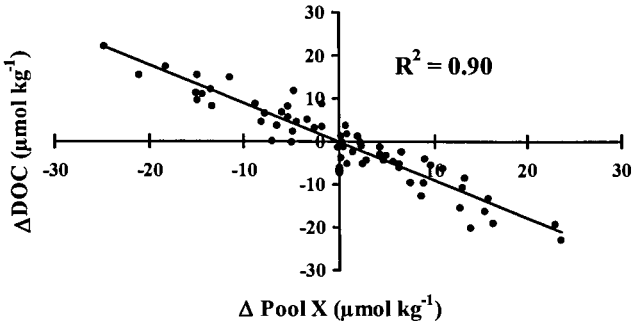

Fig. 2. Linear regression of changes in all daily total Pool X (ΣΔPC, ΔDOC, ΔCT, ΔSed, ΔGX) estimates within phase II to corresponding changes in measured DOC on the same days can be used to identify measured quantities of DOC to be unrealistic. Regression results of total Pool X to other carbon pools are given within Table 2.

biomass was rather low (Fig. 4a). Until t8, autotrophic uptake of inorganic carbon resulted in a simultaneous decrease of ΔCT, which was partly compensated by in-gassing of CO_2 from the atmosphere. Hereafter biomass decreased and PC was partly respired back into the CT pool, sedimenting out or being released as DOC_{calc}. Three days after the addition of inorganic nutrients (t16 up to t19), ΔPC build up combined with sedimentation was not leading to changes in ΔCT but was compensated by CO_2 entering the mesocosms from the atmosphere. During the first 19 days, the sum of particulate carbon produced in the control mesocosms roughly equalled the sum of inorganic carbon consumed, indicated by DOC_{calc} approaching zero during this period. Measured DOC values are included in Fig. 4b. Apparently, day-to-day variability in this dataset is much larger than the amount of carbon potentially available for the formation of DOC. This is evident from the sum of other measured carbon species shown as DOC_{calc} in Fig. 4a. Parallel variations of Pool X to DOC data (Figs. 2, 4b) identify measurement results to be unrealistic.

As shown in Fig. 4c, the temporal development of DOC_{calc} in the two control treatments was very similar. Variability of DOC_{calc} during most of the experimental time was relatively small (DOC_{calc} was on average $-0.43 \pm 2.7\,\mu mol\,kg^{-1}$ for

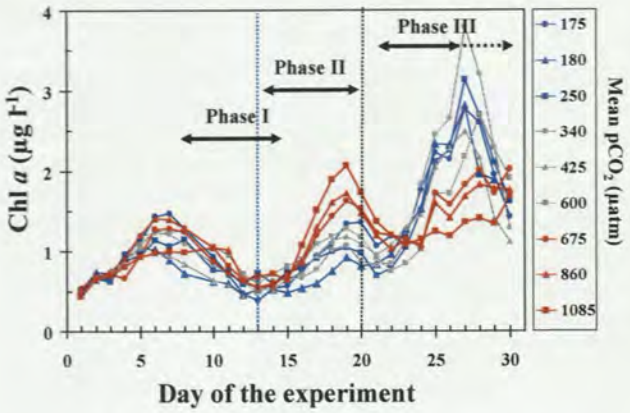

Fig. 3. Development of chlorophyll *a* concentrations during the course of the experiment. CO_2 partial pressures given in the figure legend are mean values for the experiment (day 8–26). High pCO_2 is denoted in red, intermediate in grey and low levels in blue. Within these categories, circles symbolise the lowest, triangles intermediate and squares the highest treatment pCO_2 level. The blue dashed line marks the nutrient addition (t13) at the end of phase I. The black dashed line denotes the end of phase II comprising the second bloom peak, phase III corresponds to the third bloom until the end of measurements. Arrows depict time periods used for statistical analyses.

the two controls until t19). Bias of DOC_{calc} estimates given in Table 1 could have caused a gradual increase in the DOC_{calc} of maximum 1.8 µmol kg^{-1} for this period. From t19 to t27, a phytoplankton bloom developed in the mesocosms, extensively consuming inorganic carbon. Increasing ΔPC values and cumulative sedimentation did not balance the sum of 44 µmol kg^{-1} CT taken up from the dissolved pool plus the CO_2 entering from the atmosphere (Fig. 4a). It therefore required 19 µmol kg^{-1} DOC_{calc} to close the carbon budget on t27. Within this period, biomass growing attached to the walls became visible and was estimated to account for 8.3 ± 3.1 µmol kg^{-1} of Pool X on t30 averaged over all mesocosms. This biomass was extrapolated back to the two nutrient-replete phases of the experiment based on assumed exponential growth at rates between 0.3 and 1.0, typical for ice algae communities (Hagseth et al., 1992). Even at the rather low growth rates, most of the wall grown biomass developed within the last few days before measurement, thus contributed shares to community biomass were negligible during phase I and II and moderate during phase III (Table 1). It has to be therefore assumed that carbon missing from the budget is largely dissolved organic carbon shown as DOC_{calc}. Only for phase III DOC_{calc} should be interpreted with caution. On the last sampling day (t27) undetermined pools (mainly wall growth) might have been contributing up to 5.5 of the 19 µmol kg^{-1} DOC_{calc}. Visual inspections by divers indicated that large parts of wall growth were removed by the brushing technique, but measurements most likely underestimated wall growth.

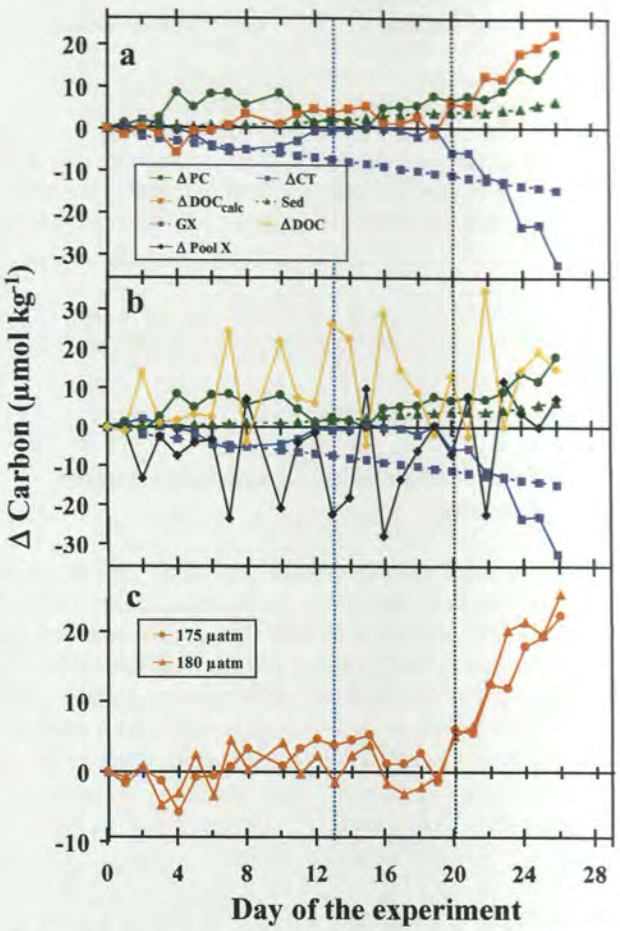

Fig. 4. Temporal development of carbon pools in the control treatment. **(a)** shows daily measured differences in particulate carbon (ΔPC), total inorganic carbon (ΔCT), dissolved organic carbon calculated from mass balance (DOC_{calc}), cumulative sedimented carbon (Sed) and CO_2 gas exchange (GX) relative to day zero for the lowest CO_2 treatment (175 µatm). In **(b)**, measured changes in dissolved organic carbon (ΔDOC) and Pool X (the carbon fraction that cannot be accounted for by changes in combined daily measured pools) are included. **(c)** compares DOC_{calc} of the 175 µatm treatment with DOC_{calc} of the second control mesocosm (180 µatm). The black dashed line denotes the end of phase II comprising the second bloom peak; phase III corresponds to the third bloom until the end of measurements.

3.3 CO_2 effects on carbon budgets

Changes in inorganic carbon concentrations between t8 and t27 (Fig. 5a) are correlated to CO_2 levels with the highest CO_2 treatment showing the strongest decrease in CT. At high pCO_2 the decrease was rather linear over time, whereas there was only a minor change in CT concentrations in the low CO_2 treatments during the first 12 days of this period. Most of these CO_2-related differences were caused by gas exchange with the atmosphere. One third (24 µmol kg^{-1}) of the CT decrease at the highest CO_2 over the whole

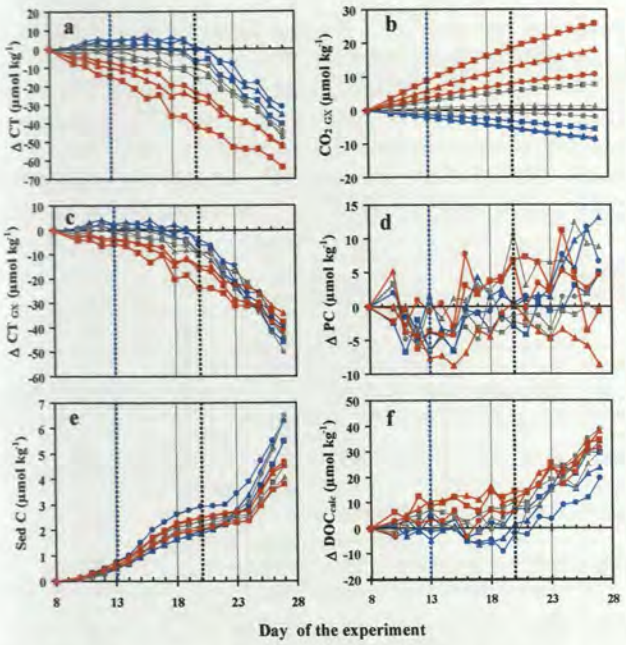

Fig. 5. Temporal development of carbon pools in all treatments relative to day 8. Changes in dissolved inorganic carbon (ΔCT) **(a)** corrected for gas exchange $CO_{2\,GX}$ **(b)** can be used to calculate biologically mediated changes in inorganic carbon concentrations (ΔCT_{GX}) **(c)**. This production estimate together with changes in particulate carbon (ΔPC) **(d)** and cumulative sedimentation of particulate carbon (Sed) **(e)** were used to estimate dissolved organic carbon from mass balance $\Delta\ DOC_{calc}$ **(f)**. CO_2 treatment levels and vertical dashed lines are coded as described for Fig. 3.

experiment can be attributed to outgassing, whereas about 25 % (10 μmol kg^{-1}) of the carbon consumed in the lowest CO_2 treatments entered from the atmosphere (Fig. 5b). The gas exchange corrected variation of ΔCT (Fig. 5c), ΔCT_{GX} is an approximation for biological net inorganic carbon fixation, as calcification was negligible during the experiment (Silyakova et al., 2012). Approximately equal amounts of inorganic carbon were consumed biologically in all treatments between t8 and t27. However, uptake rates often strongly differed among CO_2 treatments. CT was taken up immediately and rather continuously at high CO_2. At low CO_2, there was a considerable lag phase until t20, but then net uptake rates exceeded rates at high CO_2, so that all treatments ended up with similar uptake at the end of phase III. Overall, ΔPC build-up calculated from t8, with maximal 10 μmol kg^{-1} (Fig. 5d), was rather small compared to net carbon uptake ΔCT_{GX} of ~ 40 μmol kg^{-1}. Cumulative sedimentation can only account for half as much as ΔPC build-up (up to 5 μmol kg^{-1}, Fig. 5e). As the build-up of both measured particulate carbon species (ΔPC and sediment) cannot explain the measured drawdown in ΔCT_{GX}, ΔDOC_{calc} is accumulating over time (Fig. 5f).

3.4 Phase I

By separating the budget into three phases of the experiment, changes in elemental pools in the nine mesocosms can be directly compared using regression analyses.

Because inorganic nutrients were low at the beginning of phase I, there was no apparent uptake and inorganic nutrient budgets were thus not calculated. However, ΔCT_{GX} (Fig. 6a) showed a relatively strong decrease of inorganic carbon at high CO_2 compared to net heterotrophic production at low CO_2. This highly significant CO_2 effect on carbon uptake was not reflected in particulate carbon accumulation (Fig. 6b, Table 3). ΔPC was decreasing from the t8 bloom peak, while sedimentation was equally low in all treatments. This translates into a significant positive correlation of ΔDOC_{calc} to CO_2 in phase I (Table 3), causing an offset towards elevated ΔDOC_{calc} at high CO_2 that persisted over most of the experimental time (Fig. 5f).

3.5 Phase II

During phase II, dissolved inorganic matter (DIM) concentrations, comprising inorganic carbon (Fig. 6e) together with inorganic nutrients, decreased significantly stronger at high CO_2 (Table 3). Although statistical tests could not detect a significant CO_2-related increase in all pools of dissolved and particulate organic matter, significant positive trends in Chl *a* (Fig. 3), ΔPON, ΔDOP and ΔDOC_{calc} (Fig. 6h, Table 3) suggest a general positive effect of CO_2 on phytoplankton production during phase II. Mass balance indicates that surplus carbon taken up at high CO_2 accumulated in the dissolved organic pool (ΔDOC_{calc}), while nitrogen remained mainly in the particulate fraction and phosphorus was almost equally partitioned between both the particulate and dissolved organic pool (Table 3). The small sedimentation event peaking on t16 can be mainly allocated to Cirripedia larvae migrating into the sediment trap (Figs. 7a, 6g). The settling of these meroplanktonic larvae decreased metazooplankton biomass by 40–60 % (from overall average 5.0 ± 1.8 to 3.1 ± 1.1 μmol kg^{-1}) over the course of the experiment, thereby contributing ~ 60 % to the export flux during phases I and II (see also Niehoff et al., 2013). A sedimentation event caused by sticky nets of pteropods introduced into the mesocosm during phase I was not detected. The fairly large dead individuals were excluded from the sediment samples.

3.6 Phase III

In phase III, CO_2-related trends in dissolved inorganic matter uptake rates of phase II are reversed. Significantly more inorganic carbon was consumed at low CO_2 (Fig. 6i), resulting in significantly stronger build-up of PC (Fig. 6j) and export of this material (Fig. 6k). Trends in inorganic carbon uptake during phase III were parallel to trends in uptake of

Table 3. Results of F tests (regression analyses) for CO_2 dependent changes in pool sizes of C, N and P during the three phases of the experiment. Analysed delta values for each phase are calculated using the first day of the respective phase as a reference point. Mean delta concentrations of the elements in particulate organic (POM), dissolved inorganic (DIM) and dissolved organic matter (DOM) as well as sediments (Sed.) and pools calculated by mass balance (DOC_{calc} DON_{calc} POP_{calc}) were plotted against mean CO_2 concentrations during the phase. Significant trends ($p < 0.05$) are marked grey. Direction (Dir) of trends are given for correlations $p < 0.1$. "Neg." stands for negative correlation to pCO_2 and would for example mark a significantly stronger decrease in dissolved inorganic matter (DIM) with increasing pCO_2, while "Pos." stands for positive correlation to pCO_2 and could therefore mark significantly increasing concentrations, for example, POM with increasing pCO_2.

Testet period		ΔPOM			ΔDIM			ΔDOM			Sed.			ΔOM_{calc}		
		r^2	p	Dir	r^2	p	Dir	r^2	p	Dir	r^2	p	Dir	r^2	p	Dir
Phase I	Carbon T8–T15	0.01	0.78	–	0.98	< 0.00	Neg.	0.42	0.06	Pos.	0.02	0.75	–	DOC_{calc} 0.96	< 0.00	Pos.
Phase II	Carbon T14-T21	0.27	0.15	–	0.92	< 0.00	Neg.	0.01	0.77	–	0.00	0.92	–	DOC_{calc} 0.66	0.01	Pos.
	Nitrogen T14–T21	0.52	0.03	Pos.	0.87	< 0.00	Neg.	0.25	0.17	–	0.02	0.69	–	DON_{calc} 0.07	0.50	–
	Phosphorus T14–T21	0.35	0.10	–	0.93	< 0.00	Neg.	0.54	0.02	Pos.	0.02	0.71	–	POP_{calc} 0.13	0.34	–
Phase III	Carbon T21–T27	0.86	< 0.00	Neg.	0.85	< 0.00	Pos.	0.07	0.49	–	0.65	0.01	Neg.	DOC_{calc} 0.35	0.09	Neg.
	Nitrogen T21–T30	0.83	< 0.00	Neg.	0.89	< 0.00	Pos.	0.13	0.35	–	0.63	0.01	Neg.	DON_{calc} 0.25	0.17	–
	Phosphorus T21–T30	0.31	0.12	–	0.94	< 0.00	Pos.	0.15	0.31	–	0.64	0.01	Neg.	POP_{calc} 0.47	0.04	Neg.

inorganic nutrients (Table 3). As inorganic N and P were supplied in the beginning of phase II in equal concentrations (5 µmol kg^{-1} DIN, 0.32 µmol kg^{-1} DIP), stronger uptake at high CO_2 during phase II resulted in lowered concentrations of the limiting nutrients during phase III. On t20, concentrations of ~3.5 µmol kg^{-1} DIN and ~0.2 µmol kg^{-1} DIP were available in the control treatments, but only approximately half of this amount in the highest CO_2 treatment (1.76 and 0.10 µmol kg^{-1} DIN and DIP, respectively). DIN and DIP were depleted in all mesocosms at about day t28. Uptake rates were considerably faster in the still relatively nutrient-replete low CO_2 treatments. On the last days of the experiment, net community production at low CO_2 exceeded all rates observed before during this experiment. CO_2-related trends in ΔPC, ΔPON and especially in export of C, N and P could be clearly detected. Changes in nearly all of the particulate pools showed highly significant negative correlations to treatment pCO_2 (Table 3).

DOC_{calc} (Fig. 6l) was steadily increasing until day 27 in all CO_2 treatments. Major parts of the nutrients added on t13 accumulated in those pools determined by mass balance until the end of the experiment on t30 (averaged ~55% in DON_{calc} and 74% in POP_{calc}). Whereas 16% of added N and 32% of added P was measured as wall growth on t30 on average over all mesocosms. A CO_2 effect on wall growth is neither indicated by direct measurements on t30 nor by CO_2 correlations of DOC_{calc}, DON_{calc} or POP_{calc}, to which it was contributing during phase III.

3.7 Stoichiometry of particulate matter

Elemental ratios of water-column particulate matter were always close to Redfield ratios (Fig. 8). CO_2 or nutrient manipulation did not cause strong changes in elemental composition of particulate matter. C/N and N/P ratios of material sampled from the sediment traps were generally similar to ratios obtained for water-column particulate matter, with mean N/P ratios of the sediment slightly higher than respective values from the water column. During the last days (t27–t30) of the experiment, C/N ratios of water-column particulate matter increased in all mesocosms (Fig. 8a). This increase was significantly stronger for the low CO_2 treatments. The same general increase was observed in the sediment, but here C/N started to rise already on t24, reaching higher maximum values than in the water column (Fig. 8b). Diatom aggregates contributed the largest fraction of the sediment during the last week of the experiment as documented by a strong increase in biogenic silica fluxes (Fig. 7b), an elevated Si/C ratio (Fig. 7c) and microscopic inspection.

4 Discussion

4.1 Phase I

In the control treatments, dynamics in total inorganic carbon and gas exchange over the first 19 days of the experiment are well represented by measured production, export and respiration of particulate organic matter (Fig. 4a). Thus,

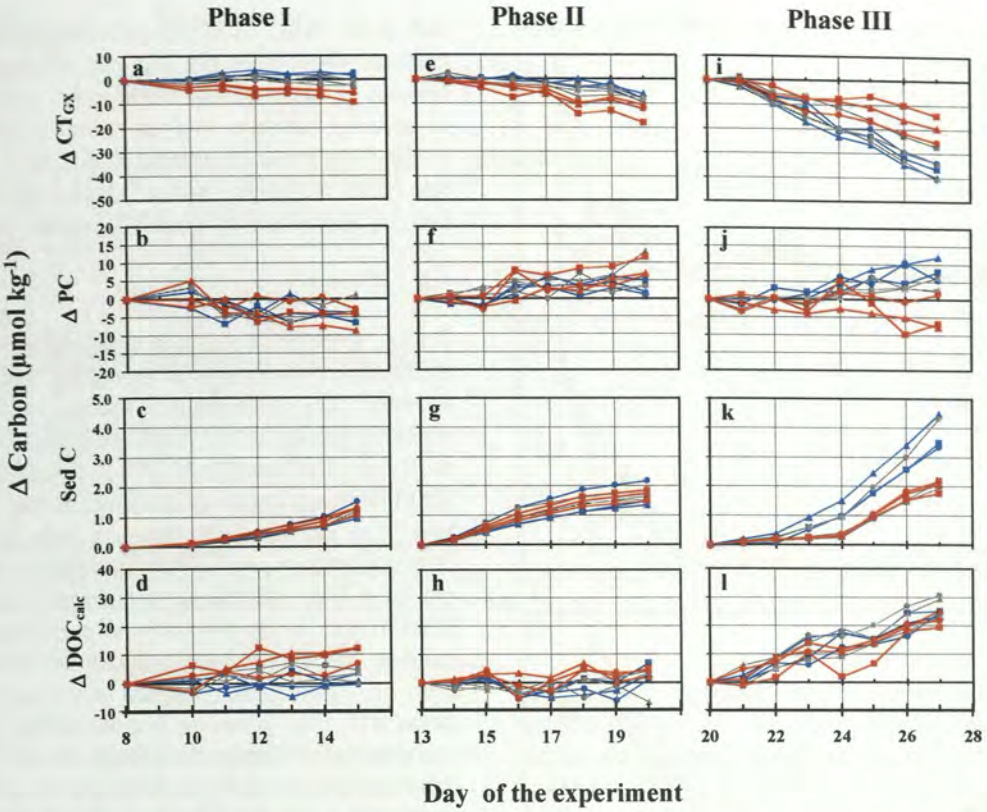

Fig. 6. Temporal development of carbon pools in all treatments for the three phases of the experiment. Biologically mediated changes in inorganic carbon concentrations (ΔCT_{GX}) together with changes in particulate carbon (ΔPC) and cumulative sedimentation of particulate carbon during each phase (Sed) were used to estimate dissolved organic carbon from mass balance ΔDOC_{calc}. CO_2 treatment levels and vertical dashed lines are coded as described for Fig. 3.

the carbon budget was closed with DOC_{calc} approaching zero at low CO_2. At high CO_2, however, there was significantly higher carbon consumption during phase I (Figs. 5c, 6a). Due to a strong vertical light gradient, ^{14}C gross primary production measured at 1 m water depth was high, showing a clear, positive correlation to CO_2 (Engel et al., 2013). In contrast, oxygen based production estimates by Tanaka et al. (2013) incubated at 3 m water depth were low and seem to be already partly balanced by respiration. The extra carbon ($\sim 13\ \mu mol\ kg^{-1}$) consumed at high CO_2 was not found in any of the particulate carbon pools (Fig. 6b, c), it was thus allocated to DOC_{calc}. Despite strong variability, statistical analyses of DOC measurements as well as ^{14}C DOC primary production measurements by Engel et al. (2013) support our interpretation of increased DOC production at high CO_2 in the phase before nutrient addition. DOC production was probably related to phytoplankton exudation but also to viral lyses of nanoplankton and microzooplankton grazing, both initiating the decline of the phase I bloom (Brussaard et al., 2013). Stronger microzooplankton grazing at low CO_2 during phase I was stated by de Kluijver et al. (2013) and Brussaard et al. (2013). Enhanced primary production at high CO_2 (Engel et al., 2013) presumably in combination with opposing strong heterotrophic loss processes at low CO_2 (Brussaard et al., 2013) were resulting in net uptake of inorganic carbon in the future CO_2 treatments and concomitant release of inorganic carbon in the low CO_2 controls (Fig. 6a). Rapid cycling of carbon during phase I obviously resulted in accumulation of DOC at high CO_2 that was not readily bioavailable and persisted at least during phase II, in which net production of DOC was considerably lower (Fig. 5f, see also Engel et al., 2013). A semi-labile nature of the produced dissolved organic matter in this experiment becomes also evident from apparent substrate limitation of heterotrophic bacteria during the entire experiment, detected by Piontek et al. (2013).

The phenomenon of inorganic carbon drawdown with low net consumption of N or P, called carbon over-consumption (Toggweiler, 1993), was enhanced at high CO_2 between t8 and t15. Such feature was already found in incubations of natural Atlantic plankton communities under high CO_2 (Schulz et al., 2008; Bellerby et al., 2008; Riebesell et al., 2007; Delille et al., 2005; Engel et al., 2004a; Egge et al., 2009; Hein and Sand-Jensen, 1997) and is also indicated by increased cumulative ^{14}C primary production observed during the experiment by Engel et al. (2013). The final product

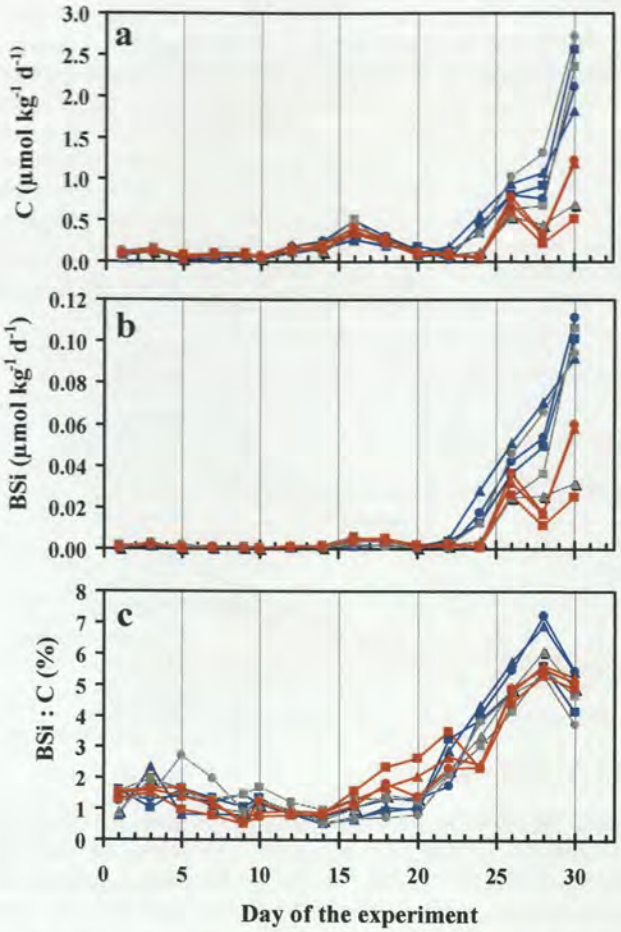

Fig. 7. Vertical fluxes for carbon **(a)** and biogenic silica **(b)** normalised to kg seawater and day. Biogenic silica to carbon ratios in the sedimented material are shown in **(c)**. Treatment levels and vertical dashed lines are coded as described for Fig. 3.

of enhanced photosynthetic activity could often not directly be measured, but was hypothesised to be released as DOC, subsequently occurring as TEP (Engel et al., 2004a). Sedimentation of aggregated DOC in the form of TEP was hypothesized to cause increased carbon loss under high CO_2 in the PEECE (Pelagic Ecosystem CO_2 Enrichment) III study (Schulz et al., 2008) and in further previous experiments (Engel et al., 2004b). In this experiment, an increased contribution of freshly fixed ^{13}C to high CO_2 sediments during phase I was argued to be caused by sinking of TEP by de Kluijver et al. (2013). TEP formation implies a flux of DOC into the PC pool, but neither increased bulk sedimentation nor increased carbon contents of sediments or of water-column particulate matter under high CO_2 were measured. Sediment fluxes were low and indication for TEP as a relevant aggregation factor was not detected. Sugars serving as precursors for TEP were possibly produced at concentrations too low to form relevant amounts of aggregates or were consumed by the bacterial community right after release (Piontek et al., 2010). DOC was therefore remaining in the water column, where it, on the long run, might support the development of the microbial community. Although an increase in bacterial numbers was not observed during the duration of the experiment (Brussaard et al., 2013), DOC accumulation rather promotes enhanced shallow remineralisation than primary production or export (Thingstad et al., 2008).

4.2 Phase II

During phase II the trends in uptake of inorganic C, N and P after nutrient addition were consistent with trends in Chl *a*. Elevated CO_2 concentrations seemed to have a stimulating effect on growth of the dominating picoeukaryotic primary producers (Brussaard et al., 2013; Schulz et al., 2013), leading to increased uptake of inorganic matter (Table 3, Fig. 6e), as well as increased cell numbers and Chl *a*. However, increasing biomass production as a result of enhanced nutrient uptake at high CO_2 during the bloom of picoeukaryotes in phase II was hardly detectable as particulate organic matter build-up and did not cause a significant sedimentation event (Figs. 6f, 5g). A peak in carbon export caused by Cirripedia larvae (t16, Fig. 7a) shows that the settling of meroplankton can seasonally account for a large portion of vertical fluxes in coastal ecosystems. This finding is in agreement with ^{13}C tracer data by de Kluijver et al. (2013). Generally low enrichment of sediment with the tracer during phases I and II can only be explained by high contents of zooplankton and "old" detrital material. Build-up of autotrophic biomass in the water column, estimated from Chl *a* as well as from biovolume of picoeukaryotes (Brussaard et al., 2013) can only account for the amount of inorganic C, N and P consumed during the first days of phase II. Thereafter, phytoplankton standing stocks were diminished and kept at a relatively low level by microzooplankton grazing and viral lyses of picoeucaryotes (Brussaard et al., 2013). Nutrient and carbon uptake continued during the time of strong biomass loss. Low C/N and C/P inorganic uptake ratios in all treatments suggest overall elevated production of organic P and N compared to organic C during phase II (Silyakova et al., 2012). Significant CO_2-correlated differences in ΔPC as well as ΔPOP_{calc} could not be detected during the entire phase II (Table 3). Dissolved organic matter is indeed showing positively CO_2-related differences in ΔDOC_{calc} (Fig. 6h) but also in ΔDOP. Release of cell contents rather than exudation may have been the source of this DOM at nutrient-replete conditions, as enhanced autotrophy at high CO_2 was strongly top–down controlled (Brussaard et al., 2013). In contrast to P and C, enhanced uptake of inorganic nitrogen at high CO_2 was also reflected in higher ΔPON and only minor amounts of N accumulated in DON_{calc}. Nitrogen was obviously preferentially incorporated into the heterotrophic community compared to C and P (Table 3).

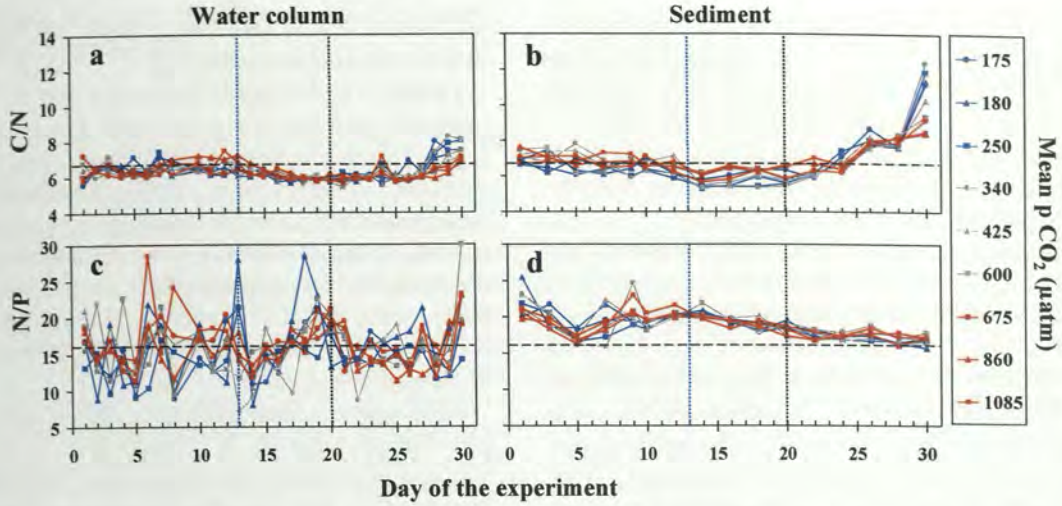

Fig. 8. Temporal development of measured carbon to nitrogen (C/N) and nitrogen to phosphorus (N/P) ratios of particles suspended in the water column (left) and particles sampled in the sediment traps (right). Dashed horizontal line marks Redfield ratios. CO_2 partial pressures given in the figure legend are mean values for the experiment (day 8–26). Vertical dashed lines are coded as described for Fig. 3.

4.3 Phase III

A relatively diverse phytoplankton community comprised of picoeukaryotes, co-dominated by diatoms and dinoflagellates established during phase III (Schulz et al., 2013; Brussaard et al., 2013). Biomass build-up resulting from fast carbon and nutrient drawdown did not seem to be limited by strong heterotrophic loss processes as observed in the previous two phases. This bloom showed higher C, N and P uptake rates at low CO_2, whereas under high CO_2 uptake was already slowing down due to nutrient depletion after the phase II peak (Fig. 6i). Reduced growth at high CO_2 in phase III was reflected by significantly lower ΔPC, ΔPON, and ΔPOP (Table 3). Diatoms, contributing relatively low biomass to the pelagic community (Schulz et al., 2013), increasingly dominated the sediment material from the beginning of phase III in all treatments. In the sediment material, this is illustrated by increasing BSi/C ratios from t20 onwards (Fig. 7c), concurring with microscopic observations of large quantities of diatom chains and their fatty acid signature detected by de Kluijver et al. (2013). Overall, higher biomass build-up seemed to be causing a sedimentation event of diatoms, forming aggregates with other particles, transporting them into the sediment trap. In contrast to the previous two phases, ^{13}C tracer concentrations indicate that there were even higher contributions of freshly fixed carbon to sediments than to water-column PC (de Kluijver et al., 2013). The retention food web, quickly recycling freshly produced biomass, seems to have shifted towards an export community in phase III (Wassmann, 1997). Strongly reduced export at high CO_2 was obviously due to nutrients being diminished by enhanced growth during phase II. Unfortunately, the total amount of export production cannot be calculated for this period, as measurements ended before peak sedimentation rates were reached (Fig. 7a). In addition to that, DOC_{calc} and wall-grown biomass, not being exported, were exponentially increasing (Fig. 4c). However, an export flux at high CO_2 comparable to fluxes observed at low CO_2 occurring after the end of our measurements (t30) seems unlikely, as inorganic N and P were depleted at t28. Until nutrient depletion, significantly less carbon uptake, PC and PON accumulation in the water column and less export of C, N and P were observed at high CO_2 during phase III.

4.4 Stoichiometry of exported particulate matter

Temporal trends in elemental composition of the sedimented particulate matter were very similar to that of the water column during most parts of the experiment (Fig. 8). Carbon isotope tracer data in sediments suggests that there was mostly an under-representation of phytoplankton biomass (de Kluiver et al., 2013). Elemental composition of sediment was overall similar to water column particulate matter. This classifies sinking material sampled at the bottom of the shallow mesocosms to be relativity fresh. Nevertheless, sinking detritus and digested material produced by the large heterotrophic community was probably responsible for the slight general offset in composition of sedimenting material towards higher C/N and N/P ratios throughout the experiment. While changes in particulate matter composition in response to future CO_2, reported from laboratory experiments on phytoplankton (Burkhardt et al., 1999; Burkhardt and Riebesell, 1997), are varying between species in strength and direction, differences in organic C/N/P ratios of primary producers growing under inorganic nutrient limitation and repletion are a common phenomenon (Klausmeier et al., 2004). The fact that we did not observe strong changes in response to nutrient or CO_2 addition, during this experiment is likely a

result of the diverse composition of POM, with phytoplankton comprising only a relatively small fraction during large parts of the experiment. Fast recycling of readily available N and P compounds during phase I were obviously covering the nutrient demand of phytoplankton (Schulz et al., 2013) and probably comprised a large part of the fluxes even during nutrient replete phases of the experiment.

The observed increase of C/N ratios in the sediment compared to the water-column particulate matter during phase III correlates with the occurrence of diatoms and increasing silicate flux (Fig. 7c). This diatom ballast or aggregation effect caused the over-representation of fresh carbon-rich particles in the sediments. The same C/N increase as in the sediment occurred later and less pronounced in the water column; here diatoms and fresh material are measured against a much larger background of other water-column particulate matter, thus diluting this signal.

On t30, higher C/N ratios at low CO_2 appeared in water-column particulate matter. Similar to the general increase of C/N in all mesocosms, also the CO_2 effect on C/N was amplified in the sediment. Mesocosms showing stronger elevated C/N ratios on the last day had also higher sedimentation rates of C, N, P and Si (Table 3). Carbon uptake beyond the day of nutrient depletion could not be determined, as the inorganic carbon dataset ends on t27. But already until t27 inorganic carbon to nutrient uptake was much higher at low CO_2 during phase III and thus even during the combined post nutrient phase (II + III) (Silyakova et al., 2012). A combination of high uptake rates and the shift towards increased C/N on the last days overcompensated initially higher uptake at high CO_2 during phase II. Elevated C or reduced N content of the phytoplankton community might have been due to growth limitation by dissolved inorganic nitrogen with concentrations below 1 $\mu mol\,kg^{-1}$ (Klausmeier et al., 2004) already since t24 in all treatments.

4.5 Synthesis

Despite all efforts in determining all relevant elemental pools of C, N and P in regular temporal intervals, budgets could not readily be closed. This was mainly because of unsatisfying precision in DOC, DON and POP as well as wall growth towards the end of the experiment. However, gaps in the budget could be narrowed down by introducing novel methodology to determine gas exchange and sedimentation. It could be demonstrated that measured pools in large mesocosms can be quantitatively evaluated against each other. Moreover, using mass balance, problematic measurement parameters as well as technical and operational problems could be identified and their relevance could be quantified. In later experiments, improved sediment traps, an improved DOC sampling strategy as well as regular cleaning of the walls solved the most prominent problems pointed out in this study (see improved methods in Riebesell et al., 2013). The particular reason for the lack in precision in DON and POP within this dataset could not be ascertained.

Future CO_2 concentrations were found to stimulate autotrophic production twice during the course of this experiment. First during phase I, when increased inorganic carbon uptake by nanoplankton at high CO_2 was directly channelled into dissolved organics. Secondly, during phase II, when enhanced growth of picoeukaryotes diminished inorganic nutrient concentrations at high CO_2, resulting in less organic matter being exported in phase III. During this experiment, both positive effects on primary producers had negative influence on carbon export.

After phase I, community composition and carbon flows had changed. Later effects were therefore a product of complex resource competition and cascading loss processes modified by CO_2 and preceding production. The dominating producers or consumers in a mesocosm had responded to the manipulation at the beginning of the experiment, any following effects were multi-causal. Growth enhancement of nanoplankton and picoeukaryotes during phase I and II (Brussaard et al., 2013; Engel et al., 2013; de Kluiver et al., 2013) might have caused most of the CO_2 effects on bloom dynamics observed during and after their occurrence. Therefore, e.g. direct physiological CO_2 effects on plankton dominating within phase III would be a matter of speculation due to the different nutrient situation already in the beginning of phase III. This demonstrates that ecological data are of substantial importance in making biogeochemical response patterns comparable between experiments. Apparently, responses found for the retention type community, which was present at the start of this experiment, are not directly comparable to earlier findings for export systems such as the coccolithophore blooms in Norwegian coastal waters compiled by Riebesell et al. (2008). Community experiments always have to be seen as case studies with results primarily valid for the specific community composition enclosed at the start of the experiment. Further experiments will show whether CO_2 enhanced DOC production and growth of smaller phytoplankton can be consistently found at similar community composition.

Laboratory studies performed on single species are ideal to detect physiological CO_2 effects, whereas the importance of these effects within a natural ecosystem is always difficult to extrapolate (Riebesell and Tortell, 2011). In this experiment, ocean acidification/carbonation affected small phytoplankton, which in turn significantly influenced principle ecosystem functioning. Whereas enhanced growth of picoeucaryotes itself had no immediate effect on carbon export fluxes, their footprint in the nutrient budget controlled export fluxes later during the experiment. Identifying species that have the potential to change biogeochemical fluxes by influencing community succession is an important task for future mesocosm experiments. Focussing from the community to the species level instead of extrapolating from the laboratory

to the field could accelerate the progress of finding general biogeochemical response patterns.

Acknowledgements. This work is a contribution to the "European Project on Ocean Acidification" (EPOCA) which received funding from the European Community's Seventh Framework Programme (FP7/2007-2013) under grant agreement no. 211384. Financial support was provided through Transnational Access funds by the European Union Seventh Framework Program (FP7/2007-2013) under grant agreement no. 22822 MESOAQUA and by Federal Ministry of Education and Research (BMBF, FKZ 03F0608) through the BIOACID (Biological Impacts of Ocean ACIDification) project. We gratefully acknowledge the logistical support of Greenpeace International for its assistance with the transport of the mesocosm facility from Kiel to Ny-Ålesund and back to Kiel. We also thank the captains and crews of M/V *ESPERANZA* of Greenpeace and R/V *Viking Explorer* of the University Centre in Svalbard (UNIS) for assistance during mesocosm transport and during deployment and recovery in Kongsfjorden. We thank the staff of the French–German Arctic Research Base at Ny-Ålesund, in particular Marcus Schumacher, for on-site logistical support.

Edited by: J. Middelburg

The service charges for this open access publication have been covered by a Research Centre of the Helmholtz Association.

References

Bathmann, U. V., Noji, T. T., and von Bodungen, B.: Sedimentation of pteropods in the Norwegian Sea in autumn, Deep Sea Res., 38, 1341–1360, 1991.

Bellerby, R. G. J., Schulz, K. G., Riebesell, U., Neill, C., Nondal, G., Heegaard, E., Johannessen, T., and Brown, K. R.: Marine ecosystem community carbon and nutrient uptake stoichiometry under varying ocean acidification during the PeECE III experiment, Biogeosciences, 5, 1517–1527, doi:10.5194/bg-5-1517-2008, 2008.

Bellerby, R. G. J., Silyakova, A., Nondal, G., Slagstad, D., Czerny, J., de Lange, T., and Ludwig, A.: Marine carbonate system evolution during the EPOCA Arctic pelagic ecosystem experiment in the context of simulated Arctic ocean acidification, Biogeosciences Discuss., 9, 15541–15565, doi:10.5194/bgd-9-15541-2012, 2012.

Bopp, L., Monfray, P., Aumont, O., Dufresne, J.-L., Le Treut, H., Madec, G., Terray, L., and Orr, J. C.: Potential impact of climate change on marine export production. Global Biogeochem. Cy., 15, 81–99. 2001.

Brussaard, C. P. D., Noordeloos, A. A. M., Witte, H., Collenteur, M. C. J., Schulz, K., Ludwig, A., and Riebesell, U.: Arctic microbial community dynamics influenced by elevated CO_2 levels, Biogeosciences, 10, 719–731, doi:10.5194/bg-10-719-2013, 2013.

Burkhardt, S. and Riebesell, U.: CO_2 availability affects elemental composition (C : N : P) of the marine diatom *Skeletonema costatum*, Mar. Ecol.-Prog. Ser., 155, 67–76, doi:10.3354/meps155067, 1997.

Burkhardt, S., Zondervan, I., and Riebesell, U.: Effect of CO_2 concentration on the C : N : P ratio in marine phytoplankton: A species comparison., Limnol. Oceanogr., 44, 683–690, 1999.

Comeau, S., Gorsky, G., Jeffree, R., Teyssié, J.-L., and Gattuso, J.-P.: Impact of ocean acidification on a key Arctic pelagic mollusc (*Limacina helicina*), Biogeosciences, 6, 1877–1882, doi:10.5194/bg-6-1877-2009, 2009.

Czerny, J., Schulz, K. G., Krug, S. A., Ludwig, A., and Riebesell, U.: Technical Note: The determination of enclosed water volume in large flexible-wall mesocosms "KOSMOS", Biogeosciences, 10, 1937–1941, doi:10.5194/bg-10-1937-2013, 2013a.

Czerny, J., Schulz, K. G., Ludwig, A., and Riebesell, U.: Technical Note: A simple method for air–sea gas exchange measurements in mesocosms and its application in carbon budgeting, Biogeosciences, 10, 1379–1390, doi:10.5194/bg-10-1379-2013, 2013b.

de Kluijver, A., Soetaert, K., Czerny, J., Schulz, K. G., Boxhammer, T., Riebesell, U., and Middelburg, J. J.: A ^{13}C labelling study on carbon fluxes in Arctic plankton communities under elevated CO_2 levels, Biogeosciences, 10, 1425–1440, doi:10.5194/bg-10-1425-2013, 2013.

Delille, B., Harlay, J., Zondervan, I., Jacquet, S., Chou, L., Wollast, R., Bellerby, R. G. J., Frankignoulle, M., Borges, A. V., Riebesell, U., and Gattuso, J.-P.: Response of primary production and calcification to changes of pCO_2 during experimental blooms of the coccolithophorid Emiliania huxleyi, Global Biogeochem. Cy., 19, GB2023, doi:10.1029/2004gb002318, 2005.

Doney, S. C.: The Growing Human Footprint on Coastal and Open-Ocean Biogeochemistry, Science, 328, 1512–1516, doi:10.1126/science.1185198, 2010.

Egge, J. K., Thingstad, T. F., Larsen, A., Engel, A., Wohlers, J., Bellerby, R. G. J., and Riebesell, U.: Primary production during nutrient-induced blooms at elevated CO_2 concentrations, Biogeosciences, 6, 877–885, doi:10.5194/bg-6-877-2009, 2009.

Engel, A.: Direct relationship between CO_2 uptake and transparent exopolymer particles production in natural phytoplankton, J. Plankton Res., 24, 49–53, 2002.

Engel, A., Delille, B., Jacquet, S., Riebesell, U., Rochelle-Newall, E., Terbrüggen, A., and Zondervan, I.: Transparent exopolymer particles and dissolved organic carbon production by Emiliania huxleyi exposed to different CO_2 concentrations: a mesocosm experiment, Limnol. Oceanogr, 50, 493–507, 2004a.

Engel, A., Thoms, S., Riebesell, U., Rochelle-Newall, E., and Zondervan, I.: Polysaccharide aggregation as a potential sink of marine dissolved organic carbon, Nature, 428, 929–932, 2004b.

Engel, A., Borchard, C., Piontek, J., Schulz, K. G., Riebesell, U., and Bellerby, R.: CO_2 increases ^{14}C primary production in an Arctic plankton community, Biogeosciences, 10, 1291–1308, doi:10.5194/bg-10-1291-2013, 2013.

Fabry, V. J., Seibel, B. A., Feely, R. A., and Orr, J. C.: Impacts of ocean acidification on marine fauna and ecosystem processes, ICES J. Mar. Sci., 65, 414–432, doi:10.1093/icesjms/fsn048, 2008.

Friedlingstein, P., Houghton, R. A., Marland, G., Hackler, J., Boden, T. A., Conway, T. J., Canadell, J. G., Raupach, M. R., Ciais, P., and Le Quéré, C.: Update on CO_2 emissions, Nat. Geosci, 3, 811–812, 2010.

Grasshoff, K., Ehrhardt, M., and Kremling., K.: Methods of Seawater Analysis., 2 Edn., Verlag Chemie, Weinheim, Germany, 1983.

Gruber, N.: Warming up, turning sour, losing breath: ocean biogeochemistry under global change, Philos. T. Roy. Soc. A, 369, 1980–1996, doi:10.1098/rsta.2011.0003, 2011.

Hansen, H. and Koroleff, R.: in: Methods of Seawater Analysis, edited by: Grasshoff, K., Kremmling, K., and Ehrhardt, M., Wiley, Weinheim, Germany, 159–228, 1999.

Hansen, J., Sato, M., Ruedy, R., Lo, K., Lea, D. W., and Medina-Elizade, M.: Global temperature change, P. Natl. Acad. Sci. USA, 103, 14288–14293, doi:10.1073/pnas.0606291103, 2006.

Hein, M. and Sand-Jensen, K.: CO_2 increases oceanic primary production, Nature, 388, 526–527, 1997.

Holmes, R. M., Aminot, A., Kerouel, R., Hooker, B. A., and Peterson, B. J.: A simple and precise method for measuring ammonium in marine and freshwater ecosystems, Can. J. Fish. Aquat. Sci., 56, 1801–1808, doi:10.1139/f99-128, 1999.

Hoover, T. E. and Berkshire, D. C.: Effects of Hydration on Carbon Dioxide Exchange across an Air-Water Interface, J. Geophys. Res., 74, 456–464, doi:10.1029/JB074i002p00456, 1969.

Klaas, C. and Archer, D. E.: Association of sinking organic matter with various types of mineral ballast in the deep sea: Implications for the rain ratio, Global Biogeochem. Cy., 16, 1116, doi:10.1029/2001gb001765, 2002.

Klausmeier, C., Litchman, E., and Levin, S.: Phytoplankton growth and stoichiometry under multiple nutrient limitation, Limnol. Oceanogr., 49, 1463–1470, 2004.

Lewis, E. and Wallace, D. W. R.: Program developed for CO_2 system calculations. ORNL/CDIAC-105. Carbon Dioxide Information Center, Oak Ridge National Laboratory, US Department of Energy, Oak Ridge, Tennessee, 1998.

Li, Q. P., Franks, P. J. S., Landry, M. R., Goericke, R., and Taylor, A. G.: Modeling phytoplankton growth rates and chlorophyll to carbon ratios in California coastal and pelagic ecosystems, J. Geophys. Res., 115, G04003, doi:10.1029/2009jg001111, 2010.

Lischka, S., Büdenbender, J., Boxhammer, T., and Riebesell, U.: Impact of ocean acidification and elevated temperatures on early juveniles of the polar shelled pteropod *Limacina helicina*: mortality, shell degradation, and shell growth, Biogeosciences, 8, 919–932, doi:10.5194/bg-8-919-2011, 2011.

Lombard, F., da Rocha, R. E., Bijma, J., and Gattuso, J.-P.: Effect of carbonate ion concentration and irradiance on calcification in planktonic foraminifera, Biogeosciences, 7, 247–255, doi:10.5194/bg-7-247-2010, 2010.

Lutz, M. J., Caldeira, K., Dunbar, R. B., and Behrenfeld, M. J.: Seasonal rhythms of net primary production and particulate organic carbon flux to depth describe the efficiency of biological pump in the global ocean, J. Geophys. Res., 112, C10011, doi:10.1029/2006jc003706, 2007.

Meehl, G. A. S., T. F., Collins, W. D., Friedlingstein, A. T., Gaye, A. T., Gregory, J. M., Kitoh, A., Knutti, R., Murphy, J. M., Noda, A., Raper, S. C. B., Watterson, I. G., Weaver, A. J., and Zhao, Z.: Global climate projections., in: Climate Change 2007, The physical science basis, edited by: Solomon, S., Qin, D., and Manning, M., Technical support unit, IPCC working group 1, Cambridge University Press, 748–845, 2007.

Millero, F. J., Woosley, R., DiTrolio, B., and Waters, J.: Effect of Ocean Acidification on the Speciation of Metals in Seawater, Oceanography, 22, 72–85, 2009.

Niehoff, B., Schmithüsen, T., Knüppel, N., Daase, M., Czerny, J., and Boxhammer, T.: Mesozooplankton community development at elevated CO_2 concentrations: results from a mesocosm experiment in an Arctic fjord, Biogeosciences, 10, 1391–1406, doi:10.5194/bg-10-1391-2013, 2013.

Oschlies, A.: Impact of atmospheric and terrestrial CO_2 feedbacks on fertilization-induced marine carbon uptake, Biogeosciences, 6, 1603–1613, doi:10.5194/bg-6-1603-2009, 2009.

Petit, J. R., Jouzel, J., Raynaud, D., Barkov, N. I., Barnola, J.-M., Basile, I., Bender, M., Chappellaz, J., Davis, M., Delaygue, G., Delmotte, M., Kotlyakov, V. M., Legrand, M., Lipenkov, V. Y., Lorius, C., P.Épin, L., Ritz, C., Saltzman, E., and Stievenard., M.: Climate and atmospheric history of the past 420,000 years from the Vostok ice core, Antarctica, Nature, 399, 429–436 1999.

Piontek, J., Lunau, M., Händel, N., Borchard, C., Wurst, M., and Engel, A.: Acidification increases microbial polysaccharide degradation in the ocean, Biogeosciences, 7, 1615–1624, doi:10.5194/bg-7-1615-2010, 2010.

Piontek, J., Borchard, C., Sperling, M., Schulz, K. G., Riebesell, U., and Engel, A.: Response of bacterioplankton activity in an Arctic fjord system to elevated pCO_2: results from a mesocosm perturbation study, Biogeosciences, 10, 297–314, doi:10.5194/bg-10-297-2013, 2013.

Qian, J. and Mopper, K.: Automated High-Performance, High-Temperature Combustion Total Organic Carbon Analyzer, Anal. Chem., 68, 3090–3097, doi:10.1021/ac960370z, 1996.

Reinfelder, J. R.: Carbon Concentrating Mechanisms in Eukaryotic Marine Phytoplankton, Annual Review of Marine Science, 3, 291–315, doi:10.1146/annurev-marine-120709-142720, 2011.

Revelle, R. and Suess, H. E.: Carbon Dioxide Exchange Between Atmosphere and Ocean and the Question of an Increase of Atmospheric CO_2 during the Past Decades, Tellus, 9, 18–27, doi:10.1111/j.2153-3490.1957.tb01849.x, 1957.

Riebesell, U.: Effects of CO_2 Enrichment on Marine Phytoplankton, J. Oceanogr., 60, 719–729, doi:10.1007/s10872-004-5764-z, 2004.

Riebesell, U. and Tortell, P. D.: Effects of ocean acidification on pelagic organisms and ecosystems, in: Ocean Acidification, edited by: Gattuso, J. P. and Hanson, L., Oxford University Press, Oxford, 99–121, 2011.

Riebesell, U., Schulz, K. G., Bellerby, R. G., Botros, M., Fritsche, P., Meyerhöfer, M., Neill, C., Nondal, G., Oschlies, A., Wohlers, J., and Zöllner., E.: Enhanced biological carbon consumption in a high CO_2 ocean, Nature, 450, 545–548, 2007.

Riebesell, U., Bellerby, R. G. J., Grossart, H.-P., and Thingstad, F.: Mesocosm CO_2 perturbation studies: from organism to community level, Biogeosciences, 5, 1157–1164, doi:10.5194/bg-5-1157-2008, 2008.

Riebesell, U., Körtzinger, A., and Oschlies, A.: Sensitivities of marine carbon fluxes to ocean change, P. Natl. Acad. Sci. USA, 106, 20602–20609, doi:10.1073/pnas.0813291106, 2009.

Riebesell, U., Czerny, J., von Bröckel, K., Boxhammer, T., Büdenbender, J., Deckelnick, M., Fischer, M., Hoffmann, D., Krug, S. A., Lentz, U., Ludwig, A., Muche, R., and Schulz, K. G.: Technical Note: A mobile sea-going mesocosm system – new opportunities for ocean change research, Biogeosciences, 10, 1835–1847, doi:10.5194/bg-10-1835-2013, 2013.

Sabine, C. L., Feely, R. A., Gruber, N., Key, R. M., Lee, K., Bullister, J. L., Wanninkhof, R., Wong, C. S., Wallace, D. W. R., Tilbrook, B., Millero, F. J., Peng, T.-H., Kozyr, A., Ono, T., and Rios, A. F.: The Oceanic Sink for Anthropogenic CO_2, Science,

305, 367–371, doi:10.1126/science.1097403, 2004.

Sarmiento, J. L. and Le Quéré, C.: Oceanic Carbon Dioxide Uptake in a Model of Century-Scale Global Warming, Science, 274, 1346–1350, doi:10.1126/science.274.5291.1346, 1996.

Sarmiento, J. L., Slater, R., Barber, R., Bopp, L., Doney, S. C., Hirst, A. C., Kleypas, J., Matear, R., Mikolajewicz, U., Monfray, P., Soldatov, V., Spall, S. A., and Stouffer, R.: Response of ocean ecosystems to climate warming, Global Biogeochem. Cy., 18, GB3003, doi:10.1029/2003GB002134, 2004.

Schmittner, A., Oschlies, A., Matthews, H. D., and Galbraith, E. D.: Future changes in climate, ocean circulation, ecosystems, and biogeochemical cycling simulated for a business-as-usual CO_2 emission scenario until year 4000 AD, Global Biogeochem. Cy., 22, GB1013, doi:10.1029/2007gb002953, 2008.

Schulz, K. G., Riebesell, U., Bellerby, R. G. J., Biswas, H., Meyerhöfer, M., Müller, M. N., Egge, J. K., Nejstgaard, J. C., Neill, C., Wohlers, J., and Zöllner, E.: Build-up and decline of organic matter during PeECE III, Biogeosciences, 5, 707–718, doi:10.5194/bg-5-707-2008, 2008.

Schulz, K. G., Bellerby, R. G. J., Brussaard, C. P. D., Büdenbender, J., Czerny, J., Engel, A., Fischer, M., Koch-Klavsen, S., Krug, S. A., Lischka, S., Ludwig, A., Meyerhöfer, M., Nondal, G., Silyakova, A., Stuhr, A., and Riebesell, U.: Temporal biomass dynamics of an Arctic plankton bloom in response to increasing levels of atmospheric carbon dioxide, Biogeosciences, 10, 161–180, doi:10.5194/bg-10-161-2013, 2013.

Sharp, J. H.: Improved analysis for "particulate" organic carbon and nitrogen from seawater, Limnol. Oceanogr., 19, 984–989, 1974.

Silyakova, A., Bellerby, R. G. J., Czerny, J., Schulz, K. G., Nondal, G., Tanaka, T., Engel, A., De Lange, T., and Riebesell, U.: Net community production and stoichiometry of nutrient consumption in a pelagic ecosystem of a northern high latitude fjord: mesocosm CO_2 perturbation study, Biogeosciences Discuss., 9, 11705–11737, doi:10.5194/bgd-9-11705-2012, 2012.

Tanaka, T., Alliouane, S., Bellerby, R. G. B., Czerny, J., de Kluijver, A., Riebesell, U., Schulz, K. G., Silyakova, A., and Gattuso, J.-P.: Effect of increased pCO_2 on the planktonic metabolic balance during a mesocosm experiment in an Arctic fjord, Biogeosciences, 10, 315–325, doi:10.5194/bg-10-315-2013, 2013.

Thingstad, T. F., Bellerby, R. G. J., Bratbak, G., Borsheim, K. Y., Egge, J. K., Heldal, M., Larsen, A., Neill, C., Nejstgaard, J., Norland, S., Sandaa, R. A., Skjoldal, E. F., Tanaka, T., Thyrhaug, R., and Topper, B.: Counterintuitive carbon-to-nutrient coupling in an Arctic pelagic ecosystem, Nature, 455, 387–390, 2008.

Toggweiler, J. R.: Carbon overconsumption, Nature, 363, 210–211, 1993.

Volk, T. and Hoffert, M. I.: Ocean carbon pumps – Analyses of reactive strengths and efficiencies in ocean-driven atmospheric CO_2 changes, in: The Carbon Cycle and Atmospheric CO_2: Natural Variations, Archean to Present, edited by: Sundquist, E. and Broecker, W., AGU Geophysical Monograph, Washington DC, 99–110, 1985.

von Bodungen, B., Antia, A., Bauerfeind, E., Haupt, O., Koeve, W., Machado, E., Peeken, I., Peinert, R., Reitmeier, S., Thomsen, C., Voss, M., Wunsch, M., Zeller, U., and Zeitzschel, B.: Pelagic processes and vertical flux of particles: an overview of a long-term comparative study in the Norwegian Sea and Greenland Sea, Geol. Rundsch., 84, 11–27, doi:10.1007/bf00192239, 1995.

Wassmann, P.: Retention versus export food chains: processes controlling sinking loss from marine pelagic systems, Hydrobiologia, 363, 29–57, 10.1023/a:1003113403096, 1997.

Welschmeyer, N. A.: Fluorometric analysis of chlorophyll a in the presence of chlorophyll b and pheopigments, Limnol. Oceanogr., 29, 1985–1992, 1994.

3. Technical and methodical improvements

Analysing the Svalbard elemental dataset revealed some weaknesses of the set-up. DOC was not measured at a satisfying precision and had therefore to be excluded from elemental budgeting. This lack of precision could be solved by switching to an acid washed sampling container in the following experiment. However, dissolved organic carbon, nitrogen and phosphorus remain the most problematic parameters also in later experiments. High background concentrations, easy contamination and the multitude of processing steps during analyses make it hard to meet precision standards of most of the other analyses. Further delicate issues like wall growth, dead volume below the sediment traps associated with potentially lost sediments as well as comparatively sparse data on zooplankton elemental composition had to be evaluated carefully. Yet, most of those drawbacks could be removed for the next experiment.

3.1 Cleaning the walls

Beside variability in DOM measurements, wall growth was another critical point when constructing the elemental budget for the Svalbard 2010 experiment. The idea of a cleaning ring was born on Svalbard, when apparent wall growth had to be quantified in order to close an elemental budget at the end of the study. On site, it was constructed from one of the mesocosms sediment trap floatation rings. Despite initial handling problems of the large heavy weighted ring, first cleaning results were rather convincing. Continuous improvements on the rope system, a closing and opening mechanism, the circumferential silicon wiper and an electric winch, made regular inside-cleaning of the bag efficient and practicable. "Easy cleaning" is important in any study as wall growth was proven not to be confined to eutrophic environments. Later studies showed benthic cyanobacteria to be competitive at inorganic nutrients on nanomolar levels. In spite of our success in keeping benthic biomass insignificant compared to plankton biomass by regular cleaning, the presence of a large surface area remains an issue when comparing mesocosm community composition to open water plankton. Providing settling ground, even only for a short duration, favours the development of benthic biofilms and microalgae. Benthic species may become enriched in the mesocosm compared to open waters over time. A clear advantage of the KOSMOS mesocosms is the low relative surface area of ~2m²/m³ compared to smaller set-ups. The cylindrical part of the mesocosm, rigid due to 200 kg heavy bottom weight and 500 µm foil, can be automatically cleaned, whereas cleaning of more light weighted constructions commonly used for mesocosm bags would be not feasible.

Efforts to reduce biofouling on the mesocosm surfaces and to improve durability of the system enables us for the first time to conduct long-term mesocosm studies in more relevant areas exposed to moderate marine weather conditions.

Long-term mesocosm studies will have the potential to firstly increase relevance of the datasets by including effects on higher, economically more important trophic levels; and secondly enhance significance of the findings through improved coverage of secondary and long-term treatment effects. With experiments lasting for several months, mechanisms relevant on a seasonal scale can be addressed. The most important cleaning tools are shown in Fig. 3.1.

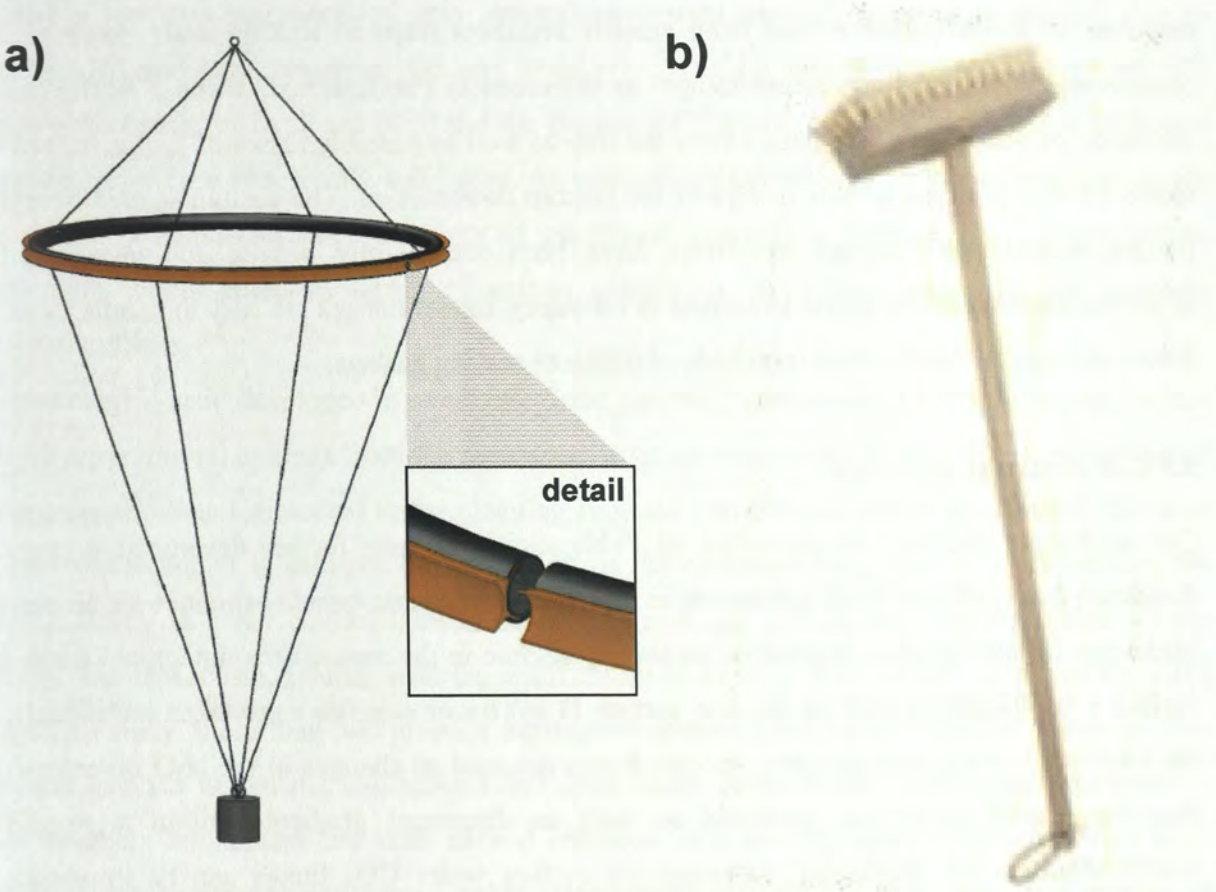

Figure 3.1. a) Weighted cleaning ring with silicon wipers used to prevent biofouling on the inside walls of the mesocosm. Ring can be opened for easier deployment (detail). **b)** Professional diving scrubber for cleaning of outer fouling. (Drawings by Detlef Hoffmann)

3.2 Sediment traps

Since the first large scale KOSMOS trials in 2007, funnel shaped sediment traps with vacuum sampling tube to the surface were installed in the bottom of the mesocosm. Due to strong variation of daily sampled sediment amounts within the first trials, sediment traps were enlarged for the 2010 study to cover the entire bottom surface of the mesocosm. The large trap should

collect all material settling and thereby account for possibly uneven distribution of sinking material among the bottom area as well as avoid trapping of resuspended material. The quantitative extraction of freshly settled material from the system eliminates the input of remineralised nutrients from below. This is a basic prerequisite for elemental budget calculations, as sediment traps on sub-units of the surface can only provide information on composition of settling material that was trapped and not on the composition of bulk exported material that underlies further degradation remaining within the system.

The large floating sediment trap as used in Svalbard 2010 was relatively quickly installed in response to inconvenient results from smaller sediment traps in a 2009 trial. However, this construction involved some disadvantages as discussed in Publications 2.1 and 2.3. The limited exchange of water with the space below the trap as well as possible losses of sediment into this space led to a principally new design of the bottom construction. The custom shaped fibreglass flanges attached and closed by divers have been successfully proven and tested in five deployments since 2010. Close to neutral in buoyancy funnel flanges are easy to handle by scuba divers and can be fitted with a multitude of different sealing gaskets.

3.3 Gas exchange estimates

Gas exchange estimates as described in Publication 2.3 were further developed to provide diapycnal fluxes of dissolved substances in stratified mesocosms, beside estimates for air-sea gas exchange. In later studies, depending on mixing regime in the mesocosms, integrated deep- and surface mixed layer as well as discrete surface (1 m) tracer samples were taken additionally to the total depth-integrated samples. Air-sea fluxes detected as changes in the N_2O inventory can thus be related to air-sea gradients as well as diapycnal gradients within a simplified stratification model. Biological influence on surface water CO_2 fluxes can be important in stratified mesocosms, especially during periods of high primary production. To improve CO_2 gas exchange estimates, the depth-integrated carbonate chemistry dataset was accomplished by routine surface (1 m) pCO_2 measurements using a HydroC™ CO_2 sensor (Contros Systems and Solutions GmbH). Uncertainties arising from estimated chemical enhancement of CO_2 air-sea gas exchange were narrowed down by continuous measurement of sea surface (10 cm) temperature within the mesocosms using HOBO precision temperature loggers.

3.4 Sampling the upper trophic levels

Many questions concerning ecological and biogeochemical responses of organisms in the size range from bacteria to metazooplankton can be answered using smaller and thus much cheaper

experimental setups. Mesocosms larger than 50 m^3, however, offer the unique opportunity to study large organisms that need considerable amounts of space and resources for their natural development within an enclosed ecosystem. Experiments on economically or biogeochemically highly relevant food web components such as fish, jellyfish, appendicularians or pteropods usually suffer limitations arising from external or artificial food supply. Within the KOSMOS mesocosms, we were able to observe the natural occurrence of fish developed from eggs enclosed in the beginning of the experiment, as well as the establishment of pteropod, jellyfish and appendicularian populations. Datasets on the abundance of those species occurring in relatively low concentrations of only several specimens per m^3 were often limited due to problems of adequate sampling. Despite large efforts in the end of the experiment, juvenile fishes observed in the Svalbard 2010 and the Bergen 2011 study could not be caught in sufficient numbers to produce statistically valid data. An appendicularien bloom, obviously responsible for the vertical transport of large amounts of gelatinous material in Bergen 2011, could not be sufficiently documented in terms of animal abundance to draw conclusions on apparent treatment effects.

Two strategies were developed to overcome these sampling limitations. Firstly, a fishing net that allows retrieving all animals from the mesocosm after an experiment is terminated, regardless of escape capabilities. Connected to the cleaning ring, the constructed net covers the full diameter of the mesocosm. It is brought to the bottom of the enclosure in a folded configuration. By putting strain on a net control line, the funnel shaped net unfolds and can be pulled slowly through the mesocosm, sealing with the walls on all sides (Fig. 3.2). In the Kristineberg 2013 long-term study, more than 500 juvenile herrings of around 5 cm length could be retrieved. The animals hatched within the mesocosms and grew much faster in the mesocosms compared to their brothers and sisters fed with natural plankton in a parallel lab experiment. Soon after hatching, larvae disappeared from weekly zooplankton samples, as they grew fast enough to escape the 20 cm net opening used during routine sampling.

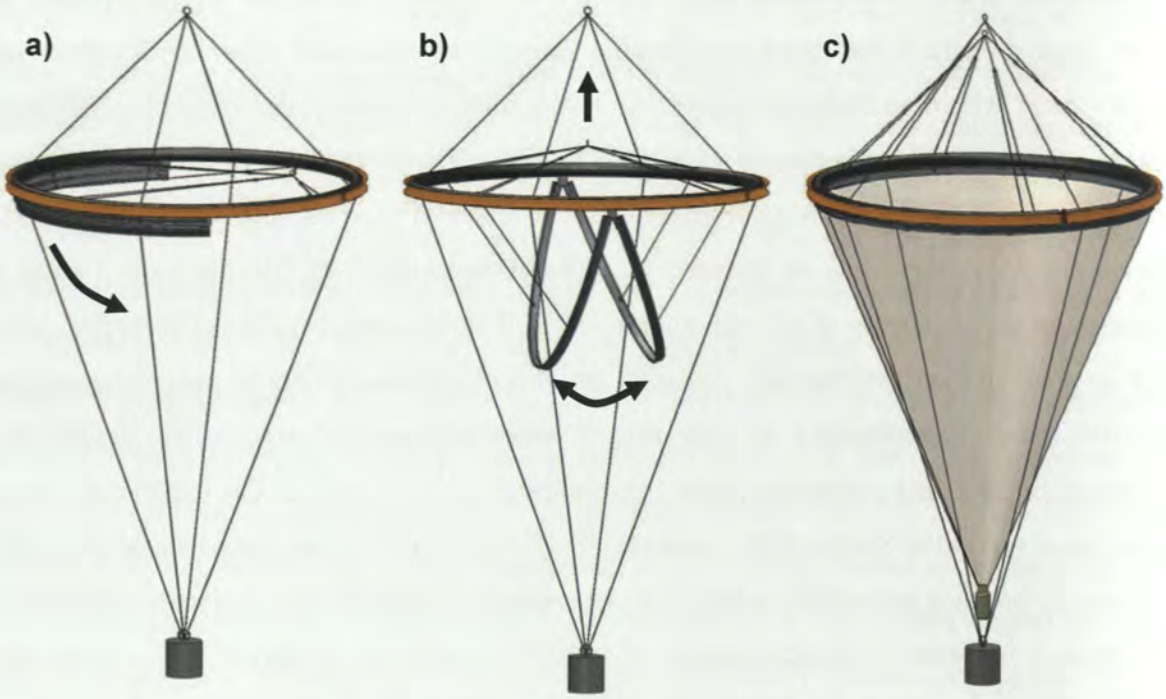

Figure 3.2. The mesocosm fishing net. **a)** Open configuration - both halves of the net ring on one side, so that cleaning ring can be opened enabling installation. During lowering, both halves of the net ring are hanging vertically to allow passage of the net below enclosed animals (net not shown). **b)** Net control line is pulled when the construction reached the bottom of the mesocosm - the net unfolds to cover the entire mesocosm surface and seals with the walls (net not shown). **c)** The unfolded net - can be slowly pulled up using the net control line. Reverse procedure for deinstalling and retrieving the sample. (Drawings by Detlef Hoffmann)

The second technical development gives timeline data on the development of large rare species. Frequent sampling of animals, present in low numbers of only a few hundred per mesocosm, would diminish the population and potentially lead to extinction of the animals from the mesocosm. Coordinated by fellow scientist Jan Büdenbender, a camera system was developed in cooperation with the company Develogic Subsea systems. Named "KielVision", this camera is designed to quantitatively screen a water column of 1.2 m^3 within the mesocosm for larger particles (Fig. 3.3). Lowered slowly down the mesocosm, KielVision is taking high resolution pictures of defined water slices every 2 cm. Based on these pictures, objects larger than ~200 µm can be non-destructively quantified and measured using the software package ZooImage (http://www.sciviews.org/zooimage/). KielVision is designed to not only create high temporal resolution abundance and growth estimates for the upper trophic levels, but also bring light into mechanisms causing sedimentation events. Observation of water column aggregation should help

connecting events of strong sediment flux to physical, biological and chemical circumstances described in the mesocosm.

Figure 3.3. KielVision. When lowered through the mesocosm, a defined water volume within the bottom frame is illuminated by red light flashes. The camera installed in the glass dome takes high resolution pictures at a frequency of up to 18 per second. An inbuilt computer connects pictures to pressure data and prepares files for later analyses. Lowered once through a 20 m mesocosm, a vertical particle profile capturing particles from 1.2 m^3 of water is recorded. Plankton organisms larger than 200 µm can be identified from automatically sorted libraries. (Drawing by Devologic)

4. Perspectives

In the following paragraphs, biogeochemical questions and hypotheses for past and future mesocosm experiments are discussed. New technical approaches to tackle those questions in the future are presented.

All past KOSMOS experiments investigated the effect of increased CO_2 concentrations on temperate to Arctic marine ecosystems. Marine regions, plankton communities and seasons varied between the experiments, leading to different CO_2 responses of the enclosed plankton communities. To move from case studies towards more general answers, improvements in experimental set-ups, sampling protocols and data analyses are needed. Specific findings of experiments performed since 2010 are not discussed within this thesis, but some general observations are used to formulate a new hypothesis for future ocean acidification experiments. Possible application of KOSMOS mesocosms for unravelling biogeochemical fluxes connected to sporadic nutrient inputs in oligotrophic oceans (e.g. eddy pumping, hurricane blooms, artificial upwelling, dust / volcanic ash events) are proposed. Funding for this important basic research may be raised with reference to risk-benefit assessment for potentially socio-economically important artificial upwelling strategies.

4.1 Optimising data acquisition and analyses

Biogeochemical results from laboratory experiments with single species and on short time scales were used to formulate most hypotheses for our community experiments. Major questions of our experiments concerning the effect of increased CO_2 levels on microbial biogeochemistry are:

- Are detrimental effects of seawater acidity on coccolithophore calcification significantly affecting future carbon export due to reduced carbonate ballast?
- Is future increased CO_2 availability leading to carbon overconsumption by phytoplankton? Will future particles thus be enriched in carbon?
- Is carbon export increased due to the formation of TEP from exuded overconsumption?
- Are CO_2 effects on cyanobacteria changing the oceans nitrogen budget?

We were the first describing all relevant parts of the system within large scale mesocosm experiments. Recorded data describe pools and fluxes of the most relevant bioactive elements as well as community composition at high temporal resolution. In general the enclosed ecosystems appeared surprisingly robust, often showing ecological and biogeochemical patterns comparable

between mesocosms and the surrounding waters for weeks and months. However, most of the questions addressed over the past years cannot yet be readily answered. We are so far unable to answer those questions with a simple yes or no, even though plenty of data on the enclosed system were collected and various CO_2 effects have been detected. The achieved data are very complex and uncertainties as to the universal applicability of the findings remain. On the ecosystem level, diverse species assemblages may often level out effects, while strong control mechanisms such as nutrient availability and grazing pressure may enhance or override CO_2 effects of single species physiology. While a coccolithophore dominated species assemblage may react to CO_2 as can be expected from monoculture experiments, coccolithophores that first have to establish their dominance in a top down controlled community may appear more CO_2 sensitive. Elemental composition of particulate matter can be stable when species composition is complex but may show large plasticity when the system becomes dominated by one blooming phytoplankton group under similar experimental conditions. Organic exudates may accumulate as DOC, aggregate as TEP or be immediately consumed by bacteria, depending on community composition.

Compared to field data, mesocosm experiments have a temporal component that allows for quantitative observation of the processing of matter within a system. However, the enclosed community sampled at one point in time can only show us a snapshot of what may happen in the given environment. Projections concerning the effect of CO_2 on biogeochemical fluxes in the future can only be made by taking into account general ecological and physiological patterns derived from as many community and single species experiments as possible. Meta-analyses of the performed experiments are necessary to reveal general patterns. Inverse modelling enables estimating carbon and nutrient fluxes between functional groups of the plankton community as well as export and accumulation of dissolved organics (Vadstein et al., 2012; Vallino, 2000). As shown in Fig. 4.1a, observations of standing stocks and rates from the experiment can be accomplished using mass balance. Models can then be tested on further mesocosm datasets featuring e.g. different starting composition of the enclosed community (Parsons, 1990). The diversity in biogeochemical ecosystem models is high (Friedrichs et al., 2007; Arhonditsis and Brett, 2004). Compiling an ecosystem model adapted to the specific observational structure and scientific questions in KOSMOS mesocosm research is the critical step. Most global models apply very simplified representations of the marine ecosystem (Fasham et al., 1990; Bopp et al., 2013) which cannot capture community changes as observed in mesocosm experiments. More complex models, describing functional types within phytoplankton, zooplankton and bacteria, as well as their specific interactions are needed (e.g. Moore et al., 2001; Quere et al., 2005).

However, it has been debated if it makes sense to increase complexity of models in consideration of current gaps in parameter constraints through lack of data, and little knowledge about modelled ecological interactions (Flynn, 2005). On a global scale, simple models usually outperform complex approaches that are better fitted to regional ecosystems (Anderson, 2005). Mesocosms are the smallest scale an ecosystem model can be applied to. Results as the one presented in this thesis seem to be ideal to test model outputs while it is realistic to actually measure, directly during the experiment, rates and quantities needed to run a complex model.

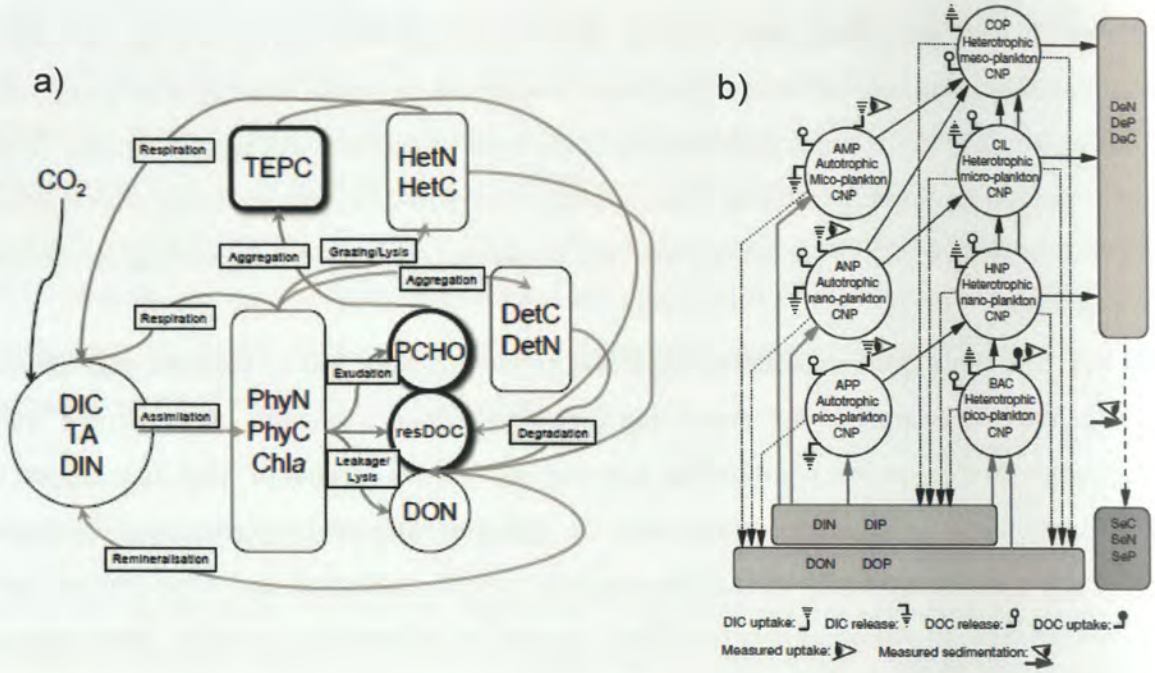

Figure 4.1. Two different model flow networks used for biogeochemical mesocosm ecosystem modelling. **a)** The model by Schartau et al. (2007) includes carbon fluxes from inorganic carbonate system to sedimentation at relatively low ecological resolution with heterotrophs and autotrophs grouped. Aggregate formation mechanisms and DOM cycling are explicitly parameterised. **b)** The model by Vadstein et al. (2012) resolves community composition by three functional groups of autotrophs and four groups of heterotrophs. Most metabolic rates for the specific groups are adopted from the literature while some are measured. Sedimentation is represented via a one-way flow from autotrophs via heterotrophs and detritus including a microbial loop via dissolved organics. Inorganic carbon and export mechanisms are not explicitly parameterised. Abbreviations: DIC-dissolved inorganic carbon, TA-total alkalinity, DOC-dissolved organic carbon, TEPC-transparent exopolymer carbon, PCHO-polysaccharides, DIN / DIP- dissolved inorganic nitrogen / phosphorus, DON / DOP-dissolved organic nitrogen / phosphorus, DeN / DeP / DeC-detritus nitrogen / phosphorus / carbon, SeN / SeP / SeC-sediment nitrogen / phosphorus / carbon, COP-copepods, CIL-ciliates, BAC-bacteria.

Fractionation of particulate matter into size classes best fitted to represent parameterized functional groups should be elaborated. Rates of nutrient uptake, carbon acquisition, respiration, growth or grazing of exactly those groups, as well as their potential CO_2 dependence, should be determined. Measuring temperature dependence of key processes, effects of global warming could be investigated once the system is mathematically described. It would be useful to agree on a standardised protocol of data acquisition for all future experiments in close cooperation with modellers. In this cooperation of modellers and analysts, sensibilities of the model and capabilities of analytics can be aligned. Units of measurement output are currently often not quantitatively comparable. Specific rates measured in side-experiments are often not representative for the whole mesocosm (Engel et al., 2013). Measurements directly within the mesocosm deliver bulk estimates on larger timescales, but are quantitatively more robust (Czerny et al., 2013; Silyakova et al., 2013). Recalibration of multiple approaches to determine elemental flow pathways and rates should be applied. Net community inorganic carbon uptake based on presented gas exchange measurements and dissolved inorganic carbon could be accomplished by daily estimated rates derived from oxygen and CO_2 logger data. Turnover rates of carbon and nutrients within functional plankton groups can be estimated by addition of stable isotope tracers at certain periods within the experiment and their detection within specific fatty acids (Van den Meersche et al., 2004). Tracing pathways of ^{13}C (de Kluijver et al., 2013) and $^{15}N_2$ (unpublished results) primarily fixed within the system was already practiced in KOSMOS mesocosms. The addition of labelled organic carbon, nitrogen or phosphorus could shed light into turnover times of dissolved organics and the activity of the microbial loop (Ducklow et al., 1986). Given the multitude of experimental approaches for unravelling the functions of enclosed ecosystems, numerical analyses of mesocosm data would help to improve concepts to constrain mechanisms for further experiments. Unprecedented interdisciplinary expertise is collaborating to describe ecosystem biogeochemistry in KOSMOS experiments. A complex picture of the ecosystem could be drawn with large gain for biogeochemical modelling with little additional efforts. Sensitivity of biogeochemical fluxes to unavoidable variability in physical forcing, enclosure size or initial composition of the community may be tested. Not only educated estimates for so called "mesocosm artefacts" can be generated; models can also provide a calculation basis for planning ecological manipulations e.g. the addition of larval fish.

4.2 Experiments on simulated eddy upwelling

Experimental plans focussing on CO_2 dependent mechanisms for particle export during tropical upwelling events will be presented. As mesocosm datasets become relevant for biogeochemistry only when describe natural events connected to relevant fluxes of matter, oligotrophic regions do not intuitively appear to be attractive research areas. Export events, by definition, can only be connected to new production and not to regenerated production when matter is recycled within the surface layer (Peterson, 1979). Seasonal thermal convection is one way nutrients can be supplied to the surface layer. Eckman transport resulting from a combination of wind and currents, modified by the Earth's rotation, is another way responsible for a multitude of convectional patterns inducing upwelling of nutrient rich deep water (Marshall and Schott, 1999). Frequent nutrient inputs to the surface layer are predominantly found at high latitudes and on the eastern margins of the Atlantic and Pacific Ocean (Levitus et al., 1993). However, sporadical upwelling can also occur within generally oligotrophic subtropical and tropical regions. "Island mass effects" create blooms and nutrient rich eddies downstream of seamounts and islands (Gilmartin and Revelante, 1974). Upwelling often occurs at hydrographical fronts and predominantly along the intertropical convergence zone, where southern and northern hemisphere weather and current systems meet. Mesoscale eddies with lifetimes usually less than three weeks and in the size range of hundreds of km^2 carry nutrient rich waters deep into oligotrophic regions (Fu et al., 2010). Important sub-mesoscale turbulence patterns with low altitude profile are commonly not detected (Levy et al., 2001). Not only horizontal propagation of productive islands through oligotrophic waters is frequent, but also multiple mechanisms for vertical nutrient upwelling in those turbulent structures exist (Siegel et al., 2011). Geochemical tracer data suggest deepwater N inputs to most oligotrophic regions such as the North Atlantic subtropical gyre, large enough to support export of 3 $molCm^{-2}yr^{-1}$ (Jenkins, 1988). The C/N ratio of the flux is assumed to be 6.5 according to Redfield. 3 $molCm^{-2}yr^{-1}$ of new production is an extraordinary high estimate for ocean deserts such as the subtropical gyre. Observations and models propose not more than half of this flux for the subtropical gyres (Oschlies, 2008). Allowing for variable and often much higher C/N ratios (~10.2) observed in trapped material would cumulate discrepancies regarding the relevance of oligotrophic oceans for global carbon fluxes (Fig. 4.2; Tamelander et al., 2013). Such discrepancies in N input and C/N ratios are relevant to global carbon flux projections, especially in respect of the vast area covered by oligotrophic regions. However, mechanisms responsible for observed variability are largely unknown.

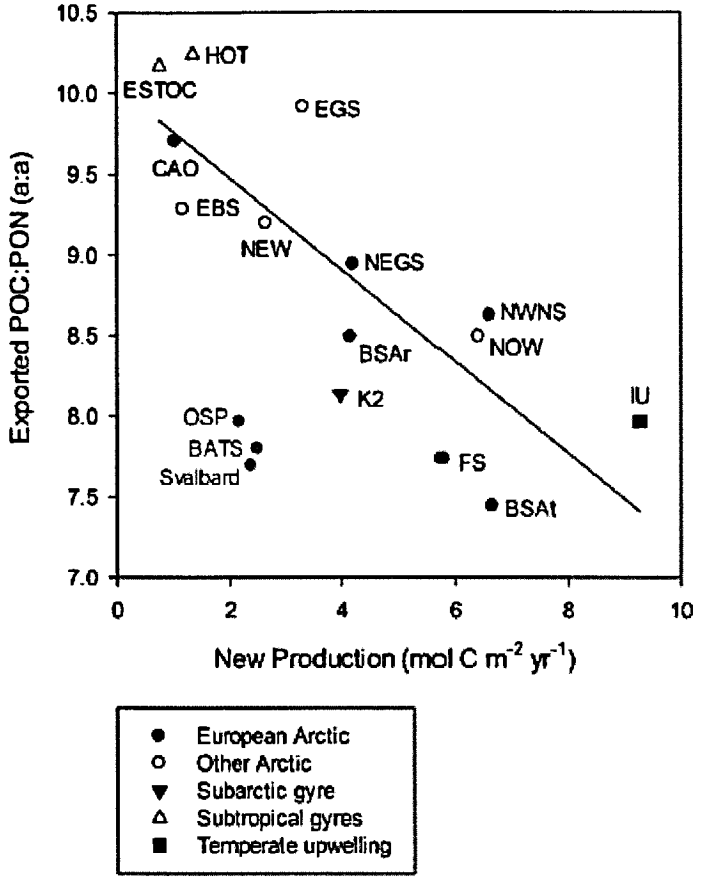

Figure 2. Mean exported C/N ratio of sinking material sampled at 400 m depth at various ocean locations against modelled average annual new production. Stations marked by grey symbols are not included in regression due its advective nature. (Figure from Tamelander et al., 2013)

Svalbard shelf break, Svalbard
Central Arctic Ocean, CAO
NE Greenland shelf, NEGS
Fram Strait, FS
Barents Sea Arctic, BSAr
Barents Sea Atlantic, BSAt
NW Norwegian shelf, NWNS
Northeast Water Polynya, NEW
North Open Water Polynya, NOW
E Greenland shelf, EGS
East Beaufort Sea, EBS
N Pacific subarctic gyre, K2
Iberian upwelling, IU
NE Atlantic subtropical gyre, ESTOC
N Pacific subtropical gyre, HOT
NE Subarctic Pacific, OSP
W Sargasso Sea, BATS

Currently, modelled enhancement of biological production by mesoscale eddies varies between 20% and 100-200%, the latter values being probably overestimates (reviewed by Oschlies, 2008). Persisting discrepancies to geochemical estimates of new production may be partly explained by sub-mesoscale events not accounted for by eddy resolving models. Furthermore, wind induced mixing of the surface layer by tropical cyclones was observed to cause phytoplankton blooms of large spatial extension (Shi and Wang, 2007). Based on long-term satellite observations of the subtropical North Atlantic, it was hypothesised that cyclone events could contribute as much nutrients to surface layer production as estimated for mesoscale eddies (Babin et al., 2004). Permanently stratified ocean regions are expected to expand as a consequence of global warming. An observed decrease in satellite-derived ocean productivity within the last decade is mainly driven by changes in those oligotrophic areas, already representing 75% of the ice free global ocean (Behrenfeld et al., 2006). The important control of global ocean productivity by the El Niño-Southern Oscillation (ENSO) is also likely to be influenced by global warming. However, direction or magnitude of future changes in ENSO is not yet predictable (Collins et al., 2010).

C/N variability of exported biomass during production events within oceanic deserts is virtually uncharacterised. Mesocosm experiments could provide first data on ecosystem biogeochemistry and CO_2 dependent export stoichiometry within such events.

From a technical point of view, artificial upwelling seems to provide nearly ideal prerequisites to perform meaningful experiments:

Plankton succession in response to sporadic upwelling events is poorly described compared to temperate regions and permanent upwelling regions. Data describing the North Atlantic spring bloom or the Peruvian upwelling system can be achieved by scheduled field campaigns. In contrast, plankton succession from nutrient input up to depletion and export within eddies can hardly be planned. Natural eddies can be well detected through sea surface height or Chl *a* measurements by satellites. But whenever water samples are taken, the system is already matured. Biogeochemical budgets are hard to construct due to on-going mixing processes.

Artificial upwelling events can be planned at any time of the year. Using deliberate deepwater upwelling into a closed mesocosm system, the initial ecosystem can be characterised before a precisely known amount of analytically characterised deepwater is added. Climatic conditions within the tropics are fairly predictable compared to e.g. the climatic situation at the onset of the North Atlantic spring bloom. The spring bloom is highly weather-depending, as it is initiated by favourable light and temperature conditions. Not only the timing of the bloom can vary by months, also the food web structure depends on temperature development and light.

Besides reproducible physical forcing, oligotrophic surface water as well as aged deepwater can be expected to have a rather constant and predictable biology (Cushing, 1989). Thus, reproducibility of deliberate upwelling experiments is further enhanced by food web structure in oligotrophic compared to eutrophic systems. Grazers specialised on large particles like diatoms, usually present at variable abundance within eutrophic or mesotrophic systems, are virtually absent in oligotrophic systems. A bloom of large phytoplankton occurring after nutrient input would be most likely bottom-up controlled and therefore characterised by freshly exported biomass at presumably variable C/N. The natural absence of benthic species in oceanic plankton would likely reduce effort and bias connected to wall grown biomass.

Other in eutrophic waters, surface water gas concentrations in oligotrophic regions are usually in equilibrium with the atmosphere. By deepwater addition, CO_2 treatment levels adjusted according to IPCC scenarios are boosted towards stronger acidification by the naturally high CO_2 concentrations in deep waters.

4.3 Potential CO_2 effects on sporadic export production in oligotrophic waters

As a general pattern from our mesocosm experiments, we observed species composition to be the first and most sensitive parameter to react to any perturbation within a community. The pico- and nano-phytoplankton nearly immediately reacted with increased growth to elevated CO_2 in almost

every experiment. Not always, however, with detectable consequences for biogeochemical fluxes. In the Svalbard experiment, nutrient uptake by picoautotrophs seemed to be affecting growth of diatoms following in the phytoplankton succession. Decreased nitrate availability within the high CO_2 treatments resulted in reduced carbon export compared to relatively nutrient replete low CO_2 treatments. Small-celled phytoplankton production at high CO_2 accumulated carbon within the dissolved organic fraction. This scenario featuring a picoplankton dominated surface water community confronted with a sudden nutrient input is the standard case for tropical upwelling events. Initially devoid of large diatoms, a CO_2 affected picoplankton community determines the growth conditions for blooming diatoms emerging after a lag phase. Also devoid of species grazing on microplankton, this community can be expected to export a large fraction of the freshly produced biomass. In earlier KOSMOS experiments, elemental composition of particles within complex species assemblages, co-dominated by several phytoplankton and zooplankton groups, was remarkably constant and close to Redfield. This was also the case in Svalbard during nearly the entire experimental duration, except of the last days when a blooming diatom-dinoflagellate assemblage became dominant. The high carbon content of those bloomers was presumably a result of nutrient limitation. With increasing sinking flux of fresh biomass, increasing carbon content in the sinking material was measured. As the ratio between picoplankton and blooming microplankton was CO_2 dependent, we could expect more fresh biomass to be exported at low CO_2. Community shifts similar to those in tropical upwelling events, featuring a transition from diverse picoplankton assemblages to blooming microplankton, are connected to airborne dust or volcanic ash input into HNLC (High Nutrients Low Chlorophyll) regions (Olgun et al., 2011; Hamme et al., 2010).

Picoplankton is grazed and most efficiently packed into fast sinking faecal pellets by salps, appendicularians and thecosome pteropods within subtropical regions. Since the large size ratio of those microphages is at least 3.5 orders of magnitude larger than their pray, carbon turnover time is affected most efficiently. Small particulate, usually short lived, organic carbon is directly passed high up the food chain or down into deepwater layers (Fortier et al., 1994; Berline et al., 2011). Within two KOSMOS experiments of the recent years, we observed appendicularian blooms to develop fast and cause significant vertical fluxes by conglomeration of particles around discarded gelatinous houses. Abundance of fast reproducing pelagic tunicates is likely to be affected by CO_2 fertilised growth of picoplankton. By grazing also on free living bacteria, microphages could represent a link from dissolved organic carbon to export and high trophic levels (Urban et al., 1992), but could also promote the conservation of DOM when bacteria are top-down controlled. This potentially exceptional importance of microphages for

biogeochemical cycles in natural food webs is virtually unexplored. Strong direct detrimental effects of increased seawater acidity on pteropods, another important subtropical food chain component, were already documented in a previous KOSMOS experiment (Büdenbender et al., in prep.). Similar to pteropods, development and food chain effects in appendicularians can only be realistically investigated using large mesocosms.

A solution to the conundrum of high nutrient input in subtropical gyres (Jenkins, 1988), currently not supported by observations and models of biological production (Oschlies, 2008), may be found by better understanding of biogeochemical dynamics during upwelling events.

4.4 Experimental set-up for simulated upwelling events in mesocosms off Gran Canary Island

The mesocosms are deployed within oligotrophic waters and left covered by a 3mm net on the upper and lower end to allow water exchange with the surrounding for several days. Thus flushed from eventual contaminations, the mesocosms are closed and volumes are measured using a purified salt solution. The enclosed ecosystem can now be characterised and treated to reach desired CO_2 concentrations. After documentation of the treatment effects on the oligotrophic ecosystem, a depth-integrated volume of 8-16m³ can be removed using a diving pump (Grundfoss SP17-5R) moving continuously up and down the mesocosm. Removal of water is necessary to create space for consequent deepwater addition.

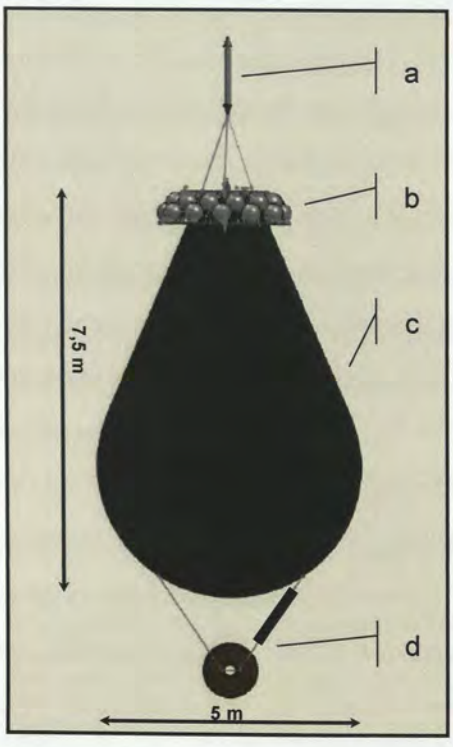

Figure 4.3. a) Expander for compensation of ship movement. **b)** Deep-sea floatation and autonomous filling mechanism. **c)** 80m³ flexible tank welded from fibre reinforced food grade PVC. **d)** Weight system with acoustic release unit. Drawing: M. Deckelnick

The water volume transferred is measured and dosed exactly using a ball valve in combination with an electromagnetic flowmeter (Endress+Hauser Promag P50). Before addition, the deepwater needs to be biologically and chemically characterised for the full set of parameters also sampled inside the mesocosms. Using the same pump as used for water removal, deepwater can be transferred from the floating 80 m³ reservoir tank to the mesocosms.

Deepwater can be sampled using two different strategies. The custom designed pump facility, used for injecting the deepwater, can also be used in combination with a CTD rosette to sample specific water layers of up to 400 m depth. The floating 80 m³ reservoir tank can either be filled using this pump or directly be lowered as deep as 900 m, where it is filled by an autonomous filling device (Fig. 4.3). The direct filling at depth is less time-consuming, but allows only water sampling from one predefined depth and not sensor operated sampling as compared to the pump. One of the two filling strategies can be chosen according to hydrographical conditions on site. The floating reservoir tank can be tugged to the mesocosm mooring site (Fig. 4.4).

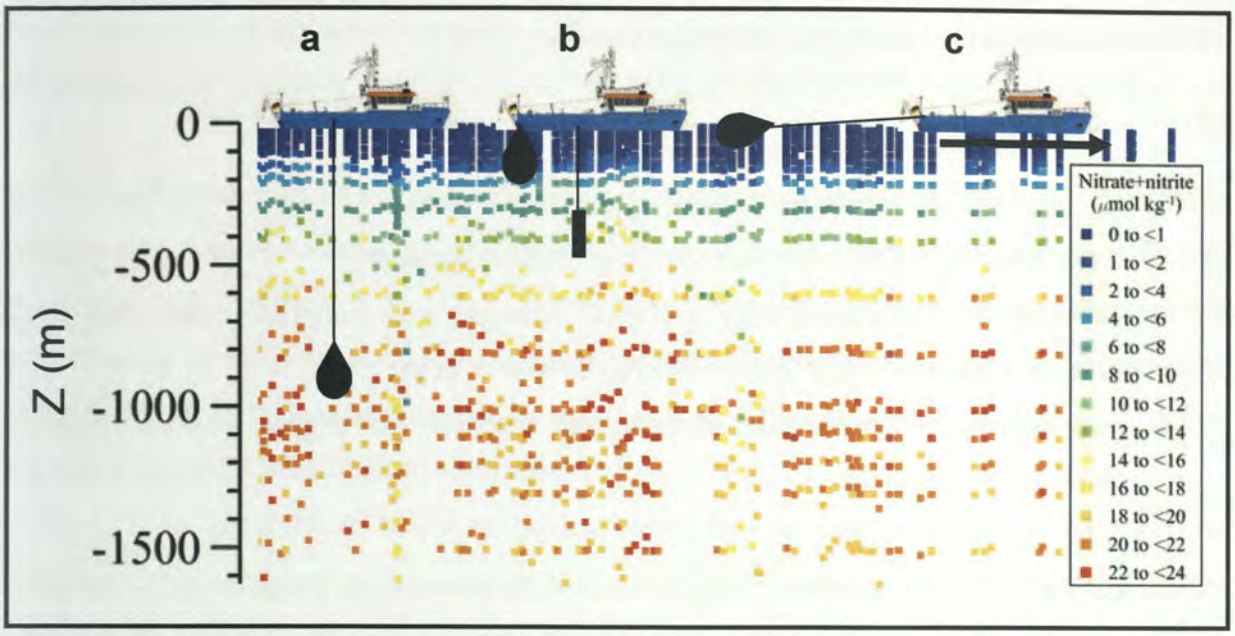

Figure 4. 4. a) Deep water sampling by filling the bag at up to 900 m depth. **b)** Deepwater sampling using the deepwater pump connected to a CTD rosette. **c)** Tugging of the bag to the mesocosm mooring site. One sampling procedure is sufficient to replace 15% of the mesocosm volume with deepwater. Depending on sampling depth, nitrate concentrations of up to 3 µmol/kg could be reached in each mesocosm. Nitrate depth distribution data are from the Canary Island Time Series ESTOC. Figure modified from a poster by O. Linas and M. Gonzalez-Davila, ESTOC (2012).

4.5 Mesocosms experiment for risk and benefit assessment of artificial upwelling strategies

Beside the basic scientific rationale for investigating ecological and biogeochemical processes connected to natural upwelling events, artificial upwelling is currently attracting commercial interests. Geo-engineering approaches targeted to sequester biologically fixed carbon in the oligotrophic open ocean were proposed for mitigate rising atmospheric CO_2 concentrations. The deployment of wave driven deepwater pipes to trigger phytoplankton blooms was proposed (Lovelock and Rapley, 2007; Karl et al., 2008) and prototypes have been tested. By vertical transport of CO_2 as well as of nutrients, upwelling is often rather a source than a sink for

atmospheric CO_2. Biogeochemical modelling suggests carbon sequestration into deep ocean waters to be negligible when Redfield composition C/N/P of upwelled nutrients as well as exported biomass is assumed (Oschlies et al., 2010). Side-effects of such an approach, in turn, may be severe. Fortunately, a ocean-wide installation of wave pipes (e.g. 1 km^{-2}; Oschlies et al., 2010) appears impossible from a technical as well as from an economical perspective. Still, artificial upwelling is well feasible and seems to offer multiple options for economic benefit on a more regional basis. Deepwater nutrients can be used to fertilise the oceans as a food source and temperature gradients to the surface water can be used to generate energy and freshwater. Technical concepts on the way to realisation include:

- air-conditioning using deepwater cooling
- ocean fertilisation to increase fishery yield (Kirke, 2003)
- large scale mariculture to cover the rising seafood demand
- production of electric energy or liquid hydrogen and deionised water using OTEC (**O**cean **T**hermal **E**nergy **C**onversion) (Nihous and Vega, 1993)
- soil cooling for production of temperate crops in the tropical regions using cold agriculture techniques
- …

Technical realisations mostly combining several of the above listed technologies are illustrated in Fig. 4.5.

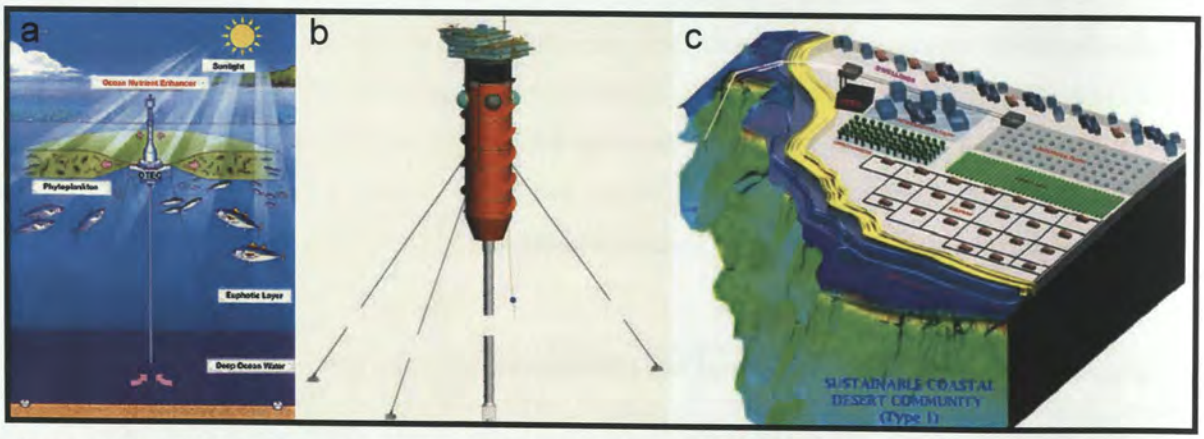

Figure 4.5. a) Schematic representation of the ocean nutrient enhancer (www.energinat.com) **b)** 100MW OTEC platform designed for deployment off Honolulu (www.oteci.com) **c)** Land based production facility combining OTEC energy freshwater, agriculture and mariculture production planned for Haiti.

Many of the listed deepwater utilisation techniques seem to be rather in a state of realisation than development. Deepwater cooling of urban air-conditioning is practiced since decades and the

first 10MW OTEC power plant is about to be constructed (Lusk, 2013). Deliberate eutrophication of oligotrophic tropical coastal waters evoking intuitive denegation by marine ecologists is presented as a "green" strategy for self-sustained renewable energy and food supply for the developing world. The Haitian "Energinat" cooperation, supported by several international companies among others Lockheed Martin, a large US armaments concern, concludes on its homepage (www.energinat.com):

"In our opinion the sustainable socioeconomic development of Haiti can only take place in a harmonious, secure and politically stable environment and will not happen unless Haitians exploit their deep ocean water resource – the nation's most valuable natural energy resource and its inexhaustible marine gold mine. THERE IS NO ALTERNATIVE. THERE IS NONE."

Possible ecological risks of eutrophication such as toxic algal blooms or coral reef destruction spontaneously coming to mind are not discussed. Plans to cover energy requirements of Hawaii by offshore OTEC presented by OTEC international LCC (www.oteci.com) appear somewhat more down to earth. Here, potential ecological impacts of artificial upwelling are discussed in the FAQ section as "potentially increasing the food source for surrounding marine live". A 100 MW plant five miles off Honolulu is planned.

Offshore OTEC in combination with mariculture could be a promising strategy to cover a rising demand for renewable energy and quality food. At the same time it could provide a perpetual source of income to less developed coastal nations that are otherwise poor in resources.

Governmental funding of research on tropical upwelling events seems probable as mesocosm experiments could help to provide a data basis for risks and benefit estimates of such approaches, which would help policy makers to create a legal basis for sustainable use of marine engineering. A pilot study employing free drifting KOSMOS mesocosms was successfully conducted in the Pacific off Hawaii in 2011. Scientific capacity building in less developed countries such as Haiti could improve on-site abilities to judge the installation of unapproved technologies in their local coastal waters.

4.6 References Perspectives

Anderson, T. R.: Plankton functional type modelling: running before we can walk?, Journal of Plankton Research, 27, 1073-1081, 2005.

Arhonditsis, G. B., and Brett, M. T.: Evaluation of the current state of mechanistic aquatic biogeochemical modelling, Marine Ecology Progress Series, 271, 13-26, 2004.

Babin, S. M., Carton, J. A., Dickey, T. D., and Wiggert, J. D.: Satellite evidence of hurricane-induced phytoplankton blooms in an oceanic desert, Journal of Geophysical Research: Oceans (1978-2012), 109 .C3, 2004.

Behrenfeld, M. J., O'Malley, R. T., Siegel, D. A., McClain, C. R., Sarmiento, J. L., Feldman, G. C., Milligan, A. J., Falkowski, P. G., Letelier, R. M., and Boss, E. S.: Climate-driven trends in contemporary ocean productivity, Nature, 444, 752-755, 2006.

Berline, L., Stemmann, L., Vichi, M., Lombard, F., and Gorsky, G.: Impact of appendicularians on detritus and export fluxes: a model approach at DyFAMed site, Journal of Plankton Research, 33, 855-872, 2011.

Bopp, L., Resplandy, L., Orr, J. C., Doney, S. C., Dunne, J. P., Gehlen, M., Halloran, P., Heinze, C., Ilyina, T., Séférian, R., Tjiputra, J., and Vichi, M.: Multiple stressors of ocean ecosystems in the 21st century: projections with CMIP5 models, Biogeosciences, 10, 6225-6245, 2013.

Collins, M., An, S.-I., Cai, W., Ganachaud, A., Guilyardi, E., Jin, F.-F., Jochum, M., Lengaigne, M., Power, S., Timmermann, A., Vecchi, G., and Wittenberg, A.: The impact of global warming on the tropical Pacific Ocean and El Niño, Nature Geoscience, 3, 391-397, 2010.

Cushing, D. H.: A difference in structure between ecosystems in strongly stratified waters and in those that are only weakly stratified, Journal of Plankton Research, 11, 1-13, 10.1093/plankt/11.1.1, 1989.

Czerny, J., Schulz, K. G., Boxhammer, T., Bellerby, R. G. J., Büdenbender, J., Engel, A., Krug, S. A., Ludwig, A., Nachtigall, K., Nondal, G., Niehoff, B., Silyakova, A., and Riebesell, U.: Implications of elevated CO_2 on pelagic carbon fluxes in an Arctic mesocosm study - an elemental mass balance approach, Biogeosciences, 10, 3109-3125, 10.5194/bg-10-3109-2013, 2013.

de Kluijver, A., Soetaert, K., Czerny, J., Schulz, K. G., Boxhammer, T., Riebesell, U., and Middelburg, J. J.: A ^{13}C labelling study on carbon fluxes in Arctic plankton communities under elevated CO levels, Biogeosciences, 10, 1425-1440, 10.5194/bg-10-1425-2013, 2013.

Ducklow, H. W., Purdie, D. A., Williams, P. J. L., and Davies, J. M.: Bacterioplankton: a sink for carbon in a coastal marine plankton community, Science, 232, 865-867, 1986.

Engel, A., Borchard, C., Piontek, J., Schulz, K. G., Riebesell, U., and Bellerby, R.: CO_2 increases ^{14}C primary production in an Arctic plankton community, Biogeosciences, 10, 1291-1308, 10.5194/bg-10-1291-2013, 2013.

Fasham, M. J. R., Ducklow, H. W., and McKelvie, S. M.: A nitrogen-based model of plankton dynamics in the oceanic mixed layer, Journal of Marine Research, 48, 591-639, 1990.

Flynn, K. J.: Castles built on sand: dysfunctionality in plankton models and the inadequacy of dialogue between biologists and modellers, Journal of Plankton Research, 27, 1205-1210, 10.1093/plankt/fbi099, 2005.

Fortier, L., Le Favre, J., and Legendre, L.: Export of biogenic carbon to fish and to the deep ocean: the role of large planktonic microphages, Journal of Plankton Research, 16, 809-839, 1994.

Friedrichs, M. A. M., Dusenberry, J. A., Anderson, L. A., Armstrong, R. A., Chai, F., Christian, J. R., Doney, S. C., Dunne, J., Fujii, M., and Hood, R.: Assessment of skill and portability in regional marine biogeochemical models: Role of multiple planktonic groups, Journal of Geophysical Research: Oceans (1978-2012), 112.C8, 2007.

Fu, L.-L., Chelton, D. B., Le Traon, P.-Y., and Morrow, R.: Eddy dynamics from satellite altimetry, Oceanography, 23, 14-25, 2010.

Gilmartin, M., and Revelante, N.: The "island mass" effect on the phytoplankton and primary production of the Hawaiian Islands, Journal of Experimental Marine Biology and Ecology, 16, 181-204, http://dx.doi.org/10.1016/0022-0981(74)90019-7, 1974.

Hamme, R. C., Webley, P. W., Crawford, W. R., Whitney, F. A., DeGrandpre, M. D., Emerson, S. R., Eriksen, C. C., Giesbrecht, K. E., Gower, J. F. R., and Kavanaugh, M. T.: Volcanic ash fuels anomalous plankton bloom in subarctic northeast Pacific, Geophysical Research Letters, 37.19, 2010.

Jenkins, W. J.: Nitrate flux into the euphotic zone near Bermuda, Nature 331, 521-523, 1988.

Karl, D. M., and Letelier, R. M.: Nitrogen fixation-enhanced carbon sequestration in low nitrate, low chlorophyll seascapes, Marine Ecology Progress Series, 364, 257-268, 2008.

Kirke, B.: Enhancing fish stocks with wave-powered artificial upwelling, Ocean & Coastal Management, 46, 901-915, http://dx.doi.org/10.1016/S0964-5691(03)00067-X, 2003.

Levitus, S., Conkright, M. E., Reid, J. L., Najjar, R. G., and Mantyla, A.: Distribution of nitrate, phosphate and silicate in the world oceans, Progress in Oceanography, 31, 245-273, http://dx.doi.org/10.1016/0079-6611(93)90003-V, 1993.

Levy, M., Klein, P., and Treguier, A.-M.: Impact of sub-mesoscale physics on production and subduction of phytoplankton in an oligotrophic regime, Journal of Marine Research, 59, 535-565, 2001.

Lovelock, J. E., and Rapley, C. G.: Ocean pipes could help the Earth to cure itself, Nature, 449, 403-403, 2007.

Marshall, J., and Schott, F.: Open-ocean convection: Observations, theory, and models, Reviews of Geophysics, 37, 1-64, 1999.

Moore, J. K., Doney, S. C., Kleypas, J. A., Glover, D. M., and Fung, I. Y.: An intermediate complexity marine ecosystem model for the global domain, Deep Sea Research Part II: Topical Studies in Oceanography, 49, 403-462, 2001.

Nihous, G. C., and Vega, L. A.: Design of a 100 MW OTEC-hydrogen plantship, Marine Structures, 6, 207-221, http://dx.doi.org/10.1016/0951-8339(93)90020-4, 1993.

Olgun, N., Duggen, S., Croot, P. L., Delmelle, P., Dietze, H., Schacht, U., Oskarsson, N., Siebe, C., Auer, A., and Garbe-Schönberg, D.: Surface ocean iron fertilization: The role of airborne volcanic ash from subduction zone and hot spot volcanoes and related iron fluxes into the Pacific Ocean, Global Biogeochemical Cycles, 25, GB4001, 2011.

Oschlies, A.: Eddies and upper-ocean nutrient supply, in: Ocean modeling in an eddying regime, edited by: Hecht, M. W., and Hasumi, H., Geophysical Monograph Series, 115-130, 2008.

Oschlies, A., Pahlow, M., Yool, A., and Matear, R. J.: Climate engineering by artificial ocean upwelling: Channelling the sorcerer's apprentice, Geophysical Research Letters, 37, L04701, 2010.

Parsons, T. R.: The use of mathematical models in conjuction with mesocosm ecosystem research, in: Enclosed Experimental Marine Ecosystems: a Review and Recommendations: A Contribution of the Scientific Committee on Oceanic Research Working Group 85, edited by: Lalli, C. M., Springer, New York, 197-210, 1990.

Peterson, B. J.: Particulate organic matter flux and planktonic new production in the deep ocean, Nature, 282, 677-680, 1979.

Quere, C. L., Harrison, S. P., Colin Prentice, I., Buitenhuis, E. T., Aumont, O., Bopp, L., Claustre, H., Cotrim Da Cunha, L., Geider, R., and Giraud, X.: Ecosystem dynamics based on plankton functional types for global ocean biogeochemistry models, Global Change Biology, 11, 2016-2040, 2005.

Schartau, M., Engel, A., Schröter, J., Thoms, S., Völker, C., and Wolf-Gladrow, D.: Modelling carbon overconsumption and the formation of extracellular particulate organic carbon, Biogeosciences, 4, 433-454, 2007.

Shi, W., and Wang, M.: Observations of a Hurricane Katrina-induced phytoplankton bloom in the Gulf of Mexico, Geophysical Research Letters, 34, L11607, 10.1029/2007gl029724, 2007.

Siegel, D. A., Peterson, P., McGillicuddy, D. J., Maritorena, S., and Nelson, N. B.: Bio-optical footprints created by mesoscale eddies in the Sargasso Sea, Geophysical Research Letters, 38.13, 2011.

Silyakova, A., Bellerby, R. G. J., Schulz, K. G., Czerny, J., Tanaka, T., Nondal, G., Riebesell, U., Engel, A., De Lange, T., and Ludvig, A.: Pelagic community production and carbon-nutrient stoichiometry under variable ocean acidification in an Arctic fjord, Biogeosciences, 10, 4847-4859, 10.5194/bg-10-4847-2013, 2013.

Tamelander, T., Reigstad, M., Olli, K., Slagstad, D., and Wassmann, P.: New production regulates export stoichiometry in the ocean, PLoS ONE, 8, e54027, 2013.

Urban, J. L., McKenzie, C. H., and Deibel, D.: Seasonal differences in the content of Oikopleura vanhoeffeni and Calanus finmarchicus faecal pellets: Illustrations of zooplankton food web shifts in coastal Newfoundland waters, Marine Ecology Progress Series, 84, 255-264, 1992.

Vadstein, O., Andersen, T., Reinertsen, H. R., and Olsen, Y.: Carbon, nitrogen and phosphorus resource supply and utilisation for coastal planktonic heterotrophic bacteria in a gradient of nutrient loading, Marine Ecology Progress Series, 447, 55-75, 10.3354/meps09473, 2012.

Vallino, J. J.: Improving marine ecosystem models: use of data assimilation and mesocosm experiments, Journal of Marine Research, 58, 117-164, 2000.

Van den Meersche, K., Middelburg, J., Soetaert, K., van Rijswijk, P., Boschker, H., and Heip, C.: Carbon-nitrogen coupling and algal-bacterial interactions during an experimental bloom: Modeling a ^{13}C tracer experiment, Limnology and Oceanography, 49, 862-878, 2004.

Contribution of authors

Technical Note: A mobile sea-going mesocosm system – new opportunities for ocean change research.

U. Riebesell, J. Czerny, K. von Bröckel, T. Boxhammer, J. Büdenbender, M. Deckelnick, M. Fischer, D. Hoffmann, S. A. Krug, U. Lentz, A. Ludwig, R. Muche, and K. G. Schulz

Klaus von Bröckel, Ulf Riebesell and Kai Schulz conceived the original design; Uwe Lentz, Detlef Hoffmann and Ronald Muche gave technical input, designed and constructed prototype mesocosms. Ulf Riebesell, Jan Czerny, Klaus von Bröckel, Kai Schulz and Sebastian Krug contributed conceptual ideas for the development of the mesocosms to operational readiness. Detailed technical design and accomplishment was performed by Detlef Hofmann, Uwe Lentz, Jan Czerny, Ronald Muche and Mario Deckelnick. Andrea Ludwig and Sebastian Krug managed the logistics of the deployments and experiments. Jan Büdenbender, Jan Czerny, Sebastian Krug and Matthias Fischer planned and performed underwater constructions and connected logistics. Within regular meetings, all authors contributed important ideas concerning all aspects during the development of KOSMOS. Ulf Riebesell wrote the manuscript. Jan Czerny, Klaus von Bröckel, Tim Boxhammer, Jan Büdenbender and Kai Schulz assisted with input to the manuscript and revision.

Technical Note: The determination of enclosed water volume in large flexible-wall mesocosms "KOSMOS"

J. Czerny, K. G. Schulz, S. A. Krug, A. Ludwig, and U. Riebesell

Jan Czerny, Kai Schulz, Sebastian Krug, Andrea Ludwig and Ulf Riebesell developed the idea. Jan Czerny designed the experimental set-up and performed experiments together with Kai Schulz, Sebastian Krug, Andrea Ludwig and Ulf Riebesell. Jan Czerny wrote the manuscript. Kai Schulz and Ulf Riebesell assisted with input to the manuscript and revision.

Technical Note: A simple method for air-sea gas exchange measurements in mesocosms and its application in carbon budgeting

J. Czerny, K. G. Schulz, A. Ludwig, and U. Riebesell

Jan Czerny, Kai Schulz, Andrea Ludwig and Ulf Riebesell developed the idea. Jan Czerny designed the experimental set-up and performed experiments with the help of Kai Schulz, Andrea Ludwig and Ulf Riebesell. Jan Czerny wrote the manuscript. Kai Schulz and Ulf Riebesell assisted with input to the manuscript and revision.

Sediment sample processing

J. Czerny, T. Boxhammer, K. von Bröckel, A. Ludwig, and U. Riebesell

Jan Czerny, Ulf Riebesell, Klaus von Bröckel and Andrea Ludwig developed the idea. Jan Czerny designed the experimental set-up. Tim Boxhammer and Jan Czerny developed the method until operational. Tim Boxhammer performed measurements. Jan Czerny wrote the article. Tim Boxhammer assisted with input and revision.

Implications of elevated CO_2 on pelagic carbon fluxes in an Arctic mesocosm study – an elemental mass balance approach

J. Czerny, K. G. Schulz, T. Boxhammer, R. G. J. Bellerby, J. Büdenbender, A. Engel, S. A. Krug, A. Ludwig, K. Nachtigall, G. Nondal, B. Niehoff, A. Silyakova, and U. Riebesell

Ulf Riebesell, Kai Schulz, Jan Czerny, Andrea Ludwig, Sebastian Krug, Jan Büdenbender, Tim Boxhammer, Richard Bellerby, Kerstin Nachtigall, Gisle Nondal, Barbara Niehoff and Anna Silyakova performed the experiment. Kai Schulz, Jan Czerny, Andrea Ludwig, Sebastian Krug, Tim Boxhammer, Richard Bellerby, Kerstin Nachtigall, Gisle Nondal, Barbara Niehoff, Anna Silyakova and Anja Engel did measurements. Jan Czerny analysed the data and wrote the manuscript. Ulf Riebesell, Kai Schulz, Jan Büdenbender, Tim Boxhammer, Richard Bellerby, Gisle Nondal, Barbara Niehoff and Anna Silyakova assisted with input to the manuscript and revision.

Danksagung

Mein besonderer Dank gilt meinem Doktorvater Ulf, der das Entstehen der Arbeit in vielfältiger Weise gefördert hat. Er hat mein, etwas zeitaufwändiges, Promotionsstudium großzügig finanziert und auch immer ein hohes Maß an Vertrauen in mich und in meine teilweise kostspieligen Projektvorschläge gesetzt. Er hatte, wenn der Projektumfang den Zeitaufwand gerechtfertigt hat, meinen oft allzu ausführlichen Darlegungen zu folgen, ein offenes Ohr für meine Ideen. Durch seinen kreativen und konstruktiven Input, und seinen unerschütterlichen Drive hat er maßgebend zu dieser Arbeit beigetragen.

Eric danke ich für seine zügige Erstellung des Zweitgutachtens und den übrigen Komiteemitgliedern für Ihre Mitarbeit im Prüfungsausschuss.

Meiner Mutter danke ich, für Ihre bedingungslose und liebevolle Unterstützung, die sie mir auf meinem gesamten Lebensweg, besonders auch während meiner Schulzeit, hat zukommen lassen.

Seit meiner frühen Kindheit war mein Vater Vorbild und Diskussionspartner in naturwissenschaftlich-technischen Fragen und hat meine Interessen in diesem Bereich maßgebend gefördert. Auch heute greife ich zeitweise auf seinen umfassenden verfahrenstechnischen Überblick zurück. Er ist jederzeit bereit, sich mit meinen Ideen zu befassen, sie zu begreifen und rechnerisch so zu erfassen, dass sie dann so funktionieren wie angedacht.

Jassi hat mich lieb und hält mir den Rücken frei, mehr als ich es verdient hätte, denn Familie ist im Grunde die wichtigere Verpflichtung. Sie ist Wochen und Monate allein Zuhause, zuerst schwanger und jetzt mit Baby. Trotzdem ist sie stark genug, um sich auch noch meine Probleme anzuhören, mir zu helfen, mich aufzubauen. Und meine kleine Tochter Paulina, noch nicht mal ein Jahr, ist durch ihre unverfälschte Lebensfreude eine wichtige Energiequelle für mich.

Die Listen der Autoren auf unseren Publikationen sind lang. Mit den allermeisten war es eine Freude zusammen zu arbeiten oder zusammen zu forschen. Ich bin allen zum Dank verpflichtet, einige will ich aber hier hervorheben.

Zu allererst Andrea. Mit ihr habe ich die meisten Expeditionen unternommen. Sie ist unersetzlich.

Ich danke Tim, da ich und wahrscheinlich auch sonst niemand die Geduld gehabt hätte, vergleichbare Ansprüche an Präzision in der Sedimentanalyse zu erfüllen.

Von Kai Schulz habe ich im wissenschaftlichen Bereich am meisten profitiert. Er hat sich immer die Zeit zum Diskutieren genommen, wenn man bei ihm ins Büro gestolpert ist. Auch beim Rotwein morgens um fünf, konnte man noch etwas lernen.

Wo ich gerade bei den Mentoren bin ...Joana hat mich geprägt!

Wenden wir uns der technischen Seite zu: Uwe und Klaus verkörpern den wissenschaftlich-technischen Erfahrungsschatz, von dem ich sehr profitiert habe.
Ronald ist hervorzuheben, er ist so etwas wie der „ Jedi-Meister des Hammers und der Schraube". Ronald kann alles und zeigte es auch geduldig jemandem mit so beschränktem technischen Grundwissen wie mir.
Detlef ist von entscheidender Bedeutung, weil er mit Liebe zum Detail konstruiert hat. Ihm haben wir „das deutsche" an unseren Mesokosmen zu verdanken, das was sie von denen der Franzosen, Griechen, Norwegern und Kanadiern usw. unterscheidet. Ich hoffe, das geht uns nicht verloren, jetzt wo er im Ruhestand ist. Detlef hat auch die meisten technischen Zeichnungen in dieser Arbeit angefertigt. Er zeichnet immer noch für mich, obwohl er es vorzieht, es aus gebührender Distanz und dafür aber ohne Bezahlung zu machen. Angekommen in der Gegenwart, danke ich Mario, Ralf und Ralf. Vom geduldeten Bittsteller habe ich mich im TLZ zu demjenigen entwickelt, der schuld ist, wenn die Mesokosmen nicht funktionieren. Ich muss deshalb bisweilen den Chef spielen, das kann ich (noch?) nicht so gut und ich muss mich für die Geduld bedanken. Des Weiteren bedanke ich mich für lebhafte Diskussionen, nicht nur über Technik.
Besondere Freunde und Kollegen sind natürlich alle unsere Taucher! Wir haben zusammen gefroren und gekämpft! Jan, Matze und Sebastian, aber auch alle die später dazukamen, ihr seid die besten, jeder auf seine eigene unterschiedliche Art!
Benni und Gerd, ihr habt einen ganz besonderen Dank verdient, weil ich mit euch mal über etwas anderes rede als über den „Wanderzirkus". Ich hoffe, das wird bald wieder häufiger!

Eidesstattliche Erklärung

Hiermit erkläre ich an Eides statt, dass die vorliegende Dissertation, abgesehen von der Beratung durch meinen Betreuer, nach Inhalt und Form meine eigene Arbeit ist und ich keine anderen als die angegebenen Quellen und Hilfsmittel verwendet habe. Ferner versichere ich, dass die vorliegende Dissertation weder im Ganzen noch zum Teil einer anderen Stelle im Rahmen eines Prüfungsverfahrens vorgelegen hat und unter Einhaltung der Regeln guter wissenschaftlicher Praxis der Deutschen Forschungsgemeinschaft entstanden ist.

Kiel, den
21.01.14

Jan Czerny